A JOURNEY ACROSS SELECTED OUTCROPS IN ALPINE CORSICA: A SHOWCASE OF THE OCEANIC AND CONTINENTAL UNITS OF A COLLISIONAL BELT

Michele Marroni*, Luca Pandolfi*,✉, Maria Di Rosa*, Chiara Frassi*, Alessandro Malasoma**
and **Francesca Meneghini***

* *Dipartimento di Scienze della Terra, Università di Pisa, Italy.*
** *Ts Lab e Geoservices Snc., Cascina, Pisa. Italy*
✉ *Corresponding author, e-mail: luca.pandolfi@unipi.it*

Keywords: *ophiolites; stratigraphy; deformation; metamorphism; subduction; continental collision; Alpine Corsica.*

ABSTRACT

This paper describes a four-day field trip across the Alpine Corsica, the southern branch of the Alpine collisional belt made up of oceanic and continental units derived from the closure of the Ligurian-Piedmont Oceanic Basin, and the subsequent collision between the continental margins of Adria and Europe plates. On the first day, the relationships between the main tectonic units, i.e., the Upper Units, the Schistes Lustrés Complex and the Lower Units, can be observed along an east-west transect from Bastia to Ile-Rousse. On the second day, the features of the Upper Units can be observed in the Balagne area, where an ophiolite sequence from the Middle to Late Jurassic period, along with its Late Jurassic to Late Cretaceous sedimentary cover, is clearly visible. This sequence, belonging to the Balagne Nappe, is characterized by the repeated occurrence of coarse-grained deposits supplied from the Europe continental margin, which makes it unique in the Alpine-Apennine belt. On the third day, the oceanic units of the Schistes Lustrés Complex in the Golo Valley will be examined. This complex comprises several ophiolite sequences that were accreted to the Alpine wedge and deformed under conditions of pressure and temperature ranging from blueschist to eclogite facies. On the fourth day, the Lower Units in the Corte, Popolasca and Ponte Leccia areas are visited. These units represent slices of the thinned continental margin of the Europe plate that were involved in subduction prior to continental collision. Overall, this paper provides a comprehensive overview of the stratigraphic, deformational, and metamorphic features of Corsica, which is one of the most significant fragments of the Alpine collisional belt in the western Mediterranean region.

INTRODUCTION

Corsica Island is a fragment of continental lithosphere surrounded by the two main back-arc basins of the western Mediterranean Sea (Fig. 1): the Liguro-Provençal Basin and the Tyrrhenian Basin. The north-eastern part of the island is occupied by a stack of oceanic and continental units known as Alpine Corsica that are classically regarded as the southern continuation of the collisional belt of the Western Alps. Data collected in Alpine Corsica may resolve key debates in Mediterranean geodynamics, including the dip of subduction during the Cretaceous-Early Tertiary period, the role of strike-slip tectonics, and the age and deformation mechanisms of continental crust during convergence processes.

This paper describes the stratigraphic and structural features of the units belonging to the Alpine Corsica that can be observed on a four-day field trip that focuses on selected, well-exposed outcrops. The trip starts describing the general geological setting along the route from Bastia to Île Rousse. Then, starting from the top and going down through the Alpine nappe stack, we will look at the outcrops of the stratigraphic and structural features of the weakly metamorphosed ophiolite sequence of the Balagne area. Next, we will examine the metamorphosed ophiolite sequence under blueschist and eclogite facies pressure (*P*) and temperature (*T*) conditions. Finally, we will analyze the high pressure (*HP*) metamorphic continental units that crop out along the boundary between the Alpine and Hercynian Corsica.

GEODYNAMIC BACKGROUND

Corsica Island is traditionally described as geologically divided into two domains (Fig. 2): Hercynian and Alpine Corsica exposed on the SW and NE sides of the island, respectively (Fig. 2a). Specifically, the Alpine tectonic stack overthrusts the Hercynian Corsica (e.g., Durand-Delga, 1984) via a NNW-SSE striking high-angle thrust that runs across the entire island (Fig. 2b).

The Hercynian Corsica (Fig. 2) is a fragment of the Europe continental margin comprising a polyphase basement that records tectono-metamorphic Panafrican and Variscan events, which was subsequently intruded and covered by Permo-Carboniferous magmatic rocks (Cabanis et al., 1990; Ménot and Orsini, 1990; Laporte et al., 1991; Rossi et al., 1994; Paquette et al., 2003; Rossi et al., 2009). This basement is covered by Mesozoic sedimentary rocks (primarily carbonates), and then by siliciclastic turbidites of Tertiary age (Durand-Delga, 1984; Rossi et al., 1994; Ferrandini et al., 2010; Di Rosa et al., 2019a). At the boundary with Alpine Corsica, slices consisting of Mesozoic-Tertiary sequences that have detached from the Hercynian Corsica have been identified as "Parautochthonous Units". The Alpine Corsica (Fig. 2) consists of continental and oceanic units that have been strongly deformed and affected by metamorphism ranging from sub-greenschist to blueschist-eclogite facies (e.g., Boccaletti et al., 1971; Durand-Delga, 1974; 1984; Mattauer and Proust, 1975; 1976; Amaudric du Chaffaut and Saliot, 1979; Mattauer et al., 1981; Dallan and Nardi, 1984; Gibbons and Horak, 1984; Bezert and Caby, 1988; Malavieille et al., 1998; Marroni and Pandolfi, 2003; Malasoma et al., 2006; Levi et al., 2007; Vitale Brovarone et al., 2012).

The present-day architecture of Corsica has mainly been shaped by the Alpine geodynamic history (Fig. 3), which began in the Middle Jurassic with the opening of the Ligurian-Piedmont Oceanic Basin (i.e., the Western Tethys)

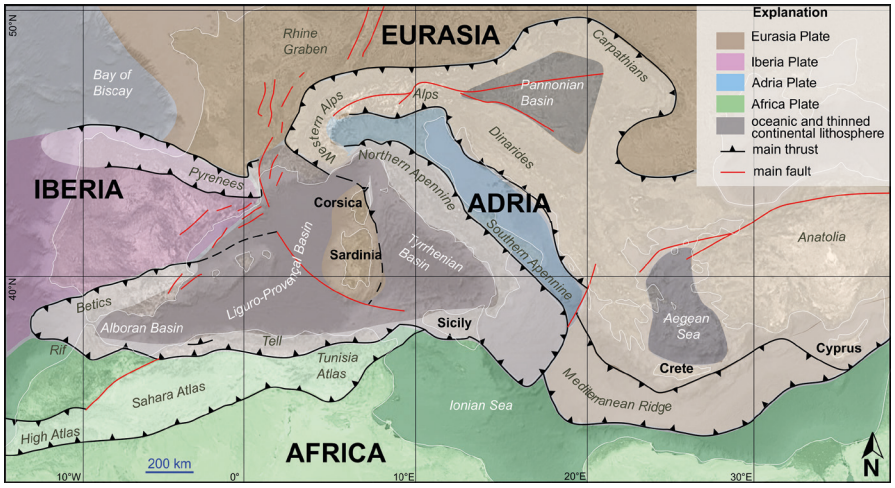

Fig. 1 - A simplified present-day geodynamic scenario of the Central-Western Mediterranean region (slightly modified after Faccenna, 2014).

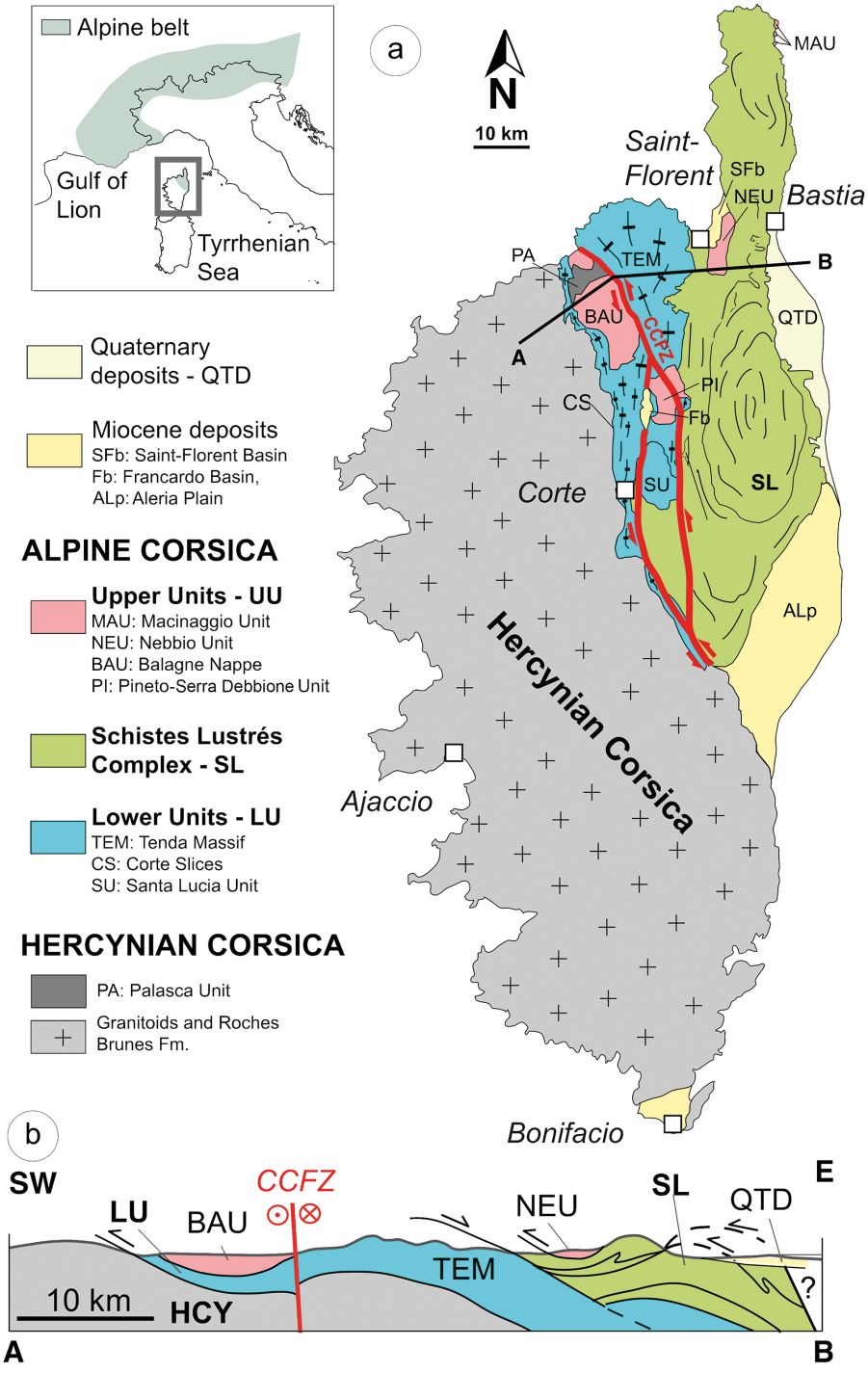

Fig. 2 - Tectonic sketch map of the Corsica Island (a) and related cross section (b). Modified from Frassi et al. (2022). CCFZ: Central Corsica Fault Zone, HCY: Hercynian Corsica.

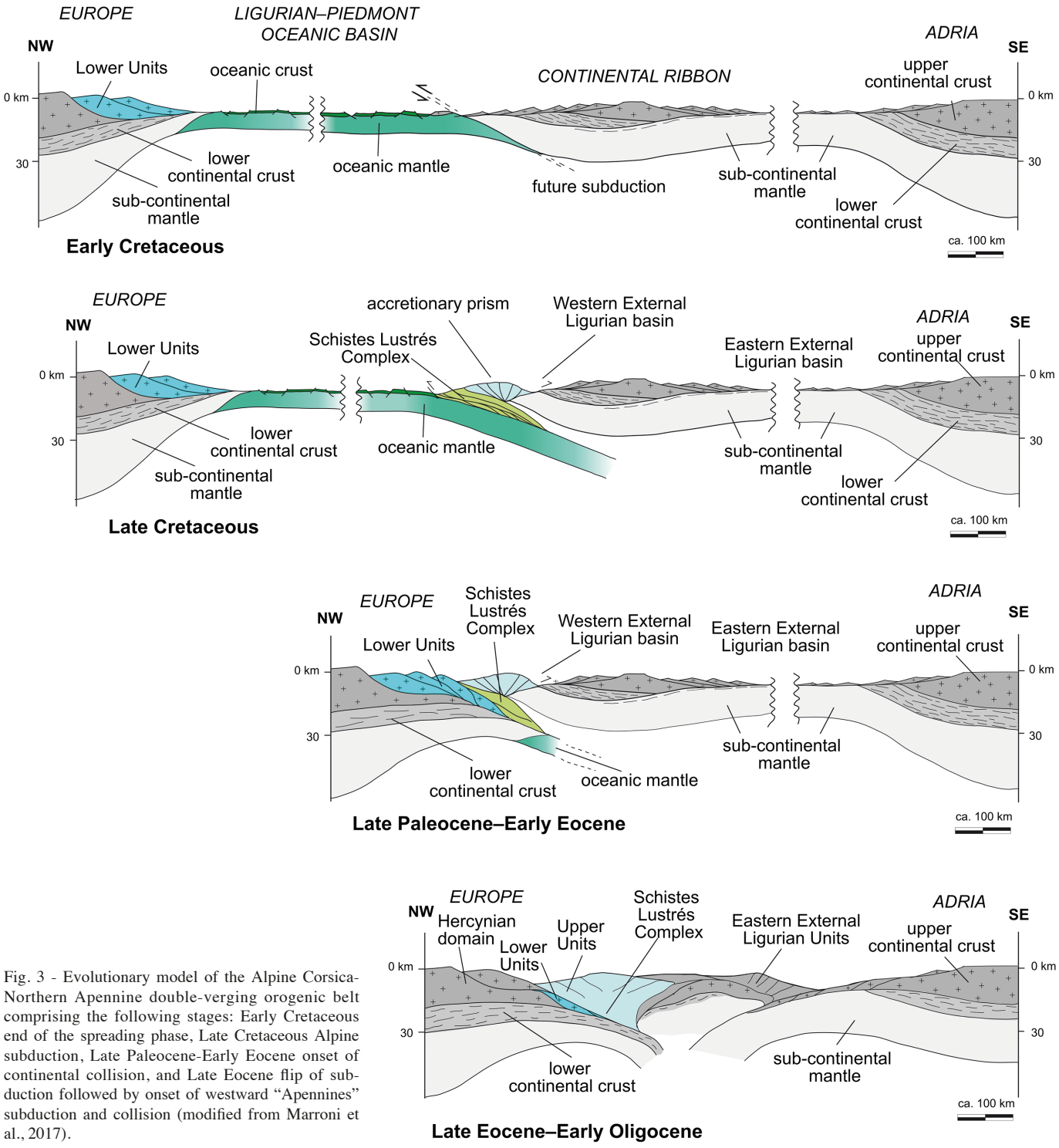

Fig. 3 - Evolutionary model of the Alpine Corsica-Northern Apennine double-verging orogenic belt comprising the following stages: Early Cretaceous end of the spreading phase, Late Cretaceous Alpine subduction, Late Paleocene-Early Eocene onset of continental collision, and Late Eocene flip of subduction followed by onset of westward "Apennines" subduction and collision (modified from Marroni et al., 2017).

between the continental margins of Europe and Adria plates (Favre and Stampfli, 1992; Manatschal, 1995; Froitzheim and Manatschal, 1996; Bill et al., 1997; Marroni and Pandolfi, 2007). This oceanic basin opened following a period of continental rifting ranging in age from the Middle/Late Triassic to the Middle Jurassic. The late-stage extensional activity of this rifting was characterized by a detachment fault system affecting a continental domain that had previously undergone polyphase tectono-metamorphic evolution achieved mainly during the Variscan orogeny (Lavier and Manatschal, 2006; Marroni and Pandolfi, 2007; Péron-Pinvidic and Manatschal, 2009; Mohn et al., 2012; Beltrando et al., 2013; Masini et al., 2013; Ribes et al., 2019). The spreading phase began in the Middle Jurassic, probably during the Bajocian, and continued until the Late Jurassic. During this time, a magma-poor, slow-spreading mid-ocean ridge system developed, producing an oceanic basin 400-500 km wide at the most (Abbate et al., 1980; Treves and Harper, 1994; Lagabrielle and Lemoine, 1997; Principi et al., 2004; Marroni and Pandolfi, 2007; Donatio et al., 2013; Sanfilippo and Tribuzio, 2013; Tribuzio et al., 2016). From the Early to the Late Cretaceous, the Ligurian-Piedmont Oceanic Basin underwent a prolonged period of stability, with no evidence of contractional or extensional tectonics. During the Campanian-Maastrichtian (Late Cretaceous), the NW to SE

directed convergence of the Europe and Adria plates produced the SE-dipping subduction of the Ligurian-Piedmont oceanic lithosphere beneath the Adria continental margin (Elter and Pertusati, 1973; Lagabrielle and Polino, 1988; Schmid et al., 1996; Michard et al., 2002; Molli, 2008; Handy et al., 2010; Malusà et al., 2015; Marroni et al., 2017).

The inception of the subduction, located at the ocean-continent transition in the Adria plate (Marroni et al., 2017), started in the Late Cretaceous, as suggested by the age of 83.8 ±4.9 Ma obtained using the Sm-Nd systematics on eclogite-facies metaophiolites (Lahondère and Guerrot, 1997). While this model is widely accepted, an alternative interpretation suggests that the Ligurian-Piedmont Oceanic Basin closed via NW-dipping subduction beneath the Europe plate in the Late Cretaceous (Principi and Treves, 1984; Lahondère and Guerrot, 1997; Jolivet et al., 1998; Brunet et al., 2000).

According to the models suggesting the SE-dipping subduction, the thinned continental margin of the Europe plate was initially part of the subduction zone and subsequently collided with the Adria plate during the Middle to Late Eocene (Gibbons and Horak, 1984; Bezert and Caby, 1988; Malavieille et al., 1998; Malasoma et al., 2006; Molli et al., 2006; Malasoma and Marroni, 2007; Maggi et al., 2012; Marroni et al., 2017; Di Rosa et al., 2017a; 2023). Shortly thereafter, the geodynamic scenario underwent a radical change due to the post-30 Ma shift in the convergence direction of the Adria-Africa plate from NW-SE to WNW-ESE (Schmid and Kissling, 2000; Ceriani et al., 2001; Handy et al., 2010; Malusà et al., 2015), causing, at the beginning of the Oligocene, the underthrusting of the southern part of the Ligurian-Piedmont Oceanic Basin under the Europe continental margin (Rosenbaum et al., 2002; Faccenna et al., 2004). The Oligocene subduction polarity inversion typically marks the onset of the Apennine orogeny, leading to the progressive deformation of the Adria continental margin, i.e., the Apennine slab (Réhault et al., 1984; Doglioni, 1991; Gueguen et al., 1998).

In this scenario, Corsica represents the upper that underwent two major extensional stages, both of which related to the rollback of the Apennine slab (Guéguen et al., 1998; Chamot-Rooke et al., 1999; Faccenna et al., 2004; Fellin et al., 2005). The first stage occurred during the Early Oligocene opening of the Liguro-Provençal Oceanic Basin, which separated the Corsica-Sardinia continental microplate from neighboring domains in the Alpine collisional belt (Figs. 1, 2a). Spreading of the Liguro-Provençal Oceanic Basin, spanning from the Aquitanian to the Langhian stages, occurred in synchrony with a counterclockwise rotation of approximately 55° of the Corsica-Sardinia continental microplate (Gattacceca et al., 2007). The second stage was linked to the Late Miocene opening of the Tyrrhenian Basin, which isolated the Corsica-Sardinia continental microplate from the Adria plate. As result, the contractional tectonics in Corsica was followed in the Early Oligocene by large-scale extension leading to the collapse of the previously thickened orogenic wedge (Jolivet et al., 1991; Fournier et al., 1991; Jolivet et al., 1991; 1998; Daniel et al., 1996; Brunet et al., 2000; Jakni et al., 2000; Zarki-Jakni et al., 2004; Pandeli et al., 2018).

Since Argand's (1924) and Staub's (1924) contributions, Alpine Corsica has been considered part of the Western Alps belt, with which it shares the same evolutionary history (Fig. 3) until the Early Oligocene (e.g., Mattauer et al., 1981; Durand-Delga, 1984; Marroni and Pandolfi, 2003; Faccenna et al., 2004; Molli and Tribuzio, 2004; Molli et al., 2006; Handy et al., 2010; Molli and Malavieille, 2011; Gueydan et al., 2017). Similarly to the Western Alps, the development since Late Cretaceous of an accretionary wedge composed of tectonically juxtaposed oceanic and oceanic-continent transition units, bearing a *HP* metamorphic imprint (Fig. 3), is also clearly identified in the tectono-metamorphic history recorded in the Alpine Corsica (e.g., Mattauer et al., 1977; Caron and Delcey, 1979; Mattauer et al., 1981; Caron et al., 1981; Faure and Malavieille, 1981; Lahondère et al., 1983; Durand-Delga, 1984 Harris, 1985; Warburton, 1986; Waters, 1990; Fournier et al., 1991; Jolivet et al., 1991; Caron, 1994; Guieu et al., 1994; Lahondère and Guerrot, 1997; Malavieille et al., 1998; Tribuzio and Giacomini, 2002; Levi et al., 2007; Chopin et al., 2008; Ravna et al., 2010; Vitale Brovarone et al., 2012; 2014; Meresse et al., 2012). Similarly, oceanic units characterized by low-grade metamorphism are considered to be involved in convergence-related deformations at higher structural level (Durand-Delga et al., 1997; Saccani et al., 2000; Marroni and Pandolfi, 2003; Pandolfi et al., 2016; Di Rosa et al., 2025). The involvement of the Europe continental margin in the subduction zone resulted in continental crust fragments detachment from the descending Europe plate and accretion to the wedge in the form of deformed and metamorphosed slices (Gibbons and Horak, 1984; Bezert and Caby, 1988; Egal, 1992; Chemenda et al., 1995; Daniel et al., 1996; Brunet et al., 2000; Tribuzio and Giacomini, 2002; Gueydan et al., 2003; Malasoma et al., 2006; Molli et al., 2006; Malasoma and Marroni, 2007; Garfagnoli et al., 2009; Molli and Malavieille, 2011; Maggi et al., 2012; Di Rosa et al., 2017b; 2019b).

TECTONIC SETTING OF ALPINE CORSICA

Alpine Corsica (Fig. 2) is composed of a stack of tectonic units that are traditionally divided into three groups based on their stratigraphic, structural, and metamorphic characteristics (e.g., Durand-Delga, 1984; Jolivet et al., 1990; Malavieille et al., 1998; Marroni and Pandolfi, 2003; Molli, 2008). From bottom to top they are: Lower Units (also known as the 'Prépiemontains' or 'Corte' Units), Schistes Lustrés Complex, and Upper Units (also known as the 'Nappe Supérieure'). Each group of units represents a specific paleogeographic and/or paleotectonic domain within the context of Alpine evolution.

The Lower Units (LU) (i.e., Tenda Massif, Palasca-Moltifao, Fuata-Pedanu, Castiglione-Popolasca, Croce d'Arbitro, Piedigriggio-Prato, Canavaggia, Pedani, Scoltola, Tour de Valletto, Venaco and Ghisoni Units) are continental-derived units that are considered fragments of the thinned Europe continental margin (i.e., comparable to the current Corsica-Sardinia continental microplate). These units were accreted at various depths to the Alpine orogenic wedge during the Tertiary period (Amaudric du Chaffaut, 1975; Amaudric du Chaffaut et al., 1976; Amaudric du Chaffaut and Saliot, 1979; Bezert and Caby, 1988; Egal and Caron, 1988; Egal, 1992; Tribuzio and Giacomini, 2002; Molli and Tribuzio, 2004; Molli et al., 2006; Malasoma et al., 2006; Malasoma and Marroni, 2007; Di Rosa et al., 2020a; 2020b).

The Schistes Lustrés Complex (SL) (Fig. 2) comprises oceanic and continental units derived from the Ligurian-Piedmont Oceanic Basin and its transition to the Europe continental margin (Caron and Delcey, 1979; Mattauer et al., 1981; Faure and Malavieille, 1981; Pequignot, 1984; Jolivet et al., 1990; Fournier et al., 1991; Lahondère et al., 1999; Rosenbaum et al., 2002; Mohn et al., 2009; Vitale Brovarone et al., 2011; Agard et al., 2011; Meresse et al., 2012; Vitale

Brovarone et al., 2014; Deseta et al., 2014) which have been deformed since the Late Cretaceous and then exhumed during the Tertiary (Jolivet, 1993). Due to the complex stratigraphy and variable metamorphic imprints, various SL classifications have been suggested (e.g., Caron and Delcey, 1979; Padoa, 1999; Rossi et al., 2001; Marroni et al., 2004; Levi et al., 2007; Vitale Brovarone et al., 2012; Vitale Brovarone and Hewartz, 2013).

The Upper Units (UU) (Fig. 2), consist of oceanic units (i.e., Balagne Nappe, and Nebbio, Macinaggio, Rio Magno, Bas-Ostriconi, and Serra Debbione-Pineto Units) made up of an ophiolite sequence with its sedimentary cover deformed under very low-grade metamorphic conditions (e.g., Mattauer et al., 1981; Dallan and Nardi, 1984; Durand-Delga, 1984; Waters, 1990; Fournier et al., 1991; Dallan and Puccinelli, 1995; Daniel et al., 1996; Malavieille et al., 1998; Marroni and Pandolfi, 2003; Molli and Malavieille, 2011; Pandolfi et al., 2016).

The LU, SL and UU underwent a different tectono-metamorphic evolution prior to their stacking at the base of the accretionary prism. While the SL and UU underwent deformation during the Late Cretaceous subduction of oceanic lithosphere, the LU were involved in continental subduction during Late Eocene-Oligocene. This evolution allowed to achieve peak metamorphism under high-pressure (HP) conditions in the LU and SL, and very low-grade metamorphic conditions in the UU (Durand-Delga, 1984; Gibbons et al., 1986; Waters, 1990; Fournier et al., 1991; Egal, 1992; Caron, 1994; Daniel et al., 1996; Malavieille et al., 1998; Marroni and Pandolfi, 2003; Molli, 2008; Molli and Malavieille, 2011; Vitale Brovarone et al., 2011; Rossetti et al., 2015; Di Rosa et al., 2020a; 2025).

The Alpine-related deformation in LU, SL and UU was only weakly modified by subsequent events that developed at shallow structural levels. In particular, the current tectonic stack of the LU, SL and UU is locally dissected by a sinistral strike-slip fault system on a regional scale, known as the Central Corsica Fault Zone (CCFZ) (Waters, 1990) and the Ostriconi Fault (Lacombe and Jolivet, 2005). This fault system also locally overprints the boundary between the Alpine and Hercynian Corsica (Lacombe and Jolivet, 2005; Di Rosa et al., 2017b). Sinistral synthetic and dextral antithetic fault systems are associated with the main fault, further complicating the relationships between the different groups of units. Maluski et al. (1973) have proposed an Eocene age, whereas Waters (1990) has indicated an Early Miocene age. By contrast, Marroni et al. (2017) suggest that the CCFZ was active during the Late Eocene-Early Oligocene.

The relationships between LU, SL and UU, and locally the CCSZ, are sealed by Burdigalian deposits that crop out in the Saint-Florent and Francardo Basins (Fig. 2) (Alessandri et al., 1977; Dallan and Puccinelli, 1995; Ferrandini et al., 1998; Cavazza et al., 2001; Cavazza et al., 2007; Gueydan et al., 2017). These basins opened during the extensional regime that affected Corsica in the post-collisional phase. The final deformation event in Alpine Corsica produced N-S trending upright folds (e.g., Fellin et al., 2005; Gueydan et al., 2017), as those of the Cap Corse, Tenda and Castagniccia antiforms, and the Saint-Florent, Balagne and Aleria synforms (Fig. 2b) that also deform the Miocene deposits of Saint-Florent, Francardo and Aleria Basins (Faure and Malavieille, 1981; Durand-Delga, 1984). They are generally associated with the late stage of Miocene extensional tectonics (Jolivet et al., 1990, 1991; Fournier et al., 1991; Egal, 1992; Marroni and Pandolfi, 2003).

In the following sections we focus on a more detailed description of the stratigraphic, structural and metamorphic characteristics of the different groups of units, that serves as a base to better follow the field journey and stops description.

The Lower Units

The Lower Units (LU) reconstructed stratigraphic log includes a Paleozoic basement composed of Late Carboniferous-Early Permian granitoids and their host rocks, covered by Permian volcanic and volcaniclastic deposits, which gradually grade into a Triassic-Eocene sedimentary sequence (Fig. 4). Each different LU recognized in literature (Tenda Massif, Palasca-Moltifao, Fuata-Pedanu, Castiglione-Popolasca, Croce d'Arbitro, Piedigriggio-Prato, Canavaggia, Pedani, Scoltola, Tour de Valletto, Venaco, and Ghisoni Units) only include part of this reconstructed succession (Table 1).

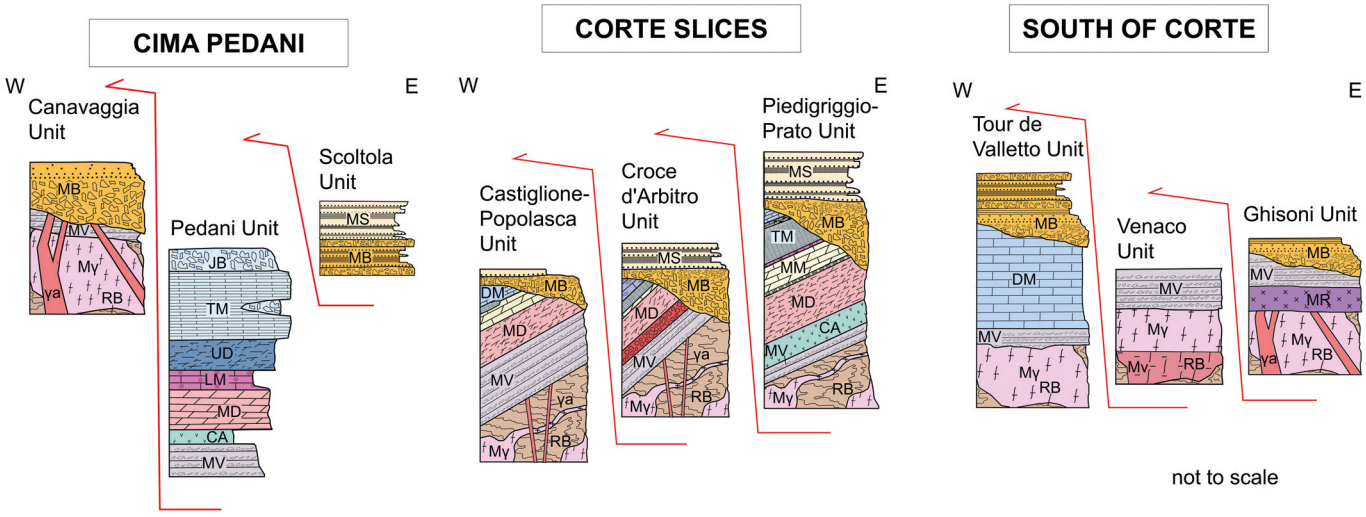

Fig. 4 - Stratigraphic logs of the three main tectonic units of the Lower Units in the central Corsica area. MB: Metabreccia Fm.; MV: Metavolcanic and Metavolcaniclastic Fm.; Mγ: metagranitoids; RB: Roches Brunes Fm.; γa: mafic dykes; JB: Jurassic Metabreccia Fm.; TM: Thin-bedded Metalimestone Fm.; UD: Upper Metadolostone Fm.; LM: Lumachella Metalimestone Fm.; MD: Metadolostone Fm.; CA: Carniole Fm.; MS: Metasandstone Fm.; DM: Detritic Metalimestone Fm.; MM: Metalimestone and Metadolostone Fm.; Mv: metagabbros; MR: metarhyolites (slightly modified after Di Rosa et al., 2019; 2020; Malasoma et al., 2020).

Table 1 - Summary of the tectonic units of the LU including their lithological and metamorphic features.

TECTONIC UNIT	LITHOLOGY	P-T PEAK METAMORPHIC CONDITIONS
PALASCA-MOLTIFAO UNIT	Variscan and Panafrican basement, Late Carboniferous to Permian metagranitoids, Permian metavolcanics, Eocene metabreccias and metasandstones	>0.4 GPa
FUATA-PEDANU UNIT	Variscan and Panafrican basement, Late Carboniferous to Permian metagranitoids, Permian metavolcanics, Eocene metabreccias and metasandstones	1.15–1.05 GPa at 280–300 °C
CASTIGLIONE-POPOLASCA UNIT	Variscan and Panafrican basement, Late Carboniferous to Permian metagranitoids, Permian metavolcanics, Triassic to Liassic metacarbonates, Eocene metasandstones	1.20–0.80 GPa at 250–330°C
CROCE D'ARBITRO UNIT	Variscan and Panafrican basement, Late Carboniferous to Permian metagranitoids, Permian metavolcanics, Triassic to Liassic metacarbonates, Eocene metabreccias and metasandstones	1.00–0.80 GPa at 200–250°C
PIEDIGRIGGIO-PRATO UNIT	Variscan and Panafrican basement, Late Carboniferous to Permian metagranitoids, Permian metavolcanics, Triassic to Liassic metacarbonates, Eocene metabreccias and metasandstones	1.05–0.80 GPa at 220–290 °C
CANAVAGGIA UNIT	Variscan and Panafrican basement, Late Carboniferous to Permian metagranitoids, Permian metavolcanics, Eocene metabreccias	1.05–0.85 GPa at 170–260°C
PEDANI UNIT	Permian metavolcanics, Triassic to Liassic metacarbonates, Eocene metabreccias	1.35–1.10 GPa at 280–360°C
SCOLTOLA UNIT	Eocene metabreccias and metasandstones	1.35–0.90 GPa at 260–280°C
TOUR DE VALLETTO UNIT	Variscan and Panafrican basement, Late Carboniferous to Permian metagranitoids, Permian metavolcanics, Triassic to Liassic metacarbonates, Eocene metabreccias	1.30–0.95 GPa at 300–350°C
VENACO UNIT	Variscan and Panafrican basement, Late Carboniferous to Permian metagranitoids, Permian metavolcanics	1.10–0.90 GPa at 260°C
GHISONI UNIT	Variscan and Panafrican basement, Late Carboniferous to Permian metagranitoids, Permian metavolcanics, Eocene metasandstones	0.81–0.72 GPa at 245–250 °C
TENDA MASSIF UNIT	Variscan and Panafrican basement, Late Carboniferous to Permian metagranitoids, Permian metavolcanics, Triassic to Liassic metacarbonates, Eocene metabreccias and metasandstones	1.20–0.80 GPa at 350–450°C

The Roches Brunes Fm. consist of polydeformed and polymetamorphic micaschists, paragneiss, quartzites, and amphibolites of Panafrican age (Rossi et al., 1994) intruded by the Permo-Carboniferous metagranitoids (Ménot and Orsini, 1990; Laporte et al., 1991; Paquette et al., 2003; Rossi et al., 2015) that in turn are cut by meta-aplite dikes and covered by the Permian Metavolcanic and Metavolcaniclastic Fm. The Mesozoic metasedimentary succession unconformably covers the basement and includes, from bottom to top:

– Norian Lower Metadolostone Fm. (Rossi et al., 1994), made of thick layers of metadolostones intercalated with purple metapelites, which are interpreted as paleosoil horizons.
– Rhaetian Metaconglomerate Fm., consisting of fragments of metadolostones and metavolcanics in a carbonate matrix, which crops out as discontinuous lenses.
– Hettangian-Sinemurian Metalimestone and Metadolostone Fm., made of medium-to-thick beds of metalimestones and metadolostones.
– Hettangian-Sinemurian Lumachella Metalimestone Fm. with well-preserved fossil associations.
– Liassic Laminated Metalimestone Fm. (Rossi et al., 1994), represented by thin beds of metalimestones alternating with very thin beds of metapelites.
– Cherty Metalimestone Fm. in discontinuous lenses.
– Liassic Detritic Metalimestone Fm., consisting of matrix-supported polymict metabreccias, often characterized by well-graded beds.

The Mesozoic succession is unconformably topped by:

– Metabreccia Fm. (cf. Volparone Breccia of Malasoma and Marroni, 2007), made up of subrounded to subangular clasts of orthogneisses, paragneisses, micaschists, metagranites, quartzites, and marbles, which are enclosed in a fine-grained matrix ranging in size from metapelites to metarenites.
– Metasandstone Fm. consists of medium-sized beds of metarenites and metapelites. The presence of *Nummulites sp*. suggests that this formation is of Middle to Late Eocene age (Bezert and Caby, 1988; Rossi et al., 1994; Ferrandini et al., 2010).

The stratigraphic relationships between the metagranitoids, their host rocks, and the Eocene deposits indicate that the latter were sedimented unconformably at the top of all Mesozoic formations, as well as at the top of the basement. The Metabreccia and Metasandstone Fms. are interpreted as foredeep deposits sedimented during Middle to Late Eocene convergence-related events when the continental crust was involved in the subduction processes, which are started in the Late Paleocene (Maggi et al., 2012 and references therein). In this setting, the Europe continental margin was affected by flexural bending, producing an uplifted forebulge deformed by extensional tectonics, with normal faulting and block tilting. These normal faults probably originated from the reactivation of former Jurassic faults as the Europe continental crust approached the foredeep basin. Extensional tectonics caused the denudation of the Triassic and Jurassic strata,

exposing them over wide areas. These areas then entered the foredeep basin, where they were swiftly covered by turbidite deposits supplied from the uplifted European continental margin (Di Rosa et al., 2017a).

Despite the differences in the *P-T* conditions of the metamorphic peak, the LU are characterized by a comparable structural setting derived from the overprinting of three phases of ductile deformation (Fig. 5) referred to as $D1_{LU}$, $D2_{LU}$ and $D3_{LU}$ (Bezert and Caby, 1988; Egal, 1992; Malasoma et al., 2006; Malasoma and Marroni, 2007; Garfagnoli et al., 2009; Di Rosa et al., 2017a; 2020b). The structures of the $D1_{LU}$ phase are almost completely obliterated during the subsequent $D2_{LU}$ phase, whose structures are the most widespread in the field, leading to the development of the most important map-scale structures. In contrast, the last $D3_{LU}$ phase does not produce any significant change to the pre-existing structural setting.

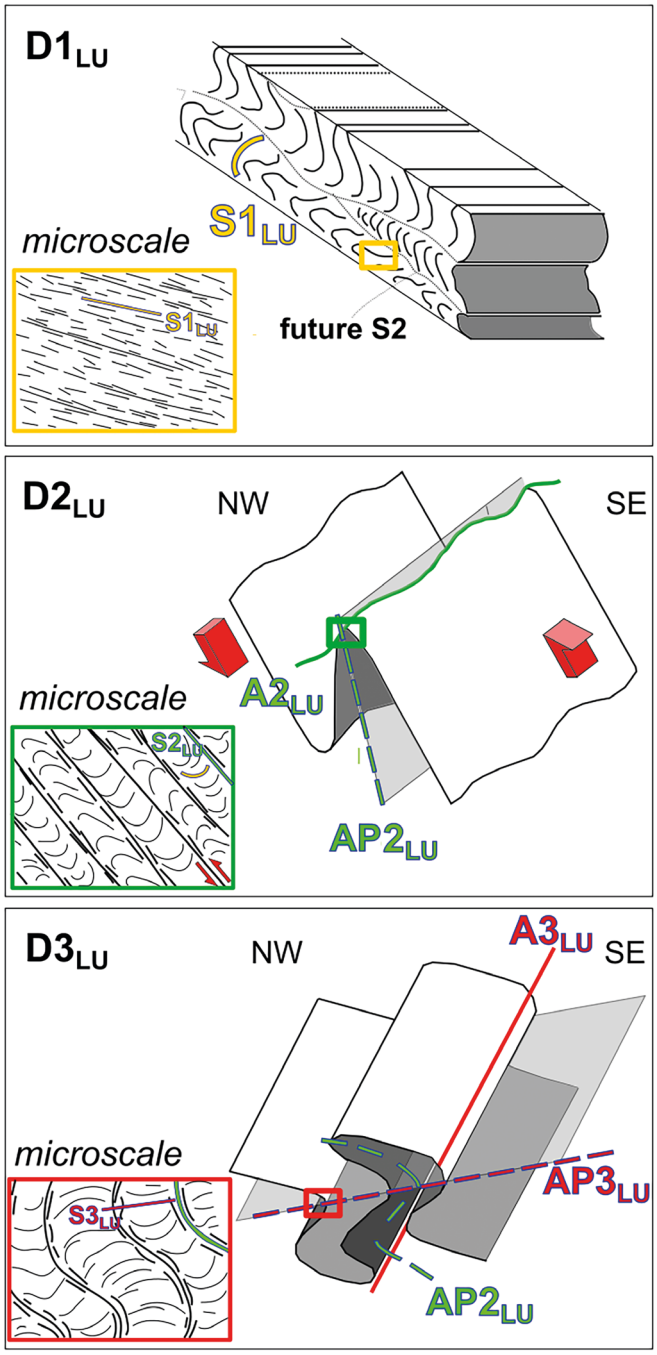

Fig. 5 - Sketches showing meso- and microscale deformation features in the Lower Units (LU).

In the field, relics of the $D1_{LU}$ phase are represented by folded Qtz veins and, occasionally, by sheath folds (Fig. 6a) which are mainly found in the Laminated Metalimestone Fm. from the North Corte area. Additionally, rare examples of $S1_{LU}$ foliation overprinted by $S2_{LU}$ have been observed in the hinges of $F2_{LU}$ folds, mostly in the Metasandstone Fm.

At the microscopic scale, relics of the $D1_{LU}$ phase have been identified in several units within metapelites-bearing formations, such as the Metabreccia and Metasandstone Fms. Here, $S1_{LU}$ is a transposed foliation preserved in the $D2_{LU}$ microlithons (Fig. 6b) and characterized by Chl + Wm + Qtz + Cal mineral assemblage (mineral abbreviations throughout the text and in the figures from Whitney and Evans, 2010 and Warr, 2021; Wm = white mica).

The $D2_{LU}$ phase is the most penetrative at the field scale. In metalimestones, metapelites, metarenites, metabreccias and metagranitoids (Fig. 6c), the $S2_{LU}$ foliation is a pervasive and continuous planar anisotropy. In the Metabreccia Fm., the well-developed $S2_{LU}$ foliation is characterized by flattened coarse-grained clasts. The strike of the $S2_{LU}$ foliation remains consistent across different areas, ranging from NNW-SSE in the North Balagne region to N-S in the Ponte Leccia-Francardo, North Corte, South Corte, and Vezzani-Ghisoni regions. A clearly visible mineral lineation ($L2_{LU}$) on the $S2_{LU}$ foliation is defined by elongated Chl, Qtz and Wm grains. In the metalimestones, the $L2_{LU}$ stretching lineation is mainly represented by boudinaged millimetric Cpx and elongated Qtz grains with oriented growth of Cal fibers. Similarly, to the foliation strike, the $L2_{LU}$ lineation shows a constant E-W trend. The $S2_{LU}$ foliation is associated with sub-isoclinal to isoclinal $F2_{LU}$ folds that are well-developed at all scales, typically showing necking and boudinage along stretched limbs. The trend of the $A2_{LU}$ axes ranges from NNW-SSE to N-S from N to S.

In metapelites and metarenites thin sections sampled the principal anisotropy along the limbs of the $F2_{LU}$ folds, is a continuous and pervasive $S2_{LU}$ - $S1_{LU}$ composite foliation where the metamorphic minerals recrystallized during the $D2_{LU}$ phase are superimposed on the pre-existing $D1_{LU}$ phase minerals. In the $F2_{LU}$ hinge-zone, $S2_{LU}$ foliation is a crenulation cleavage characterized by smooth cleavage domains showing a gradational to discrete transition to the microlithons where the $S1_{LU}$ foliation is still preserved. $S2_{LU}$ foliation is characterized by a metamorphic mineral assemblage of Wm + Qtz + Cal + Chl + Ab (Fig. 6d). In the meta-limestones, associated to the $D2_{LU}$ phase, pervasive Cal recrystallization occurs, with development of a fine-grained granoblastic texture.

The $S2_{LU}$ foliation in the metagranitoids from the Croce d'Arbitro and Ghisoni Units is mylonitic (Fig. 6e) and characterized by a mineral assemblage of Qtz + Kfs + Pl + Chl + Wm ± Cal ± Ep ± Bt (Di Rosa et al., 2017a; 2019c). Mylonitic fabric is defined by discontinuous, lepidoblastic layers of Wm ± Bt, as well as granoblastic layers of fine-grained Qtz + Pl. cm-sized Qtz and K-Fsp grains occur as σ-type porphyroclasts (Fig. 6f). The largest Qtz grains exhibit undulatory extinction, deformation lamellae, deformation bands and incipient sub grain recrystallization.

$D2_{LU}$ N-S striking m-scale shear zones mark the boundary between the units (Fig. 6e). Kinematic indicators such as the asymmetric tails of white mica around σ- and δ-type porphyroclasts of Qtz and Fsp, S-C/C' fabrics, mica fish and bookshelf structures in Fsp point to a top-to-W sense of shear. These ductile/ductile-brittle shear zones are overprinted by brittle deformation producing cataclasites.

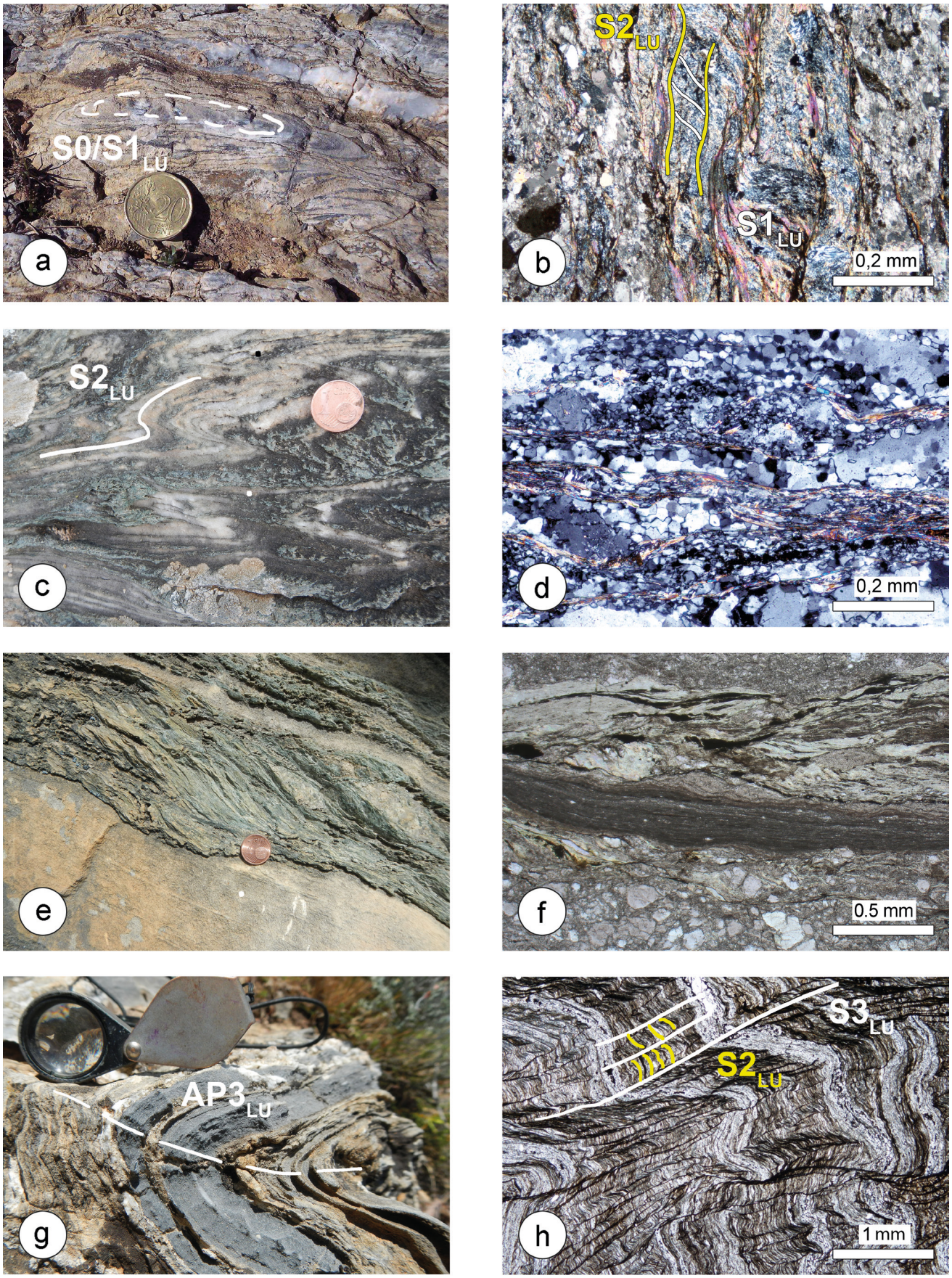

Fig. 6 - (a) $F1_{LU}$ sheath fold in the Laminated Metalimestones Fm. (b) $S1_{LU}$ foliation within the microlithons along the $S2_{LU}$ foliation in the Metasandstone Fm, CPL. (c) $S1_{LU}$ foliation deformed by $F2_{LU}$ folds within the Metabreccia Fm. (d) Photomicrograph of the $S2_{LU}$ foliation in the metagranitoids, CPL. (e) Mesoscale shear zone. (f) Photomicrograph of the shear zone associated to the $S2_{LU}$ foliation in the metagranitoids, PPL. (g) $F3_{LU}$ folds in the Metalimestones Fm. The axial plane of the $F3_{LU}$ is indicated as $AP3_{LU}$. (h) Photomicrograph of the $S3_{LU}$ foliation in the Metasandstones Fm., the $S2_{LU}$ foliation is also indicated, PPL.

The $D3_{LU}$ phase is primarily characterized by open roughly recumbent $F3_{LU}$ folds with rounded hinges (Fig. 6g) and N-S trending and sub-horizontal plunging $A3_{LU}$ axes. At the outcrop scale, the $S3_{LU}$ foliation occurs as convergent, fanning, axial-plane crenulation cleavage in the metapelites and metarenites, whereas in the metalimestones, it is represented by disjunctive cleavage. The $F3_{LU}$ folds deform the shear zones at the LU boundaries.

At the microscale, the $S3_{LU}$ foliation in metapelites can be classified as crenulation cleavage, where the main deformation mechanisms are pressure solution and the reorientation of pre-existing tabular grains, which are locally associated with minor recrystallisation of Qtz, Cal and Fe-oxides (Fig. 6h). Recrystallized calcite crystals exhibit twins belonging to Type 1 of the Burkhard (1992) classification indicate deformation temperatures below 200 °C.

The determination of P-T equilibrium conditions for LU along the Hercynian-Alpine Corsican boundary has been the subject of several studies over the past two decades (Malasoma et al., 2006; Malasoma and Marroni, 2007; Di Rosa et al., 2017a; 2019c). The metamorphic P-T paths of the Fuata-Pedani Unit (North Balagne area), the Castiglione-Popolasca, Piedigriggio-Prato, and Tour de Valletto Units (from Ponte Leccia to S of Corte) and the Ghisoni and Venaco Units were reconstructed by studying the metapelites (Malasoma and Marroni, 2007; Di Rosa et al., 2019c; 2023), whereas the P-T conditions for the Croce d'Arbitro Unit (from the Ponte Leccia to the N of Corte) were based on estimates obtained for the meta-aplite dikes (Malasoma et al., 2006). The P-T conditions of the Castiglione-Popolasca Unit were also constrained through the Na-Amp + Wm + Qtz + Ab + Ep association found in a meta-aplites dike in the Ponte Leccia-Francardo area (Malasoma et al., 2006).

Two foliations ($S1_{LU}$ and $S2_{LU}$) with the mineral association Chl + Wm + Ab + K-Fsp + Qtz ± Cal were distinguished in all the investigated samples. Di Rosa et al. (2020b and references therein) observed that the analyzed Chl and Wm related to the $S1_{LU}$ foliation in the Castiglione-Popolasca, Piedigriggio-Prato and Ghisoni Units have different compositions, which they interpreted as representing two distinct generations. A third generation of Chl and Wm was identified as growing alongside the $S2_{LU}$ foliation.

Thermobarometric estimates are summarized in Fig. 7. The highest P conditions (P = 0.8-1.2 GPa for T = 250-330°C) were registered by the Castiglione-Popolasca Unit during the early $D1_{LU}$ phase. Lower P conditions (0.55-0.80 GPa) were recorded by the Castiglione-Popolasca Unit during the T-peak (320-350 °C) in the late $D1_{LU}$ phase. Conversely, the Piedigriggio-Prato Unit reached the highest T conditions of 340-400 °C in association with a P range of 0.5-0.8 GPa during the late $D1_{LU}$ phase. This unit registered the P peak at 0.80-1.05 at 220-290°C. Overall, the LU follows two different trends: an 'isothermal' path (e.g., the Castiglione-Popolasca Unit), in which the T increase during exhumation is less than 100 °C; and a 'warm' path (e.g., the Piedigriggio-Prato Unit), in which the temperature between the P- and T-peaks increase by at least 150 °C. This causes the T-peak to be reached during the late $D1_{LU}$ phase, at temperatures between 300 and 400 °C. Despite the differences relating to the $D1_{LU}$ phase, all samples registered the $D2_{LU}$ phase (i.e., that associated with the P-T equilibrium conditions of the third Chl-Wm generation) at lower P-T.

The relationships between the LU and SL have been thoroughly investigated in the western edge of the Tenda Massif. The Tenda Massif is the largest of the LU and crops out at the core of a broad antiform that is part of the N-S trending upright fold system deforming at island-scale the unit stack defined during Alpine subduction and collision (Fig. 2b). The Tenda Massif is made up of metagranitoids intruded by metagabbros, both of Permian age (Lahondère et al., 1999; Tribuzio et al., 2009), and is regarded as a slice of European continental crust that underwent blueschist facies metamorphism (Tribuzio and Giacomini, 2002) at 47 Ma, followed by retrograde greenschist facies metamorphism up to 25 Ma (Brunet et al., 2000). The massif is bounded on the E and W side by two important tectonic boundaries of regional significance.

The East Tenda Shear Zone (ETSZ) is a km-thick shear zone developed on the eastern boundary of the Tenda Massif with a long (>20 Ma) and complex kinematic evolution developed at different crustal levels. The structure of the Tenda Massif is the result of two main events ($D1_{LU}$ -$D2_{LU}$). The first event ($D1_{LU}$) was responsible of burial of the continental slice up to 30-40 km during early Eocene (54± 8 Ma: Maggi et al., 2012; 46.6 ± 1.2 Ma; Brunet et al., 2000). Peak-metamorphic conditions is marked by celadonite-rich phengite + riebeckite-ferro-glaucophane + jadeite-bearing aegirine or clinopyroxene + rutile metamorphic assemblage constraining pressure and temperature conditions in a range of 0.8-1.2 GPa at 350-450°C (Fig. 8) (Gibbons and Horak, 1984; Maggi et al., 2012; Molli et al., 2006; Molli and Tribuzio, 2004; Rossetti et al., 2015; Tribuzio and Giacomini, 2002). This event is characterized by a dominant top-to-SW sense of shear. The main fabrics documented in the field both in the ETSZ (and within the Tenda Massif) were acquired during the $D2_{LU}$ event under retrograde greenschist facies metamorphic conditions. The post-D1 event has three different interpretations:

Model 1 (Jolivet et al.,1990, 1991; Daniel et al., 1996; Gueydan et al., 2003): $D2_{LU}$ event recorded the post-orogenic exhumation producing $F2_{LU}$ folds, $S2_{LU}$ crenulation cleavage and shear zones with a top-to-NE kinematics like a Cordillera-type core complex.

Model 2 (Molli and Tribuzio, 2004; Molli et al., 2006). $D2_{LU}$ event produced the syn-convergent exhumation of the Tenda Massif and the SL, within a kilometer-scale $D2_{LU}$ shear zone whose lower boundary is represented by the ETSZ and the upper is in the overlying SL. The exhumation started in in blueschist facies conditions and evolved up to early greenschist facies. ETSZ was finally reactivated as meter to cm-thick localized top-to-the-NE shear zones (associated to $F3_{LU}$ open to close folds) at the end of exhumation until brittle conditions ($D3_{LU}$) (T = 300-400°C; P<0.5GPa).

Model 3 (Maggi et al. 2012, 2014; Rossetti et al., 2015). Most of the exhumation was syn-orogenic and was accommodated by a dominant top-to-NE sense of shear (even if the top to the SW shearing was still present). $D2_{LU}$ phase produced also strain gradient from gneisses to phyllonites that recording a top-to-SW shearing accommodated the final stages of exhumation during the post-collisional extension.

The ages of 34-37 Ma (Priabonian), reported by Vitale Brovarone and Hewartz (2013) and by Brunet et al. (2000), constrain the exhumation of the Tenda Massif at 25-30 km of depth (Molli et al, 2006). This picture is recently confirmed by Beaudoin et al. (2020), that constrain the end of burial and exhumation at ~34 and ~22 Ma (Priabonian and Aquitanian), respectively.

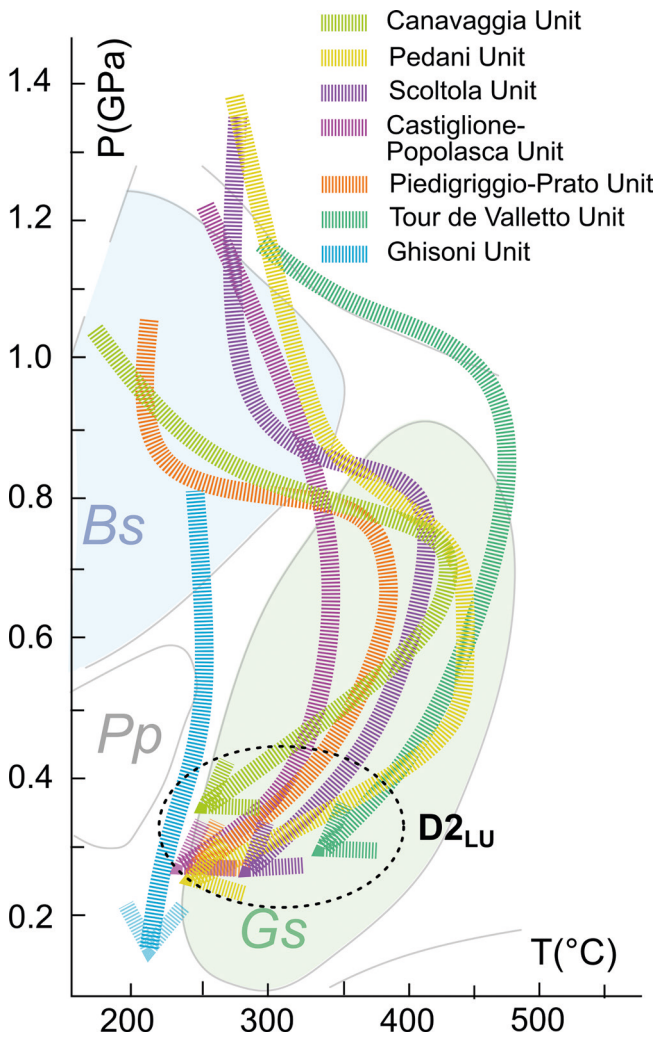

Fig. 7 - Summary of the pressure-temperature-deformation (P-T-d) paths available from the Lower Units. The stacking of the Lower Units occurred during the late D2 phase. Bs: blueschist facies; Gs: greenschist facies; Pp: prehnite-pumpellyite facies.

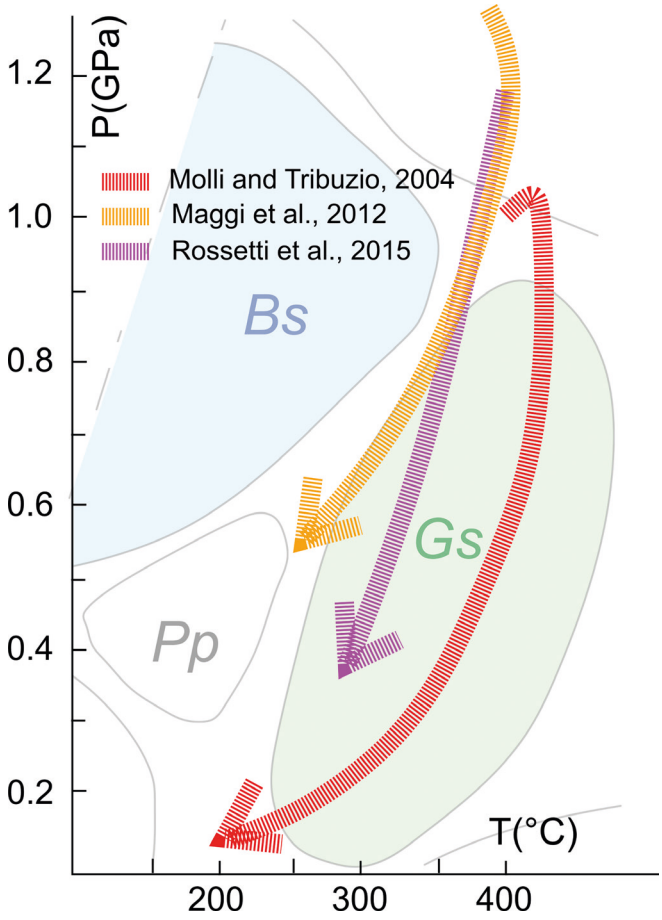

Fig. 8 - Comparison between the Pressure-Temperature deformation paths estimated for the continental rocks of the Tenda Massif. Bs: blueschist facies; Gs: greenschist facies; Pp: prehnite-pumpellyite facies.

The west border of the Tenda Massif is defined by a high-angle, left-lateral strike-slip and transtensive fault system belonging to a wide deformation zone up to 100 km long, known as the Central Corsica Fault Zone (CCFZ). It lies between the Tenda Massif and the large-scale Balagne synform, where very low-grade oceanic units of the UU formations are exposed (Nardi et al., 1978; Marroni and Pandolfi, 2003).

The Schistes Lustrés Complex

The Schistes Lustrès ocean-derived units are represented by serpentinized peridotites, metagabbros and metabasalts, topped by quartzites, marbles and calcschists, that are considered as the metamorphic equivalent of the trilogy of Radiolarite, Calpionella Limestone and Palombini Shale Fms. of the Northern Apennines, spanning in age from Late Jurassic to Late Cretaceous. Recently, De Cesari et al. (2024) have described at the top of the calcschists a sequence of metaturbidites, of likely Late Cretaceous age.

The SL continental units consist of slices of upper continental crust, primarily metagranitoids, with rare remnants of sedimentary cover in the form of quartzites, paragneisses, marbles, and micaschists. Some of these slices have been interpreted as originating from the transition between oceanic and continental crust, representing former extensional allochthons inherited from the final stage of the Ligurian-Piedmont Oceanic Basin opening (Vitale Brovarone et al., 2011; Meresse et al., 2012).

Based on stratigraphy, metamorphic imprint, and tectonic position, several groups of tectonic units are classically identified in the SL (Table 2). They will be briefly decried in the following, together with a reference to the various nomenclature occurring in literature. The structurally lowest group is represented by the Castagniccia Units (crf. Brando Unit of Lahondère and Lahondère, 1988), made of metasediments with interlayered metabasites, deformed during blueschist and eclogite metamorphism (Caron and Péquinot, 1986; Lahondère, 1991; Jolivet et al., 1998). The metasediments can be subdivided into a lower succession of calcschists interlayered with marbles and quartzites, and an upper succession of only micaschists and quartzites. The oceanic or continental origin of the Castagniccia Units remains a matter of debate.

The Prasinite Unit (cfr. Sisco and Mandriale-Lavasina Units of Lahondère and Lahondère, 1988) crops out at the top of the Castagniccia Units (Dallan and Puccinelli, 1995) and is characterized by blueschist facies metamorphism (0.8-1.0 GPa and 350 ± 25 °C; Lahondère, 1991), accompanied by syn-kinematic growth of Na-Amp + Lws (Dallan and Puccinelli, 1995; mineral abbreviations are from Warr, 2021).

Table 2 - Summary of the tectonic units of the SL including their lithological and metamorphic features.

TECTONIC UNITS GROUPS	LITHOLOGY	METAMORPHISM
UPPER SLICES COMPLEX including Inzecca-Lento-Casaluna Units	Metaophiolites and related metasediments	Blueschists facies metamorphism
OLETTA-SERRA DI PIGNO UNIT	Metagranitoids and related metasediments	Blueschists facies metamorphism
LOWER SLICES COMPLEX including Campitello-Morteda-Volpajola- Farinole Units	Metaophiolites, metasediments and metagranitoids	Blueschists and eclogite facies metamorphism
PRASINITE UNIT including Sisco-Mandriale-Lavasina Units	Metaophiolites	Blueschists facies metamorphism
CASTAGNICCIA UNITS including Brando and Sisco Units	Metasediments with scarce metaophiolites	Blueschists and eclogite facies metamorphism

The Lower Slices Complex (see Morteda, Volpajola and Campitello Units of Lahondère and Lahondère,1988, and Brunet et al.,2000), is located at the top of the Prasinite Unit. This complex consists of slices of serpentinized peridotites, metagabbros, and metabasalts, as well as slices of metasediments and metagranitoids (orthogneisses). All these lithotypes have been affected by eclogite facies metamorphism (P = 2.0 GPa and T ~500 °C in paragneisses; Lahondère and Guerrot, 1997), as well as by retrograde blueschist facies metamorphism (P = 0.8-1.0 GPa and T = 350 ± 25 °C; Lahondère and Lahondère, 1988; Lahondère, 1991). The age of eclogite metamorphism is estimated to be 83.8 ±4.9 Ma (Sm-Nd dating by Lahondère and Guerrot, 1997), whereas blueschist metamorphism is estimated to range from 34 to 37 Ma (Brunet et al., 2000; Vitale Brovarone and Herwatz, 2013). For this complex, Lahondère and Lahondère (1988) also reported the occurrence of a slice of orthogneisses with eclogite facies metamorphism (minimum P = 1.5 GPa and T = 600 ± 50 °C). According to Vitale Brovarone et al. (2011) and Meresse et al. (2012), evidence of tectonic relationships predating *HP* metamorphism between metagranitoids, metaperidotites and metabasalts indicates the presence of slices inherited from the ocean-continent transition.

The Lower Slices Complex is topped by the Oletta-Serra di Pigno-Farinole Unit, which consists of metagranitoids and metasediments interpreted as representative of continental crust (Dallan and Puccinelli, 1995). This unit has undergone blueschist-facies metamorphism (P = 0.6-0.8 GPa and T = 300 ± 50 °C; Lahondère, 1991) at 65 Ma (^{40}Ar-^{39}Ar dating by Brunet et al., 2000).

The Oletta-Serra di Pigno-Farinole Unit overthrust the Upper Slices Complex, which includes the Inzecca (Padoa, 1999) and Lento (Levi et al., 2007) Units that are also collectively known as the Inzecca-Lento Unit and consist of an intensively folded and sheared ophiolite sequence featuring lenticular slices of serpentinized peridotites, metagabbros, metabasalts, metaradiolarites, and calcschists. Of these, the Lento Unit displays the best-preserved ophiolite sequence of the SL. Although the litholtypes are like those described for the Lower Slices Complex, the metamorphism of the Upper Slices is referable to *P-T* conditions that do not exceed blueschist facies (P = 0.8 ± 0.2 GPa and T<450 °C; Levi et al., 2007).

All SL Units display relics of an early deformation event (D1) characterized by top-to-W kinematics, which developed under *HP* metamorphic conditions ranging from low-grade blueschist to eclogite facies (Mattauer and Proust, 1976; Mattauer et al., 1977; Faure and Malavieille, 1981; Malavieille, 1983; Waburton, 1986; Fournier et al., 1991; Dallan and Puccinelli, 1995; Malavieille et al., 1998). This event produced $F1_{SLa}$ sheath folds associated with the $S1_{SLa}$ schistosity which exhibits a well-developed $L1_{SLa}$ stretching lineation trending from NE-SW to E-W (Faure and Malavieille, 1981; Malavieille, 1983; Harris, 1985; Waburton, 1986). Mylonite shear zones are parallel to the $S1_{SLa}$ foliation and occur inside and at the boundaries of the tectonic units with top-to W kinematics. This deformation event produced also $F1_{SLb}$ isoclinal folds that overprinted the previously sheath folds and a N-S trending $L1_{SLb}$ stretching lineation. According to Levi et al. (2007), the late stage of the $D1_{SLb}$ was acquired during the exhumation of oceanic slices in the accretionary wedge and developed everywhere under *HP* metamorphic conditions. Previously, Lahondére (1988) suggested a similar process to explain the observed eclogite facies mineral assemblages transposed by a main regional foliation showing syn-kinematic glaucophane recrystallization.

The later deformation (D2 event) produced N-S trending, open to close $F2_{SL}$ folds, $S2_{SL}$ axial-plane foliation and brittle-ductile shear zones with S-C structures pointing to a top-to E shearing (Harris, 1985; Fournier et al., 1991; Jolivet et al., 1991 and 1998; Daniel et al., 1996; Brunet et al., 2000; Levi et al., 2007). These structures were interpreted as produced during the progressive exhumation at lower structural levels under greenschist facies metamorphism during the a long-lived extension (Fournier et al., 1991; Jolivet et al., 1991 and 1998; Daniel et al., 1996; Brunet et al., 2000). The $S2_{SL}$ foliation bears an E-W trending $L2_{SL}$ lineation.

The final deformation stages are characterized by broad, km-scale N-S trending antiforms and synforms associated with brittle deformations such as fractures and faults. These plicative structures are interpreted as hanging-wall rollover folds related to the activity of normal listric faults (Fournier et al.,1991) or as developed during an Early Pliocene shortening event (Fellin et al., 2005).

The Upper Units

The Upper Units (UU) occur as isolated klippen at the top of the SL or the LU and include 5 units (Table 3): Nebbio, Macinaggio, Rio Magno, and Serra-Debbione-Pineto Units and Balagne Nappe. These units preserve different portions of the typical Middle to Late ophiolite sequence (including its Late Jurassic to Late Cretaceous sedimentary cover). Since the Balagne Nappe provides the most complete ophiolite sequence and sedimentary cover, it can be considered representative of the UU and its stratigraphy and deformation history will be described in detail.

The Balagne Nappe is divided into four sub-units, from top to bottom: the Navaccia, Alturaja, Toccone, and Bas-Ostriconi Units. The Navaccia Unit can be subdivided into the San Colombano, Novella, and Punta Corbajola Subunits (Marroni and Pandolfi, 2003; Pandolfi et al., 2016), and show the most complete stratigraphic section representative of the nappe (Fig. 9), from Jurassic ophiolites to Late Cretaceous sedimentary cover (Bosma, 1956; Lacazedieu, 1974; Nardi et al., 1978; Dallan and Nardi, 1984; Durand-Delga, 1984; Marroni et al., 2000). The Jurassic ophiolite section comprises an oceanic basement represented by lherzolite and gabbroic complexes, that is locally covered by ophiolitic breccias. Both the basement and the ophiolitic breccias are topped by a volcanic

Table 3 - Summary of the tectonic units of the UU including their lithological features, basalts geochemistry and amount of continental debris.

TECTONIC UNIT	LITHOLOGY	BASALT GEOCHEMISTRY	CONTINENTAL DEBRIS
NEBBIO UNIT	Middle to Late Jurassic ophiolites (basalts) and Late Jurassic to Turonian pelagic and turbidite deposits	E-MORB	scarce
MACINAGGIO UNIT	Early to Late Cretaceous pelagic and turbidite deposits	no basalts	scarce
RIO MAGNO UNIT	Middle to Late Jurassic ophiolites (basalts) and Late Jurassic to Cenomanian pelagic and turbidite deposits	N-MORB	absent
PINETO-SERRA DEBBIONE UNIT	Middle to Late Jurassic ophiolites (peridotites, gabbros with basaltic dikes) and Late Jurassic to Cenomanian pelagic and turbidite deposits	N-MORB	scarce
BALAGNE NAPPE	Middle to Late Jurassic ophiolites (peridotites, gabbros and basalts) and Late Jurassic to Campanian pelagic and turbidite deposits	E-MORB	relevant

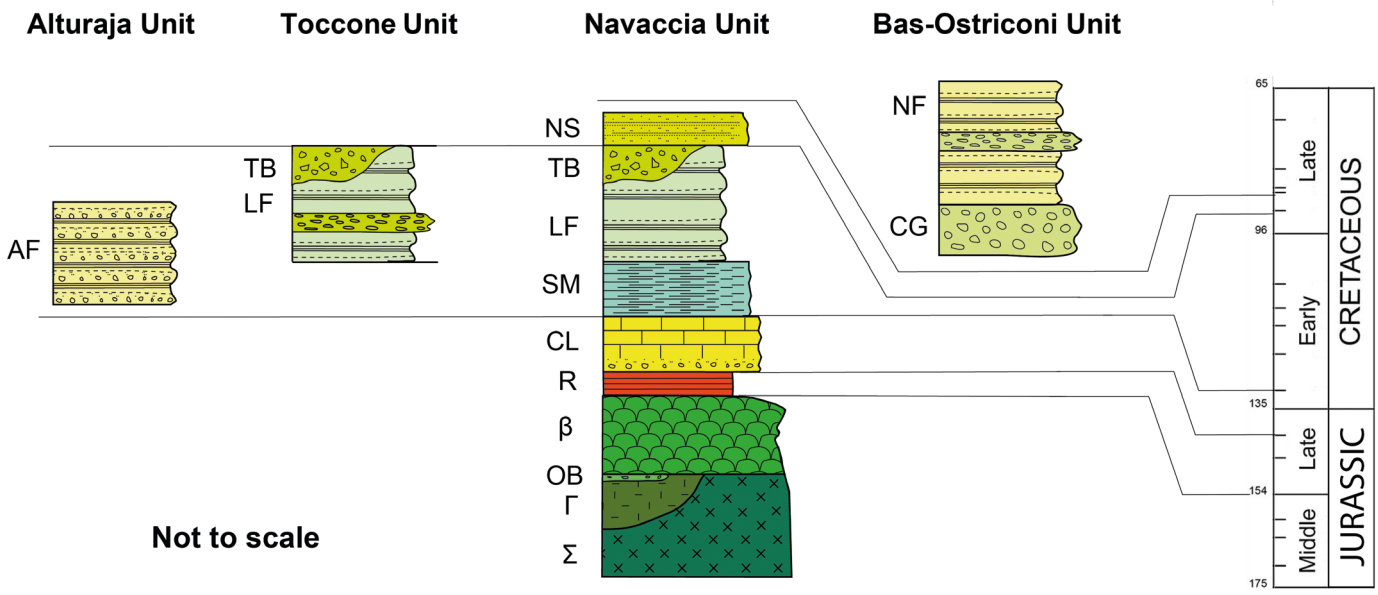

Fig. 9 - Schematic logs of the stratigraphic successions from Balagne Nappe including Navaccia, Bas-Ostriconi, Toccone and Alturaja Units (modified after Marroni and Pandolfi, 2003 and Pandolfi et al., 2016). NF: Narbinco Flysch; CG: Conglomerate Member; NS: Novella Sandstone; TB: Toccone Breccia; AF: Alturaja Fm.; LF: Lydienne Flysch; SM: San Martino Fm.; CL: Calpionella Limestone; R: Radiolarites; β: Basalts; OB: Ophiolitic Breccia; Γ: Gabbros; Σ: Serpentinites.

sequence consisting of massive and pillow lava basalts, which are cut by basaltic dikes with a porphyritic texture. The geochemical features of the basalts reveal a typical affinity for crust developed during the initial stage of oceanic spreading (Saccani et al., 2000; 2008; Durand-Delga et al., 2005; Sanfilippo and Tribuzio, 2013; Sanfilippo et al., 2015; Renna et al., 2018). Within the volcanic sequence, Durand-Delga et al. (1997) described levels of continental-derived debris containing quartz and extra-basinal carbonate fragments (see also Renna et al., 2017). The basalts are covered by a sedimentary cover comparable to that typical of the Northern Apennines ophiolites comprising Radiolarites (Callovian-Early Kimmeridgian; Conti et al., 1985; De Wever et al., 1987) and Calpionella Limestone (Tithonian-Early Berriasian; Lacazedieu, 1974; Routhier, 1956; Nardi, 1968b) locally containing continental-derived debris (Durand-Delga et al., 1997) (Fig. 9). The Calpionella Limestone passes upwards to the San Martino Fm., which consists of calcareous turbidites represented by 100 m-thick limestones and shales, interbedded with minor siliciclastic turbidites made up by alternating Qtz-rich siltstones and shales. This formation is correlated with the Palombini Shale Fm. of the Northern Apennines (Nardi, 1968a; Durand-Delga, 1984; Marroni et al., 2000). The base of this formation has been assigned to the Early Berriasian, while the top has been referred to as the Late Hauterivian to Early Barremian (Marroni et al., 2000). The San Martino Fm. shows a transition to the Lydienne Flysch, which Marroni et al. (2000) dated from the Late Hauterivian to Early Barremian at the base to the Early Turonian at the top. The 300 m thick Lydienne Flysch consists of thinly bedded mixed turbidites that show stratigraphic transition with the Novella Sandstone (cf. Gare de Novella), a 200 m-thick formation comprising amalgamated beds of coarse-grained arenites and rudites. The Novella Sandstone displays Middle to Late Cenomanian

foraminifera (Durand-Delga et al., 1978), whereas an assemblage of nannofossils no older than Late Albian has been found by Marino et al. (1995). According to Sagri et al. (1982) and Durand-Delga et al. (1997), both the deposits from the Lydienne Flysch and the Novella Sandstone Formations were supplied by the Corsica crystalline basement.

In the Toccone Unit, the stratigraphic succession includes the San Martino Fm., the Lydienne Flysch, and the Toccone Breccia. The latter is represented by coarse-grained continental-derived breccias. In turn, the Alturaja Unit is characterized by the Alturaja Fm., a thick succession of siliciclastic turbidites of Early-Middle Aptian age (Marroni et al., 2004). The Toccone Breccia and the Alturaja Fm. were probably heteropic with the Lydienne Flysch and Novella Sandstone. The youngest deposits of this sequence are probably preserved in the Bas-Ostriconi Unit. This unit comprises only the Late Cretaceous Narbinco Flysch, which consists of carbonate turbidites containing lenses of coarse-grained polymictic conglomerates (Conglomerate Member of Pandolfi et al., 2016). According to Marino et al. (1995), the nannofossils found in the Narbinco Flysch suggest a latest Coniacian age.

Throughout the Balagne Nappe succession, the occurrence of deposits supplied from a continental margin that can be identified in Hercynian Corsica is noteworthy, i.e., the Variscan basement and its carbonate cover (Fig. 10). This suggests that the succession's paleogeographic location was close to the Europe continental margin (Durand-Delga, 1984; Durand-Delga et al., 1997, 2005; Marroni and Pandolfi, 2003; Pandolfi et al., 2016).

The four subunits of the Balagne Nappe share a similar complex deformation history (Waters, 1990; Egal, 1992, Marroni and Pandolfi, 2003). According to Di Rosa et al. (2025), this history consists of four distinct deformation phases (hereafter referred as $D1_{UU}$, $D2_{UU}$, $D3_{UU}$ and $D4_{UU}$), which developed at upper structural level. The $D1_{UU}$ phase is mainly represented by noncylindrical, tight to isoclinal folds with sub-rounded and thickened hinge zones. Boudinage of the fold limbs and associated necking are very common features that developed during the $D1_{UU}$ phase. The $A1_{UU}$ fold axes are scattered with two main clusters ranging from NE-SW to N-S with NE and N plunges respectively (Fig. 11). The $D1_{UU}$ mesoscopic structures generally face W to NW. All $F1_{UU}$ folds are characterized by a well-developed, continuous $S1_{UU}$ axial-plane foliation, generally parallel to or at a low-angle to the bedding surfaces. In the shales, the $S1_{UU}$ axial-plane foliation is a slaty cleavage characterized by the metamorphic mineral assemblage Qtz ± Cal ± Ab ± Chl ± Ilm ± Fe-oxides. In the massive basalts, a widespread recrystallization occurred during the $D1_{UU}$ phase of Prh ± Pmp ± Qtz ± Ab ± Cal ± Fe-oxides (Dal Piaz et al., 1977), although Lws formation has also been reported (Baud et al., 1974). A $L1_{UU}$ mineral lineation trending NW-SE is marked by Cal and/or Qtz fibers infilling pressure shadows around Py crystals. In the antitaxial veins, Cal fiber twins indicate formation temperatures during the $D1_{UU}$ phase ranging from 150 to 200 °C. The estimated *P-T* conditions are 0.55-0.60 GPa and 240-260 °C for the Navaccia Unit, 0.50-0.60 GPa and 250-270 °C for the Toccone Unit and 0.35-0.50 GPa and 215-250 °C for the Bas-Ostriconi Unit. These values indicate *P-T* conditions pertaining to the prehnite-pumpellyite metamorphic facies (Di Rosa et al., 2025).

The $D2_{UU}$ phase deformation is responsible for the map-scale structures documented in the Balagne Nappe. $F2_{UU}$ asymmetric and overturned folds with roughly parallel geometry, rounded to acute hinges, and interlimb angles that range from 70 to 140° are commonly documented in the field. The axial planes dip steeply (50 to 80°) towards N-NE and the $A2_{UU}$ fold axes mainly trending N-S, gently dip both towards N and S (Fig. 11). The $S2_{UU}$ axial-plane foliation in the shales is a convergent fanning zonal crenulation. Low-angle thrusts, marked by foliated cataclasites with widespread S-C structures are often associated to $F2_{UU}$ folds. Kinematic indicators point to a top-to-W sense of shear.

The $D2_{UU}$ phase was followed by a mild $D3_{UU}$ phase, which is characterized by $F3_{UU}$ asymmetric folds with roughly parallel geometry (classes 1b, 1c and 2; Ramsay 1967), more pervasive in the less competent formations, such as the San Martino Fm. or the Lydienne Flysch. These folds typically exhibit clear eastward vergence. The interlimb angles range from 45° to 80°, the axial planes are sub-horizontal or gently dipping exhibiting an eastward vergence and the $A3_{UU}$ fold axes trend from NNE-SSW to NNW-SSE (Fig. 11) Marroni and Pandolfi, 2003). $F3_{UU}$ folds are characterized by well-spaced fracture cleavages that are recognized as sub-horizontal surfaces everywhere. The bedding-cleavage intersection lineation is well developed and runs parallel to the $A3_{UU}$ fold axes. During this phase, the previous top-to-W shear zones are overprinted by brittle deformations with top-to-E shear kinematics (Di Rosa et al., 2025). On a regional scale, the entire stack of tectonic units was deformed by km-scale $F4_{UU}$ syncline. This structure is probably connected to the Ostriconi Fault, which marks the boundary between the Balagne Nappe and the Tenda Massif.

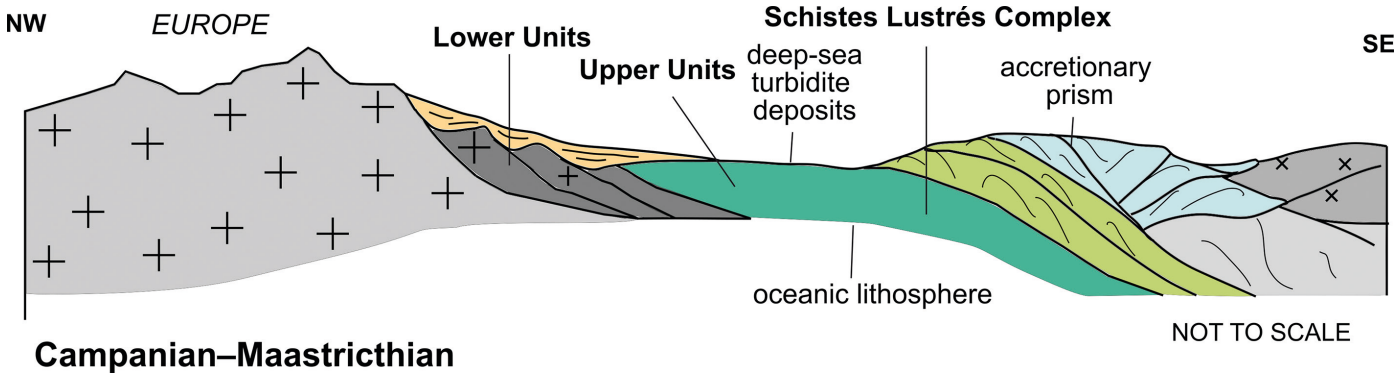

Fig. 10 - Palaeotectonic 2D sketch maps of the evolution of Ligurian-Piedmont Oceanic Basin along the Corsica-Northern Apennine transect during Late Cretaceous. Modified from Pandolfi et al., (2016).

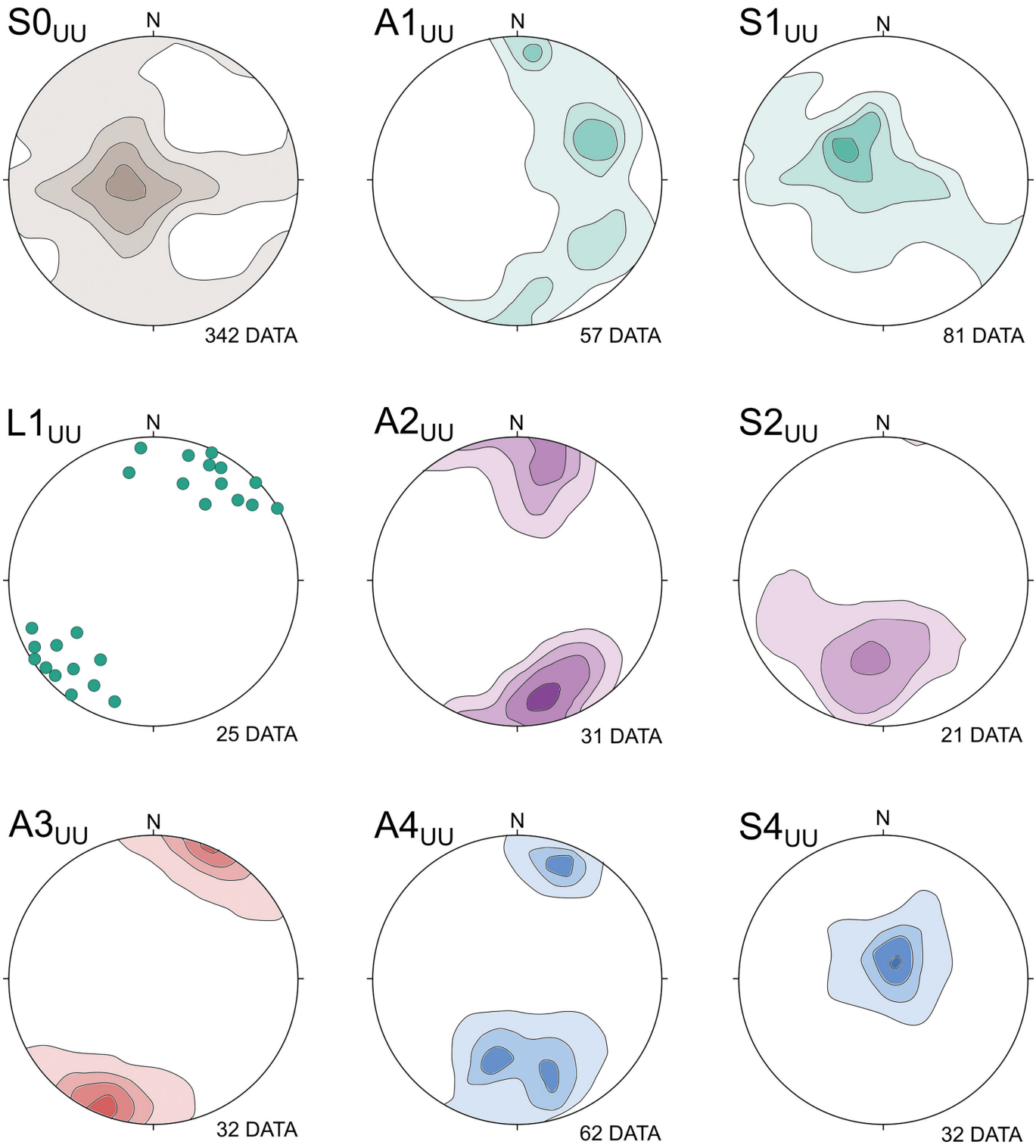

Fig. 11 - Equal area, lower hemisphere stereographic representation of $S0_{UU}$ and $D1_{UU}$, $D2_{UU}$, $D3_{UU}$ and $D4_{UU}$ structural data in the Balagne Nappe. (A= axes, S0= bedding; S= foliation; L= mineral lineation). Slightly modified after Marroni and Pandolfi (2003).

The reconstructed deformation history can be interpreted within the context of the geodynamic evolution of the Ligurian-Piedmont Oceanic Basin. Within this framework, the $D1_{UU}$ phase relates to the latest Cretaceous/Paleocene accretion into the accretionary wedge, which is associated with an E-dipping subduction zone. This is followed by the Late Eocene $D2_{UU}$ phase, which is associated with the emplacement onto the Europe/Corsica continental margin. The subsequent $D3_{UU}$ phase $D4_{UU}$ phases occurred during Early Oligocene-Late Miocene extensional processes associated with the collapse of the Alpine belt.

DAY 1: A CROSS SECTION THROUGH THE ALPINE CORSICA FROM BASTIA TO ÎLE ROUSSE

The first day focuses on an east to west traverse through northern Corsica, that offers a first snapshot of the tectonic architecture of Alpine Corsica, as well as the relationship between UU, the SL, and the LU. Along this traverse (Fig. 1.1), a specific focus on the SL is made. Starting from the town of Bastia, the SL will firstly be observed along the Cap Corse antiform, where beautiful outcrops are exposed in the road-cuts along the D81 road towards Saint-Florent. Then, we will cross the units cropping out along the Nebbio synform and arrive at the eastern flank of the Tenda antiform, where the East Tenda shear zone can be observed. To the W of Tenda, the low-grade sedimentary successions of the UU are exposed along the Balagne synform and will be examined in detail on the second day.

DAY 1 STOPS DESCRIPTION

ITINERARY: Bastia, Col de Teghime, Saint-Florent, Defilè de Lancôme, Saint-Florent, Lozari, Île Rousse.

STOP 1.1 - Monserrato Village - VIEW ON THE BIGUGLIA PLAIN AND THE EASTERN FLANK OF THE CAP CORSE ANTIFORM (42°69'24.8"N 9°44'16.1"E)

This stop is located on the RD81 road towards **Î**le Rousse, just after the center of Bastia, and offers a beautiful view of the Biguglia Plain, which is filled with Quaternary alluvial deposits. The western border of the plain is formed by the hills where the eastern, east-dipping flank of the Cap Corse antiform crops out. This structure affects a stack of SL Units, ranging from the lowest Castagniccia Unit to the uppermost Oletta-Serra di Pigno-Farinole Unit. The recent alluvial deposits of the Biguglia plain are partially covered by the Biguglia marshland and are separated from the Tyrrhenian Sea by beach deposits.

STOP 1.2 - near the Suerta Village: GLAUCOPHANE-BEARING METABASITES OF THE PRASINITE UNIT (42°41'10.6"N 9°24'34.6"E)

Moving forward RD81 towards Île Rousse, near the village of Suerta, there is a well-exposed outcrop of metabasites from the Prasinite Unit (Mandriale-Lavasina Unit of Lahondère, 1981). This unit consists of a body of metabasites up to 500 m-thick, showing a polyphase tectono-metamorphic history acquired under conditions ranging from blueschist facies to retrograde greenschist *P-T* conditions. In this outcrop, the metabasites (Fig. 1.2a) are deformed by N-S trending, gently dipping foliation, showing NE-SW trending mineral lineation.

The main foliation visible at outcrop-scale is marked by Ep-rich levels and can be correlated with the greenschist facies $D2_{SL}$ deformation phase, although relics of the prograde blueschist facies metamorphism (0.8-1.0 GPa and 350 ± 25 °C; Lahondère, 1991) can also be observed at microscale as a Gln + Lws mineral assemblage foliation (Fig. 1.2b). Particularly, the outcrop shows well-preserved Na-Amp minerals aligned along the thin, 10-15 mm-thick, blue layers. The post-$D2_{SL}$ phase deformation in this area is represented by NE-SW trending subvertical crenulation cleavage. Later subvertical faults, which are generally interpreted as being related to the development of the Cap Corse antiform, also occur in these outcrops.

STOP 1.3 - near the "station de traitment des lordures" - METAGRANITOIDS OF THE OLETTA-SERRA DI PIGNO - FARINOLE UNIT (42°40'47.1"N 9°24'41.2"E)

Further along the same road, before the intersection with the road to Montesoro, the outcrop offers good exposures of the continental slices involved in the subduction. In this outcrop the Oletta-Serra di Pigno-Farinole Unit consists of mylonitic orthogneiss are characterized by cm-scale porphyroclasts of Qtz and Fsp in a fine-grained matrix (Fig. 1.2c) locally preserving felsic and basic boudins. The protolith is the Permian granitoids cut by aplitic and basaltic dikes, as found in the Hercynian Corsica batholith. The orthogneiss exhibits E-W striking and N-dipping mylonitic foliation and a NE-SW trending stretching lineation.

In thin section, relics of the magmatic association (porphyroclasts of Qtz, K-Fsp and Pl) are wrapped by a foliation consisting of Wm-rich and recrystallized Qtz layers (Fig. 1.2d). The occasionally presence of syn-kinematic recrystallisation of Wm, Na-Amp, Ab and Jd indicated that these rocks achieved blueschist facies metamorphic conditions constrained at 65 Ma (Brunet et al., 2000). Lahondère (1991) estimated the *P-T* conditions of metamorphic peak to be 0.6-0.8 GPa and 300 ± 50 °C.

STOP 1.4 - south of Montebello: METAGABBROS OF THE UPPER SLICES COMPLEX (46°67'82.3"N 9°40'29.7"E)

We continue along the RD81 road towards Saint-Florent. After 1 km from the landfill, we can observe along the road-cut a well-exposed outcrop of metagabbros from the Upper Slice Complex (Fig. 1.2e).

The metagabbro crops out as a lenticular-shaped tectonic slice wrapped around by calcschists, and it is a clear example of the heterogeneous distribution of deformation in the SL (Fig. 1.2e) At the boundaries of the slice, the metagabbro is intensively sheared and characterized by gently dipping, NE-SW trending, fine-grained foliation bearing E to W trending

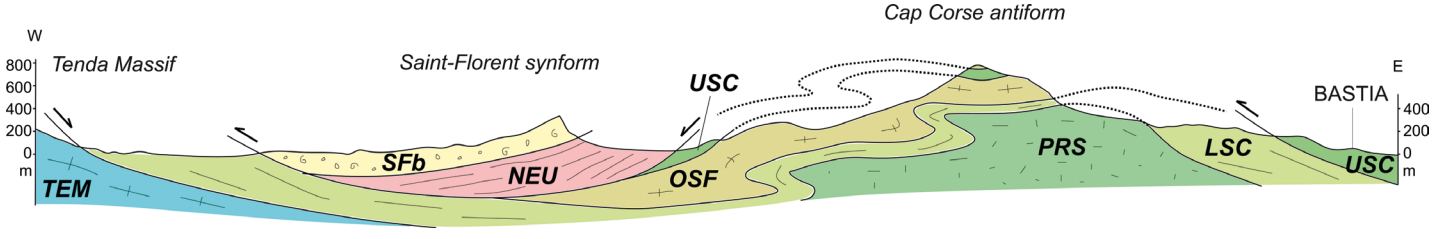

Fig. 1.1 - Geological cross-section from Bastia to the Tenda Massif (based on Dallan and Puccinelli, 1995). TEM: east flank of the Tenda Massif belonging to the Lower Units, SFb: Miocene of Saint-Florent Basin; NEU: Upper Units of the Nebbio area; USC: Upper Slice Complex of the Schistès Lustrès Complex; OSF: Oletta-Serra di Pigno-Farinole Units of the Schistès Lustrès Complex; LSC: Lower Slice Complex of the Schistès Lustrès Complex; PRS: Prasinite Unit of the Schistès Lustrès Complex.

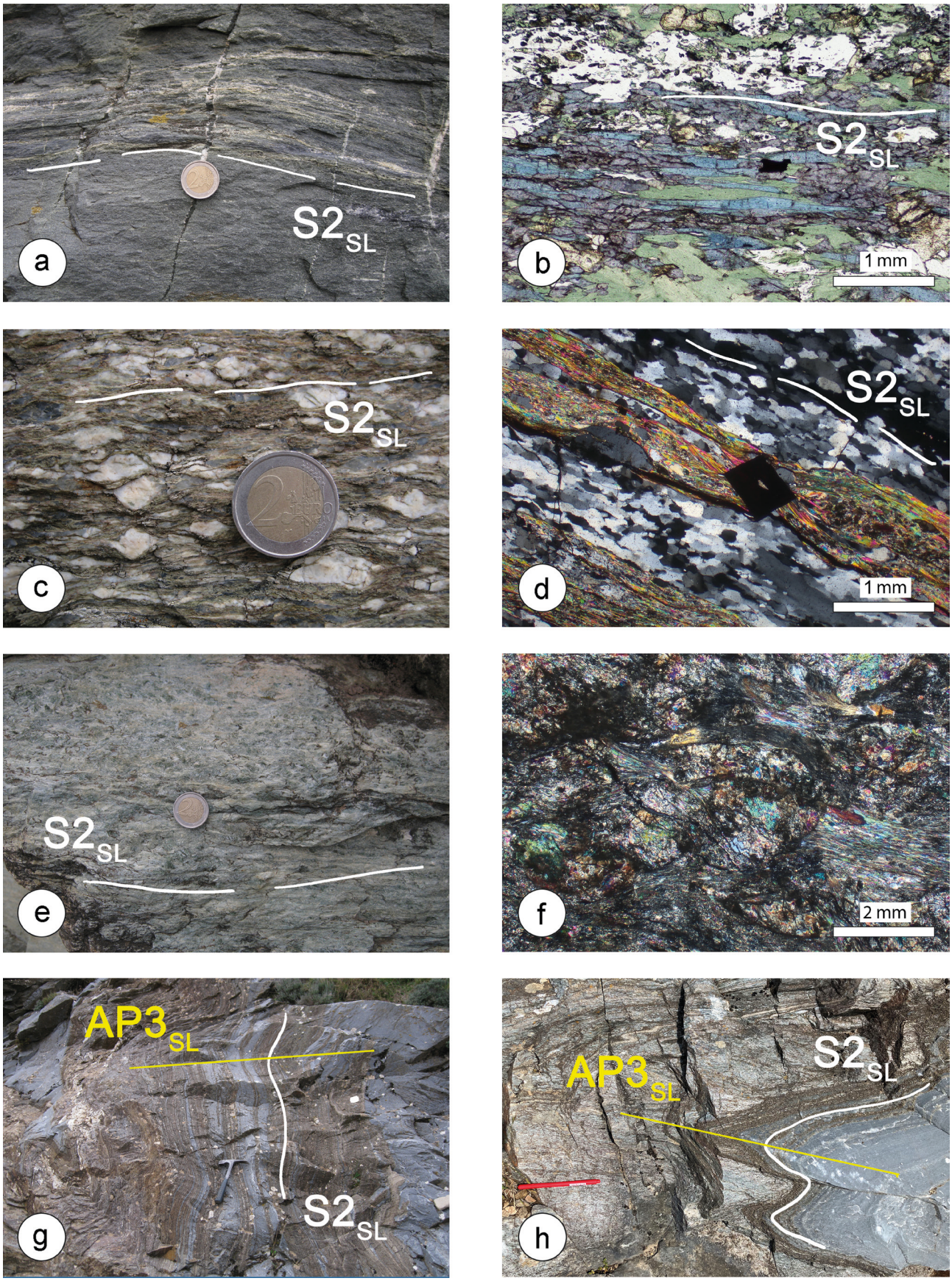

Fig. 1.2 - (a) Close-up of the metabasalts belonging to the Prasinite Unit. Yellowish, epidote-rich levels and dark, glaucophane-rich levels can be observed. (b) Thin section of metabasalt from the Prasinite Unit. Glaucophane partly replaced by chlorite is aligned along the $S2_{SL}$ foliation, PPL; (c) Close-up of the orthogneisses belonging to Oletta-Serra di Pigno-Farinole Unit. (d) Photomicrograph of orthogneisses belonging to Oletta-Serra di Pigno-Farinole Unit, CPL; (e) Close-up of the metagabbros belonging to Upper Slices Complex. (f) Photomicrograph of metagabbros belonging to the Upper Slices Complex, which preserves relics of pristine magmatic paragenesis, CPL. Close-up of the metalimestones (g) and metaquartzites (h); Oletta-Serra di Pigno Unit. Labels: $S2_{SL}$: foliation S2; $AP3_{SL}$: F3 Axial plane.

mineral lineation. In these zones, the obliteration of the original magmatic paragenesis is complete. Moving towards the core of the slice, the grain size of metagabbros increases and relics of magmatic Cpx can be observed (Fig. 1.2f). A few km S of this area, in the Lento Unit, Levi et al. (2007) estimated *P-T* conditions of the blueschist metamorphism of the Upper Slice Complex as 0.8 ± 0.2 GPa and <450 °C.

STOP 1.5 - ancient carriere de ruines (Rnes): METALIMESTONES AND METAQUARZITES OF THE OLETTA-SERRA DI PIGNO-FARINOLE UNIT (42°40'46.0"N 9°23'26.8"E)

Moving on the RD81, about 200 m before the Col de Teghime pass, there is a nice outcrop of strongly deformed alternating marble and quartzite layers (Fig. 1.2g,h) near an old quarry. The stratigraphic interpretation of these metasediments is still a matter of debate. They can be regarded as representative of the Early Cretaceous sedimentary cover of an oceanic crust, like the Calpionella Limestone found in the Northern Apennine ophiolites, or alternatively, as Triassic or Early Jurassic cover of a continental crust, comparable to the orthogneisses found in the Oletta-Serra di Pigno Unit. In this outcrop, a detail of the multiphase deformation that affect the SL can be observed. Specifically, $D2_{SL}$ sheath folds are seen as deformed by the open-to-close $D3_{SL}$ folds, which have sub-horizontal axial planes. The $D2_{SL}$ folds exhibit well-developed $L2_{SL}$ stretching lineations represented by Qtz rods that are parallel to the $A2_{SL}$ axes everywhere. Relics of the $D1_{SL}$ phase are visible only at thin section-scale, preserved in the microlithons aligned along the $S2_{SL}$ foliation.

STOP 1.6 - Col de Teghime: PANORAMIC VIEW ON THE WESTERN FLANK OF THE CAP CORSE ANTIFORM AND NEBBIO SYNFORM (42°40'36.6"N 9°22'57.6"E)

We arrive at the Col de Teghime pass, and we stop at the panoramic viewpoint, located ca. 100 m towards Saint-Florent from the pass. The point offers a beautiful view of the Nebbio area (Fig. 1.3). From NNE to SSW, we can observe:

- the western flank of the Cap Corse antiform, represented by a W-dipping pile of SL units. The hinge zone of this large-scale structure is visible in the landscape as a change in the dipping of the main foliation.
- the SL units dip below the UU of the Nebbio area, which corresponds to an area characterized by smooth morphology.
- the UU are unconformably covered by Burdigalian to Langhian deposits of the Saint-Florent Basin, which crop out along the coastal cliffs. The UU, as well as the Saint-Florent Basin deposits, are deformed on a large scale synform with a subvertical axial plane, showing the same age and origin as the Cap Corse antiform.
- the eastern flank of the Tenda Massif antiform can be observed in the skyline.

From the Pass we can continue along the main road and cross the outcrops of the UU ophiolites and Miocene deposits until Saint-Florent. Alternatively, we can take the road RD38 to Olmetta di Tuda at the crossroad immediately after the panoramic viewpoint, to reach the outcrop of Stop 1.7.

STOP 1.7 - detour to the Défilé de Lancôme: ECLOGITE FACIES METABASALTS (parking: 42°40'36.6"N 9°22'57.6"E)

From the Col de Teghime pass we take the road RD38 towards Olmetta di Tuda and we continue until Col de Santo Stefano. Then, we take the RD62 road until a parking spot close to first house, from where walk back for about 100 m to observe the outcrops of eclogite facies metabasalts (Fig. 1.4a). The road cuts offer spectacular sections of well-preserved eclogitized pillow lavas belonging to the Lower Slices Complex. According to Ravna et al. (2010), the fine-grained eclogitized pillow lava and inter-pillow matrix appear

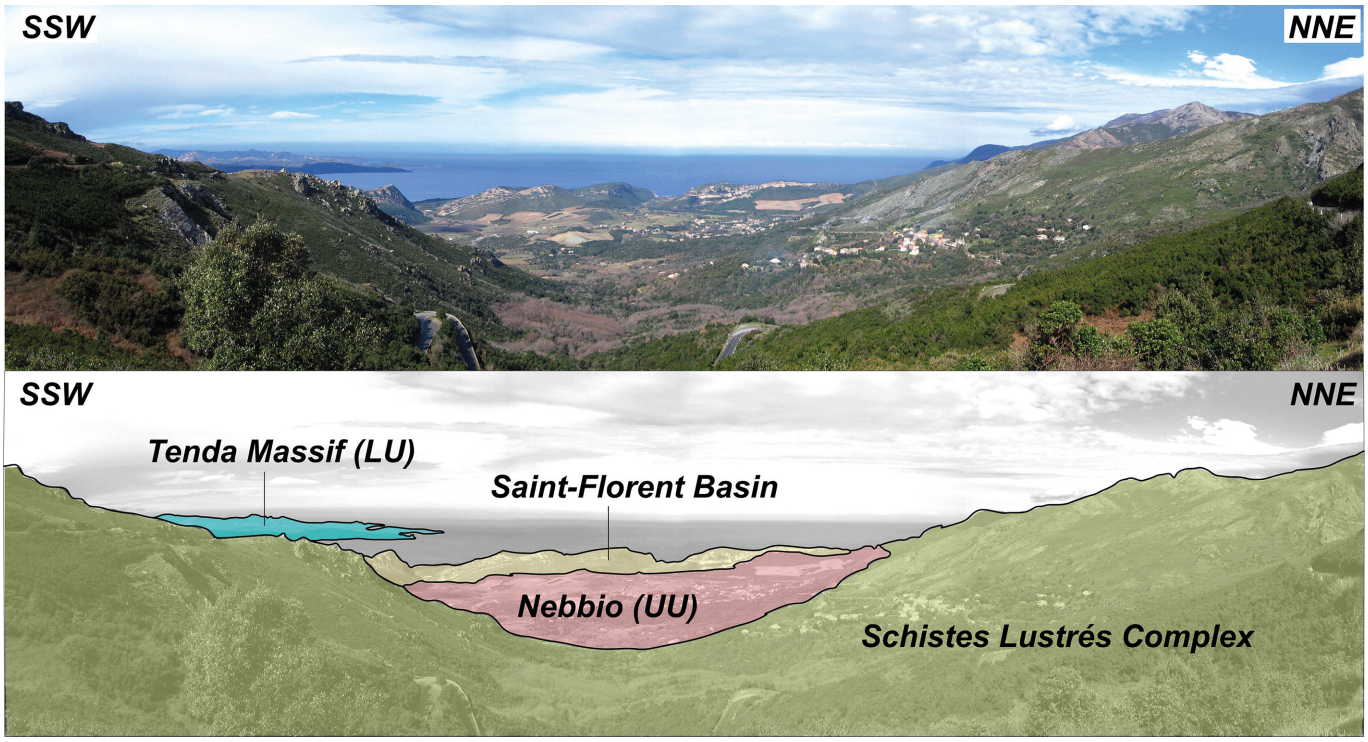

Fig. 1.3 - Panoramic view of the Nebbio area. The view faces to W.

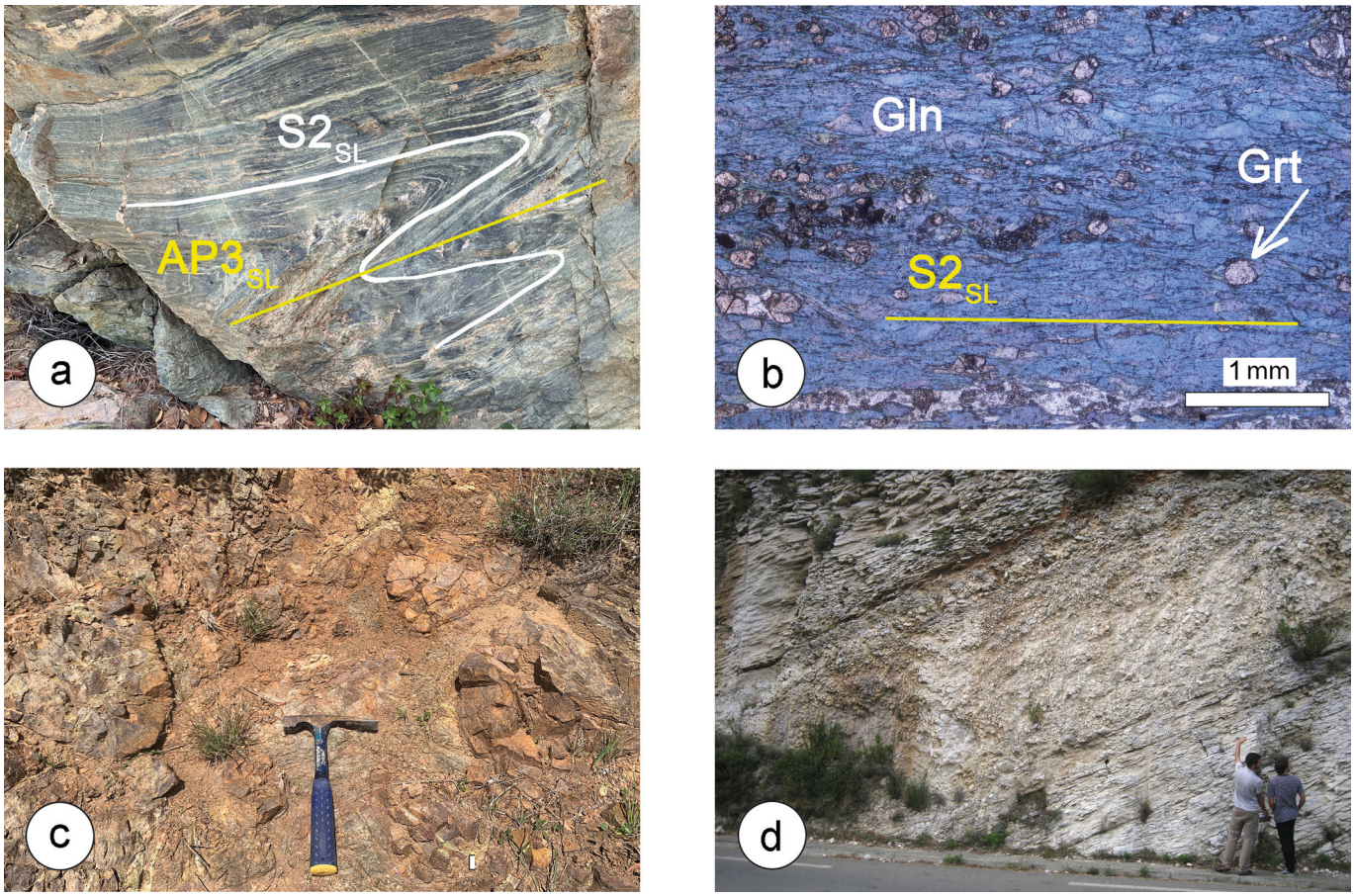

Fig. 1.4 - Défilé de Lancôme: (a) Close-up of the eclogite-facies metabasalts; (b) Photomicrograph of metabasalts characterized by glaucophane (Gln), albite, epidote and garnet (Grt). (c) Pillow lava basalts of the UU from the Nebbio Nappe; (d) Miocene deposits of the Saint-Florent Basin.

extremely fresh, showing clear evidence of retrograde path under blueschists facies P-T metamorphic conditions (Fig. 1.4b). The peak assemblages in the massive pillows and the weakly foliated inter-pillow matrix both consist of zoned, idiomorphic, Mg-poor (less than 0.8 wt% MgO) Grt + Omp + Lws + Chl + Ttn.

Locally, the Omp and Grt are replaced by the lower-grade Gln + Ab assemblage. Pseudosections of the compositions of the massive pillows, the inter-pillow matrix, and the cross-cutting veinlets indicate similar *P-T* conditions, with maximum P of 1.9-2.6 GPa and T of 335-420 °C (Ravna et al., 2010). Retrogression during the initial decompression of the studied rocks is very localized. Late Ab + Gln veinlets, not associated with lawsonite breakdown, indicate that the rocks remained in a cold environment during exhumation.

We return to the panoramic viewpoint at Col de Teghime and follow the main D81 road towards Saint-Florent. After passing through Patrimonio, we reach a roundabout and continue for 200 m until a small road intersection.

STOP 1.8 - Nebbio area: PILLOW BASALTS OF THE UPPER UNITS OPHIOLITE SEQUENCE (42°41'43.6"N 9°21'07.9"E)

Moving towards west along the D81 for ca. 12 km we turn left in correspondence of the wastewater treatment plant in Strada Imperiale. After 200 m, before the sharp turn right, we can observe the pillow lava basalts of the Nebbio Unit in a small outcrop along the road cut (Fig. 1.4c).

The pillow lavas exhibit a clear westward dipping attitude. The pillows are set in an abundant hyaloclastite matrix and are characterized by varioles filled with zeolite. As in the Balagne Nappe (see Day 2), these slightly-metamorphic basalts are covered by Callovian-Early Kimmeridgian Radiolarites that show a gradual transition to Tithonian-Early Berriasian Calpionella Limestone (Dallan and Puccinelli, 1995).

STOP 1.9 - Saint-Florent Basin: MIOCENE DEPOSITS (42°39'22.2"N 9°03'21.2"E)

We continue along the D81 road for approximately 1.2 km until we reach an intersection with a small road on the right, just before a small bridge. This outcrop provides a well-exposed section of the Miocene deposits of the Saint-Florent Basin (Fig. 1.4d). According to Cavazza et al. (2007), these deposits lie unconformably on the units of Alpine Corsica and consist of a succession including the age-unknown Albino Conglomerates Fm., topped by the Torra Fm., that progressively pass to the Monte S. Angelo Fm., both of Late Burdigalian-Early Langhian age. These formations are made up of calcarenites and conglomerates, which record thin transitional deposits that evolve vertically into fully marine sediments. The top of the succession is represented by the Late Langhian to Early Serravallian Farinole Fm., which consists of foraminifera-rich marls and calcarenites. This outcrop exposes a small section of the Monte S. Angelo Fm characterized here by cross-bedded calcarenite, made up of well-sorted, coarse- to very coarse-grained intrabasinal bioclastic sandstone (biosparite and biomicrosparite), with a subordinate extrabasinal siliciclastic detrital component. Rhodoliths

(i.e., concentrically encrusted nodules of red corallinacean algae) are very common in this formation.

We then move forward to the village of Saint-Florent, and after the village, we continue along the D81 road and stop after about 3 km in front of an old quarry.

STOP 1.10 - near Monte Guppio: EAST TENDA SHEAR ZONE (parking: 42°39'23.0"N 9°16'21.4"E)

This stop allows documenting the heterogeneous distribution of $D2_{LU}$ shear strain within the ETSZ affecting Permian granitoids and mafic dykes in the eastern Tenda Massif. Walking for ca. 600 m towards north, it is possible to recognize along the road cut the $D2_{LU}$ crenulation cleavage and cm-thick $D2_{LU}$ ductile shear zones wrapping dcm- to m-thick less deformed domains of orthogneiss (Fig. 1.5a), occasionally preserving relics of $S1_{LU}$ foliation mainly defined by Qtz + Wm + Ep and (relict) feldspars + rare Na-amph (non-visible at the outcrop scale) (e.g., Molli et al., 2006).

Moving towards N-NE (i.e., towards the SL), the number and the thickness of shear zones progressively increase, as well as the development of $D2_{LU}$ crenulation cleavage (Fig. 1.5b). The S2 mylonitic foliation is oriented NW-SE, dips less than 30° towards NE and it is highlighted by phengite, quartz, albite, epidote, and microcline. It bears stretching and object lineations which are oriented NE-SW and shallow dipping mainly towards NE. Kinematic indicators, both at the meso- and at the microscopic scale, are represented by asymmetric feldspar porphyroclasts and S-C-C' fabrics both indicating a main top-to-E-NE (locally top-to-W-SW) sense of shearing (Fig. 1.5c). Rare 5-10 cm thick basalt doleritic dykes, characterized by epidote-blueschist assemblages with Rbk/Fe-Gln grew both along the $S1_{LU}$ and $S2_{LU}$ crenulation cleavage (Fig. 1.5d) clearly indicated that $D2_{LU}$ deformation started under blueschist facies conditions.

STOP 1.11 - road D81 south of Bocca di Vezzu: TRANSITION FROM PANAFRICAN BASEMENT ROCKS TO CARBONIFEROUS - PERMIAN SEQUENCE INTO THE TENDA MASSIF (42°39'50.7"N 9°08'12.0"E)

We continue along the D81 road until we reach the Bocca di U Vezzu. After this, we continue for about 3 km until we reach a sharp bend. We stop here and walk about 100 m back towards Bocca di U Vezzu.

This outcrop reveals a section of the host rocks of the Permian granitoids. These pre-Alpine, polyorogenic continental basement rocks record tectono-metamorphic Panafrican and Variscan events. Within this section, the 'Panafrican' micaschists are covered by Late Carboniferous-Early Permian metaconglomerates, which grade into metavolcaniclastics and metavolcanics of Early Permian. The metamorphic imprint was acquired during the Alpine orogeny, probably in the Early Tertiary.

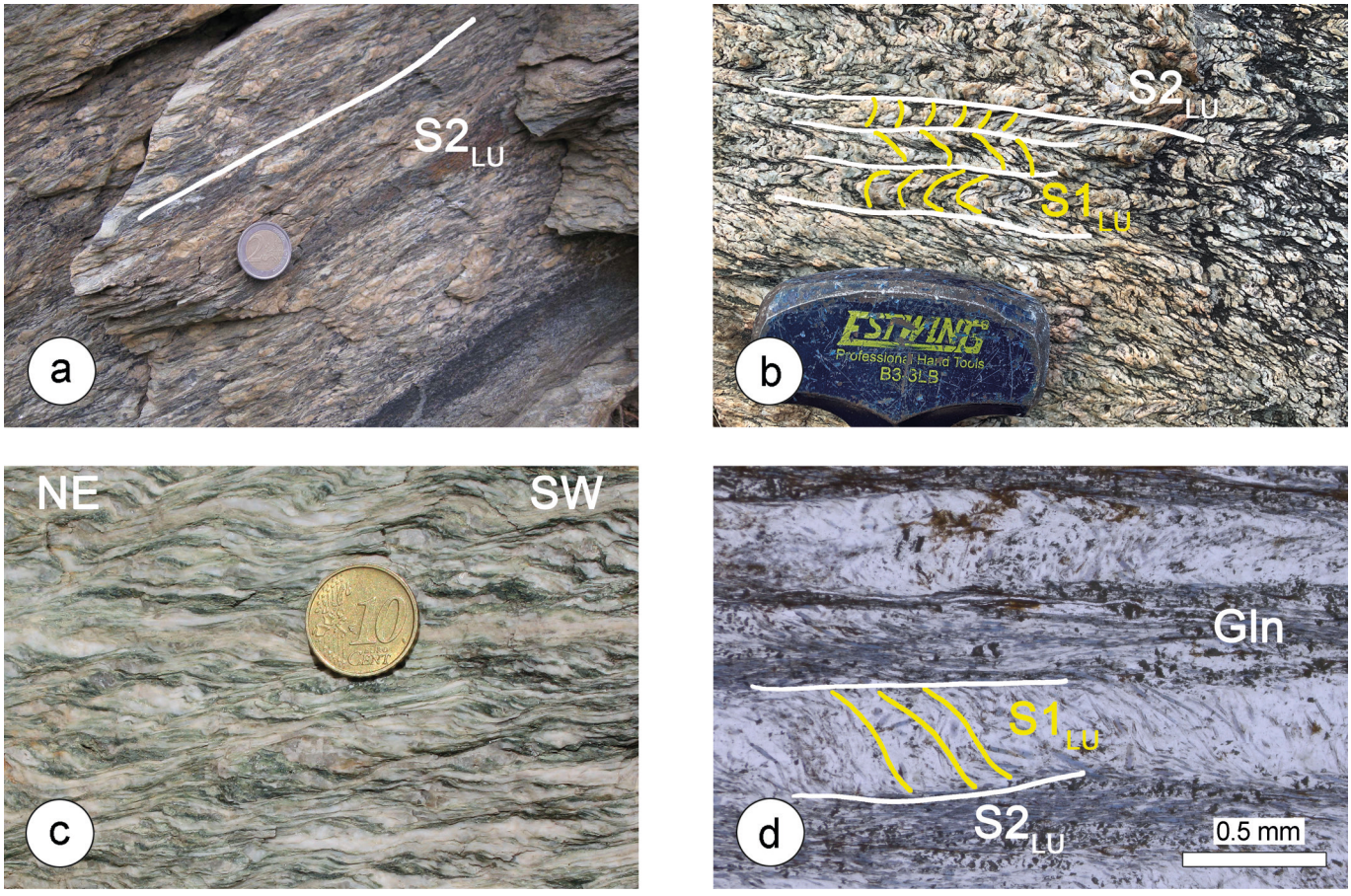

Figure 1.5 - Examples of meso- and microdeformation in the orthogneisses of the Tenda Massif along the East Tenda Shear Zone. (a) Mylonitic fabric. The attitude of the $S2_{LU}$ *foliation is indicated; (b)* $S1_{LU}$-$S2_{LU}$ foliations structural relationship within a $F2_{LU}$ *hinge zone; (c)* S-C' fabric suggest a top-to-NE sense of shear, and (d) $S2_{LU}$ foliation marked by the dynamic recrystallization of glaucophane (Gln) and albite. Relics of the $S1_{LU}$ foliation preserved in microlithons are also observed (parallel nicols).

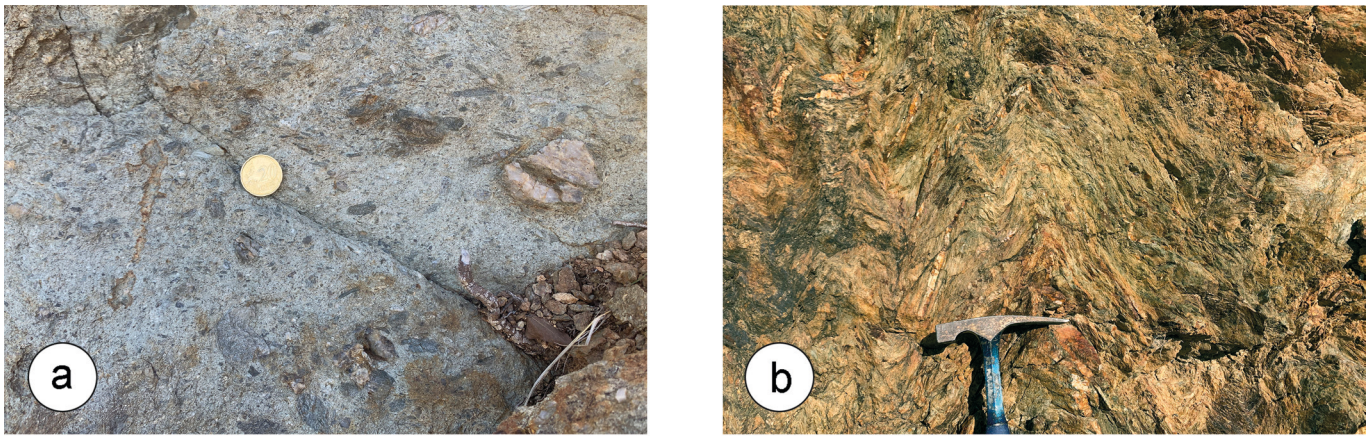

Fig. 1.6 - Bocca di Vezzu Stop 1.11, transition from Panafrican basement rocks to Carboniferous-Permian sequence. (a) Late Carboniferous-Early Permian metaconglomerates (b) Panafrican Micaschists (cf. Roches Brunes Fm. Auctt.).

This transition is clearly visible along the road cut, where metavolcanoclastics and metavolcanics pass to metadacites and metarhyodacites interspersed with volcaniclastics. The geochemistry of the metavolcanic rocks indicates a calc-alkaline affinity. Rossi et al. (1994) obtained ages of 291 ±2 Ma and 283 ±3 Ma (Early Permian) for the metadacites. The metavolcaniclastics and metavolcanics are intercalated with metarkoses of rhyolite composition, as well as levels of metaconglomerates consisting of volcanic rock fragments and Qtz in a volcaniclastic matrix. The metavolcanics and metavolcanoclastics lie over metaconglomerates which are probably of Late Carboniferous-Early Permian age (Fig. 1.6a). These metaconglomerates, which are about 30-40 m thick, contain fragments of micaschists and Qtz veins in an abundant matrix of arkose metarenites.

The metaconglomerates, in turn, lie unconformably over the micaschists (Fig. 1.6b). These metamorphic rocks consist of polydeformed and polymetamorphic metapelites and metasiltstones, and bodies of amphibolites have also been recognized. Rossi et al. (2001) obtained a U-Pb age of 2.28 ±0.09 Ga. The amphibolites, in turn, provide an Sm-Nd model age of 600 Ma (Rossi et al., 1994). These micaschists correspond to the so-called Roches Brunes Fm. This sequence is intersected by dikes of alkaline microgranite granitoids. After this, we continue to **Î**le Rousse.

DAY 2: A DAY WITHIN THE UPPER UNITS OF THE BALAGNE NAPPE

The second day focuses on the Balagne Nappe (Fig. 2.1) and its relationships with the LU and Hercynian Corsica. This nappe, which extends over an area of around 100 km^2 to the SE of Île Rousse, represents, like all the already described UU, a fragment of the Ligurian-Piedmont Oceanic Basin that escaped *HP* metamorphism. The Balagne Nappe can be correlated with the Serra Debbione and Pineto Units, which crop out to the E and S of the Balagne area, respectively.

The Balagne Nappe crops out at the core of a large-scale open synform with an N-S axis that occupy the entire Balagne area and that deforms a stack of units that is juxtaposed directly on the Hercynian Corsica. (Fig. 2.2). To the W and S, the Balagne Nappe is thrust over Hercynian Corsica, here represented by the Variscan basement and its Eocene sedimentary cover (Nardi, 1968a; Nardi et al., 1978; Dallan and Nardi, 1984; Durand-Delga, 1984; Rossi et al., 2001; Marroni and Pandolfi, 2003). The Parautochthonous Units, mainly represented by the Palasca Unit, occur between the Variscan basement and the Balagne Nappe. To the east, the main NNW-SSE-striking Ostriconi fault separates the nappe from the N-S-trending Tenda antiform, where the Variscan basement is exposed.

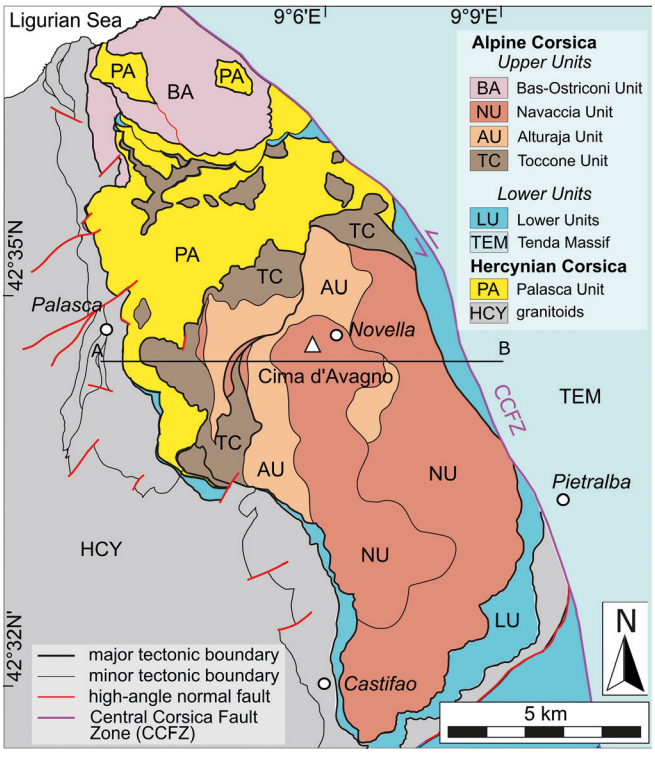

Fig. 2.1 - Tectonic sketch map of the Balagne area (modified from Marroni and Pandolfi, 2003). The trace of the cross-section shown in Figure 2.2 is indicated as A-B. Key: HCY: Hercynian Corsica; PA: Palasca Unit; TEM: Tenda Massif; LU: Lower Units; TC: Toccone Unit; NU: Navaccia Unit; AU: Alturaja Unit; BA: Bas-Ostriconi Unit.

DAY 2 STOPS DESCRIPTION

ITINERARY: Île Rousse, Piana, San Colombano, Belgodere, Ostriconi, Île Rousse.

STOP 2.1 - Carnispola Bridge: TRANSITION FROM GABBROS TO BASALTS (42°30'47.54"N 9°08'55.76"E)

From *Île* Rousse, we head back towards Ponte Leccia. Before reaching Ponte Leccia, we take the road RT301 (old RN197) towards Piana. At the Carnispola bridge, the left bank of the Tartagine River exposes a section representative of the base of the basalts of the Balagne ophiolite sequence. Despite being affected by low- and high-angle brittle faults, it is possible to observe a transition from 5 m-thick ophiolitic breccia to pillow lava basalts. The breccia comprises Mg-gabbros, Fe-gabbros, and Fe-basalts, which are intersected by veinlets of plagiogranites fragments in a fine-grained matrix (Fig. 2.3a). Plagiogranites yielded U-Pb zircon ages of 169 ±3 Ma (Rossi et al., 2002). In thin section (Fig. 2.3b), the matrix displays fragments of gabbros, plagiogranites and basalts. However, a typological study of the zircon population in the breccia matrix using Pupin's (1980) classification indicates that the population is bimodal. Some grains are characteristic of zircons derived from gabbro and trondhjemite, while others are typical of continental granites. This finding suggests that this breccia, which was deposited in an oceanic environment prior to basaltic lava flows, was fed by both oceanic and continental material. In the southern corner of the outcrop, coarse-grained Cpx and Pl bearing gabbro are exposed. This outcrop has been interpreted as the stratigraphic top of the gabbroic basement (Rossi et al., 2002).

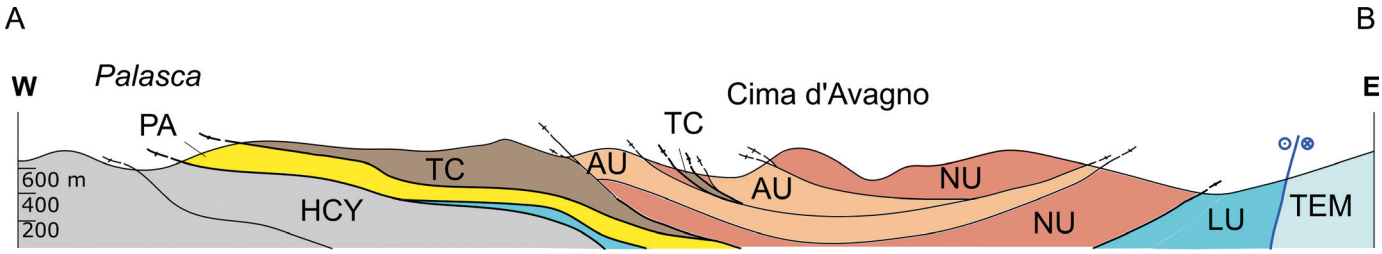

Fig. 2.2 - Geological cross-section of the Balagne area (the location of the trace A-B is shown in Fig. 2.1). Key: HCY: Hercynian Corsica; PA: Palasca Unit; TEM: Tenda Massif; LU: Lower Units; TC: Toccone Unit; NU: Navaccia Unit; AU: Alturaja Unit (modified after Marroni and Pandolfi, 2003).

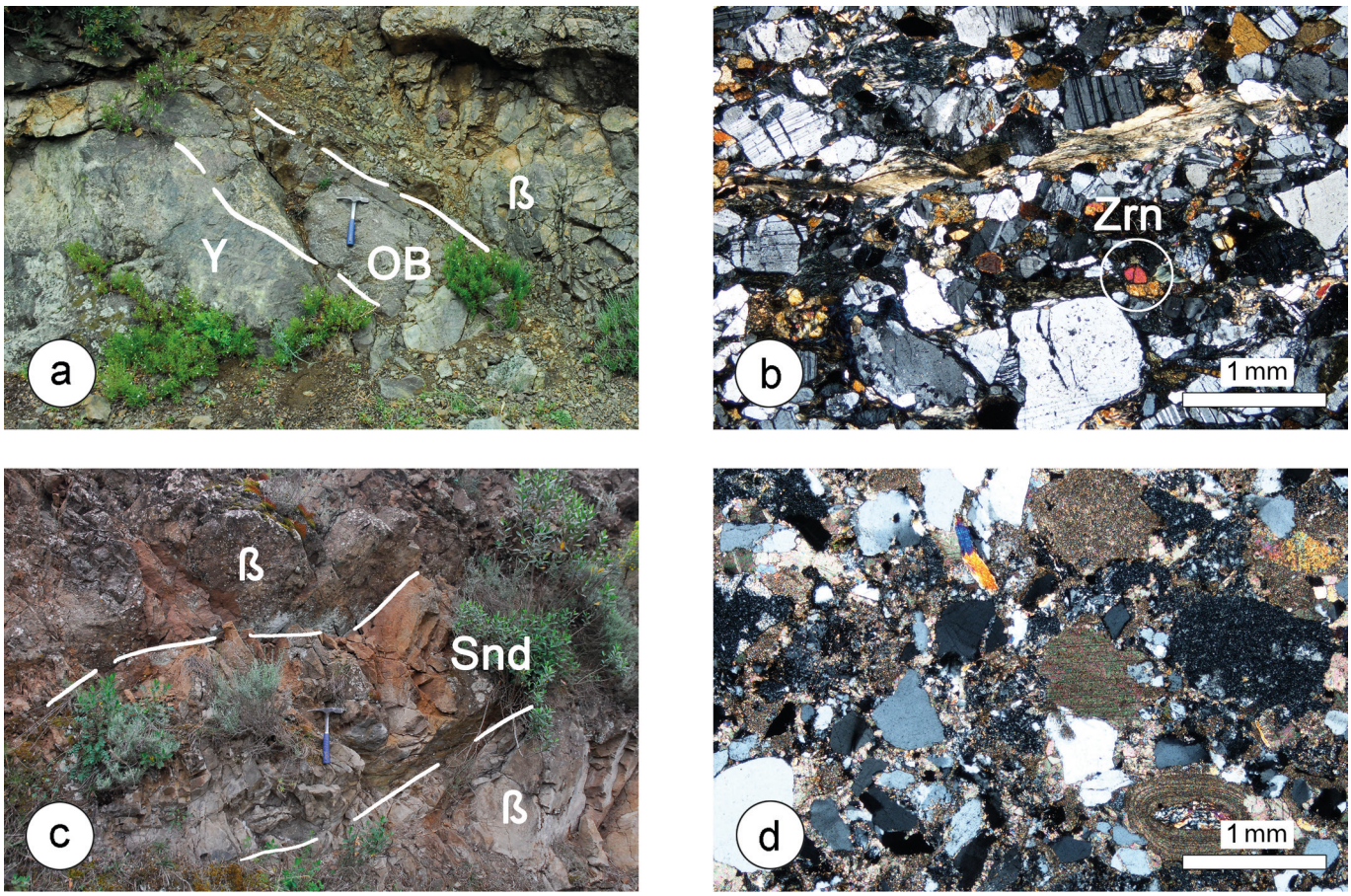

Fig. 2.3 - Carnispola Bridge: (a) field occurrence of the transition from gabbros (Y) to basalt (β) in the Balagne ophiolite sequence. The transition is characterized by the presence of ophiolitic breccia (OB). The thin section of this fine-grained breccias (b) shows the presence of zircon (Zrn) fragments, CPL. Piana di Castifao, (c) arenite intercalations (Snd) sandwiched between two pillow basalts lava (b). (d) The coarse-grained arenites show a mixed (carbonatic-siliciclastic) composition, CPL.

STOP 2.2 - Piana: PILLOW LAVA BASALTS (42°30'53.0"N 9°07'32.6"E)

We continue along the road towards Piana. At the junction with the road to Moltifao, there is a well-exposed section of pillow lava basalts with sub-horizontal orientation and clear normal polarity. Structures such as pipe vesicles filled with glassy material can be seen. These basalts have chemical compositions that fall along the N-MORB-OIB array, closer to N-MORB (Marroni et al., submitted). The co-variation of Th, Ta, Nb, Hf, La, and Ce with Zr demonstrates that the Balagne basalts are enriched in incompatible elements relative to other N-MORB Alpine Corsica ophiolitic and metaophiolitic rocks. Saccani (2003) suggested that the basalts of the Balagne Nappe originated from a mantle source that was variably enriched by components derived from plumes, which were probably related to magmatic activity at the beginning of oceanic opening. In addition, Renna et al. (2018) highlight significant differences with the basalts from the Internal Ligurian Units, suggesting that the Balagne ophiolites originated at the margin of the oceanic basin.

STOP 2.3 - Piana di Castifao: ARENITE INTERCALATIONS IN PILLOW LAVA BASALTS (42°51'67.1.5"N 9°12'33.3"E)

We continue along the road towards Piana, a small village on the southwestern edge of the Balagne region. Along the D457 road near Piana di Castifao, about 50 m southeast of the Tartagine bridge a 3 m-thick layer of arenites intercalated with pillow lava basalts can be observed in the lower section of the basalts (Durand-Delga et al., 1997; Peybernès et al., 2001; Renna et al., 2017).

Along the roadcut, it is possible to observe the full thickness of the arenites, which exhibit graded bedding, as well as some mm-thick bands of black mica-bearing pelites (Fig. 2.3c). The coarse-grained arenites (Fig. 2.3d) contain mm-sized fragments of Qtz, carbonates, micaschists and, in the uppermost levels, basalts. Due to the presence of carbonate rocks, these arenites can be classified as mixed arenites. These arenites are characterized by minerals such as Zrn, Py, Ca-Amp, Bt, Chl, Grt (Alm and Adr), Cr-Spl, Hem, Tur, and Ap. Zrn derived from magnesian-potassic, calc-alkaline granites. According to Pupin's diagram (1980), the plotted field overlaps that of zircons from calc-alkaline granites of the Corsican batholith. This interpretation is confirmed by U–Pb zircon geochronology, which revealed a 280 Ma dominant component. (Renna et al., 2018). The top of the arenites is represented by a thick layer of pillow lava basalts commonly with a variolitic rim.

STOP 2.4 - Old Road Ponte Leccia-Île Rousse: BASALTS-SEDIMENTARY COVER TRANSITION (42°32'51.1"N 9°07'25.1"E)

From Stop 2.3, we retrace our steps along the old RN197 road to the railway bridge. The roadcuts along the way offers impressive examples of pillow lava intruded by sills of dolerite. We stop at km 59, where the transition from basalts to its sedimentary cover is clearly visible along the railway track.

There is a well-exposed sequence of pillow lava basalts along the road. The pillow lavas generally exhibit normal polarity with a dip towards the NW. Along the railway track, the pillow lava basalts are topped by pillow breccias, which show a transition to a sedimentary cover (Fig. 2.4). The sedimentary succession begins with 2 m of black, siliceous shales, followed by the radiolarites. This formation consists of 10 m of red radiolarites beds interspersed with green and white beds, which are probably silicified carbonates. Callovian to Early Kimmeridgian radiolarian assemblages have been found within these radiolarites (Conti et al., 1985; de Wever et al., 1987).

Radiolarites are in turn topped by an alternation of 6 m-thick carbonate, pelites and radiolarites beds representing the transition to the Calpionella Limestone. At this level, *Lamellaptychus gr. beyrichi* (Kimmeridgian-Early Berriasian) has been found in the radiolarites beds. The Calpionella Limestone, represented by marly limestones and marls, occurs at the top with a thickness of about 5 m and has yielded calpionellids (*Calpionella elliptica and Calpionellopsis oblonga*) of Middle to Upper Berriasian age. The succession is topped by thick level of pelites, which probably represent the base of the San Martino Fm.

STOP 2.5 - Road to Novella: SAN MARTINO FM. AND LYDIENNE FLYSCH (42°32'51.1"N 9°07'25.1"E)

After Stop 2.4, we follow the old RN197 road until we reach the junction with the road to Novella. We stop by a railway cut along this road and we walk along the railway where the transition from the San Martino Fm. to the Lydienne Flysch can be observed at the core of a $D1_{UU}$ anticline of the San Martino Fm., which was refolded during the second folding phase. The San Martino Fm. succession, which is up to 60 m-thick, consists of fine-grained limestones (calcilutites and rare fine calc-siltstones) alternating with marlstones, shales, and minor siliciclastic, fine-grained turbidites.

The sedimentological analyses indicate the presence of pure and subordinate traction, as well as fall-out structures such as plane and convolute laminae and ripples, suggesting that they originated from low-density turbidity currents (F9a facies of Mutti, 1992). The Te Bouma interval consists of marlstones and silty marlstones, while carbonate-free shales represent hemipelagic background sedimentation. The calcilutites consist of calcareous nannofossils-bearing micritic mudstones with subordinate amounts of monocrystalline Qtz, Fsp and undetermined phyllosilicate fragments. Pervasive Cal recrystallisation and scattered silicification affect both the limestones and marlstones beds. Furthermore, widespread silicification can replace over 50% of the original carbonate framework in the calcilutites, while scattered authigenic Qtz (less than 5% of the original framework) affects the marlstones.

The upper part of the San Martino Fm. is characterized by the presence of siliciclastic turbidites, which consist of Qtz-rich siltstones and shales. The presence of these beds indicates a gradual transition to the overlying Lydienne Flysch.

The Lydienne Flysch (Fig. 2.5a) consists of thin-bedded turbidites (Fig. 2.5b) ranging in grain size from medium arenites to siltstones, which are interbedded with lenticular (Fig. 2.5c), coarse-grained beds characterized by megaripples and cross-stratification (F6+F9 facies of Mutti, 1992). In the Lydienne Flysch, coeval calcareous debris is almost absent, and the beds have a mixed siliciclastic-carbonate composition. By comparing the available data with that from the ophiolite sedimentary cover of the Northern Apennines, the San Martino Fm. has been correlated with the lower part of the Palombini Shale Fm. In this context, the Lydienne Flysch can be considered time-equivalent to the upper part of the Palombini Shale Fm. This is corroborated by the presence of several medium- to coarse-grained beds with the same composition as the Lydienne Flysch (Pandolfi, 1997).

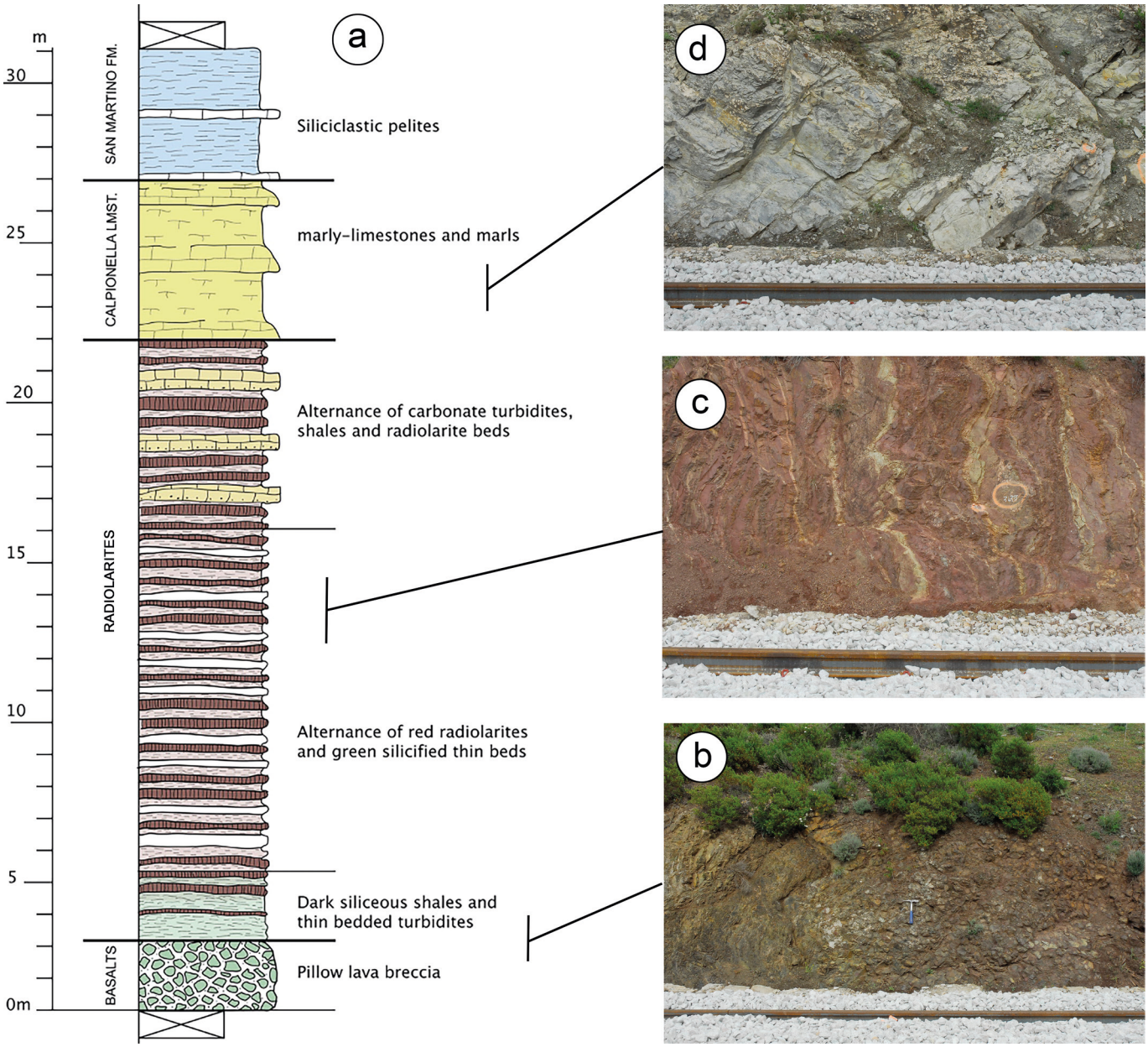

Fig. 2.4 - (a) Stratigraphic log of the transition from basalts to Calpionella Limestone along the railway track parallel to the RT301 (old RN197). Along the stratigraphic section the transition from Basalts (β) to Radiolarites (c) to Calpionella Limestone (d) is well exposed.

STOP 2.6 - Gare di Novella: NOVELLA SANDSTONE (42°34'51.15"N 9°06'38.29"E)

We continue along the road RN197 until we reach the Novella railway station. Along the railway cut, a nearly complete section of the Novella Sandstone (up to 250 m-thick) is exposed. Detailed stratigraphic sections show that the Novella Sandstone is stacked in an overall upward trend of coarsening and thickening. The beds exhibit limited lateral continuity, characterized by a gentle lenticular shape. The Novella Sandstone is characterized by beds ranging in thickness from 0.5 to 3 m and in grain size from coarse arenites to fine rudites. The pelitic interval is generally lacking, or if present, the sand-to-shale ratio is greater than 10. The Novella Sandstone was formed through processes involving erosion, as evidenced by bottom sedimentary structures such as scours, amalgamated beds and groove casts, as well as the widespread presence of intraformational clasts. Several beds are characterized by poor sorting and a lack of internal organization, as well as the presence of crudely bedded material, rare fluid escape features, crossbedding, and traction carpets.

As in the Lydienne Flysch, abrupt changes in grain size are common, with coarse-grained beds grading into incomplete Bouma sequences, which are generally represented by centimetric siltite Te Bouma intervals. According to these data, the deposits recognized in the Novella Sandstone are mainly produced by gravelly, high-density turbidity currents, and can generally be referred to the F4 and F5, and subordinate F5+F9, facies of Mutti (1992).

A modal analysis was performed on twenty thin sections from the Lydienne Flysch, the Toccone Breccia, and the Novella Sandstone (Bracciali et al., 2007). No differences in framework composition were recognized among the arenites from the Lydienne Flysch, the Toccone Breccia, and the Novella Sandstone. These sublitharenites and subarkoses

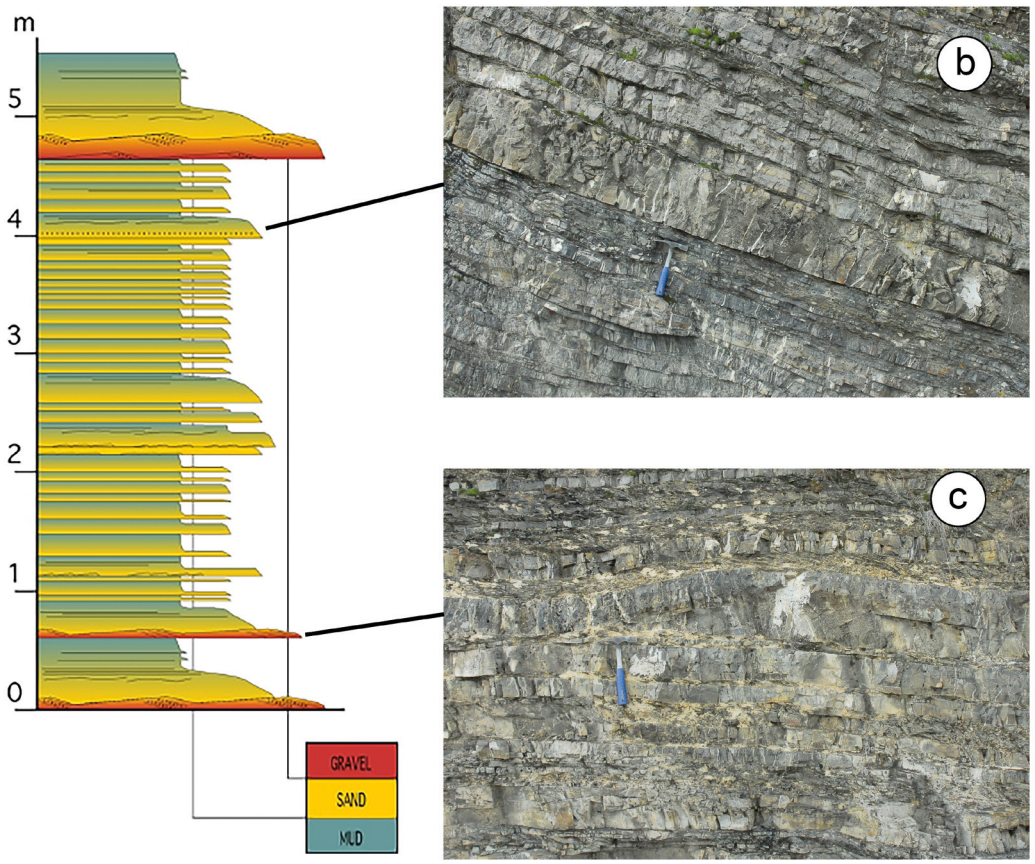

Fig. 2.5 - Detailed stratigraphic log of 5 m of Lydienne Flysch (a). The typical thin-bedded turbidites (b) showing megaripple and cross-stratification (c) can be observed in the two pictures.

($Q_{40}F_{27}L_{33}$, Fig. 2.6) are characterized by a mixed siliciclastic-carbonate framework composition (NCE78NCI+CI1CE21, Fig. 2.6), as well as a volcaniclastic composition of fine-grained lithic fragments ($Lm_{28}Lv_{70}Ls_{<1}$, Fig. 2.6). The extrabasinal siliciclastic framework is characterized by the widespread presence of moncrystalline and polycrystalline Qtz (31 ± 14%), Pl (7 ± 3%) and K-Fsp (13 ± 3%). Lithic volcanic fragments are widespread (18 ± 9%) and include rhyolites and dacites fragments with porphyritic texture (Fig. 2.6). Intrusive-derived lithic fragments, such as granitoids, are widespread as coarse-grained rock fragments (7 ± 3%). Metamorphic rocks clasts include coarse-grained gneisses, fine-grained low-grade schists, micaschists and metaquartzites (fine-grained lithic fragments: 7 ±2%). Lithic sedimentary fragments (fine-grained arenites and siltstones) are scarce or absent. Ophiolite-derived fragments, such as serpentinites, gabbros, MOR basalts and radiolarites, have never been observed. Carbonate extrabasinal fragments represent a significant proportion of the total framework (21 ±11%). This group is represented by limestone fragments, which are generally composed of grainstones and mudstones.

STOP 2.7 - Road to Novella: DEFORMATION IN LYDIENNE FLYSCH (outcrop: 42°34'29.9"N 9°06'53.9"E)

We head back towards the RN197 road. Along the road, some of the deformation structures affecting the ophiolite sedimentary cover can be seen (Fig. 2.7). The outcrop is characterized by sub-isoclinal to isoclinal $F1_{UU}$ folds with strongly dipping $A1_{UU}$ axes and sub-vertical axial planes. Penetrative foliation related to the $A1_{UU}$ folds can only be observed in the thin pelites alternating with arenites. The $F1_{UU}$ folds show axes that are scattered across their axial plane. The $F1_{UU}$ folds are deformed by the $D3_{UU}$ deformation phase, which is characterized by gentle folds with a low-angle axial plane. Only a very sparse fracture cleavage is associated with these folds. According to Marroni and Pandolfi (2003), all the piles of tectonic units exposed in this area are deformed by $F3_{UU}$ folds. A few m from this outcrop, an example of an $F2_{UU}$ fold with a high-angle axial plane can be observed.

STOP 2.8 - San Colombano Hill: SECTION IN THE SAN COLOMBANO SUBUNIT (parking: 42°34'46.1"N 9°04'15.4"E)

We continue along the RN197 road, and we park at San Colombano pass, where there is a beautiful view of the coast from Île Rousse to Lozari. Between the San Colombano pass and Castle hill, along the east-west dirty road, the entire San Colombano Subunit is exposed, tectonically sandwiched between the Toccone and Alturaja Units (Fig. 2.8). This section comprises several slices bounded by brittle shear zones. The stratigraphic and structural features can be fully observed in each slice.

The first part of the section is occupied by the top of the Toccone Unit, represented by the Lydienne Flysch and Toccone Breccia, which are folded with the San Martino Fm. The Lydienne Flysch is here pervasively deformed with isoclinal folding. The Toccone Unit is topped by a slice of strongly deformed San Martino Fm. The boundary is a brittle shear zone with top-to-E kinematics (Di Rosa et al., 2025). Above the San Martino Fm., a slice including San Colombano Limestone (referred to in the figure as Calpionella Limestone) and Radiolarites occurs. Radiolarites does not crop out along the road. This outcrop, well known in geological literature as the Grand Rocher, is characterized by coarse-grained breccias in a carbonate matrix. Pebbles comprise igneous (intrusive and

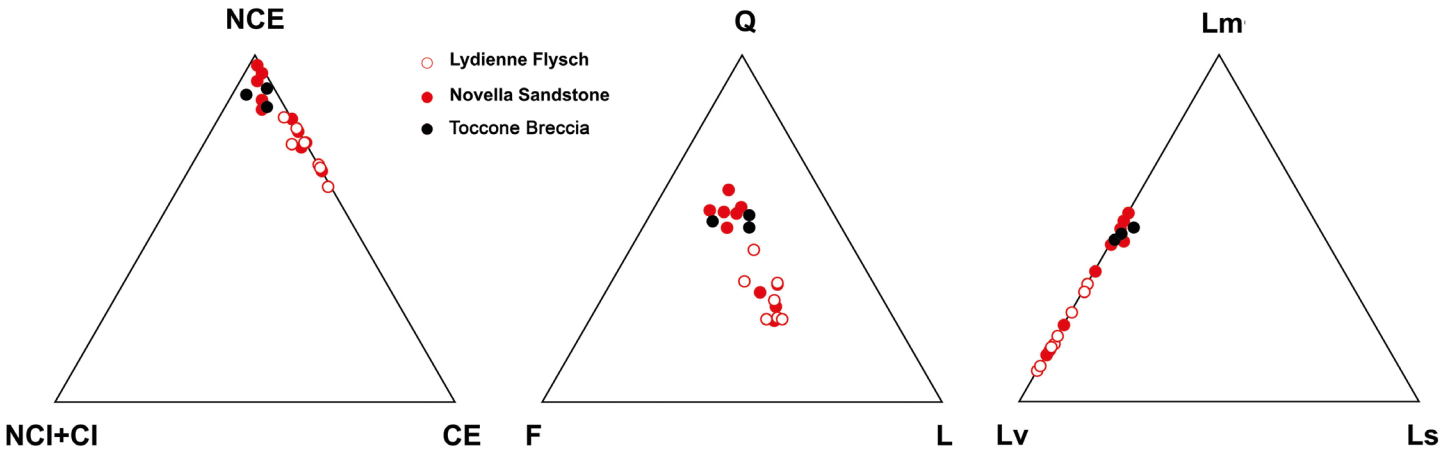

Fig. 2.6 - Modal compositional data of arenites from Balagne Nappe plotted on (NCE CI+NCI CE, Zuffa, 1980), (Q F L, Dickinson, 1985) and (Lm Lv Ls, Ingersoll and Suczek, 1979). Ternary plots show framework modes of arenites from Balagne Nappe (20 samples) from Lydienne Flysch, Toccone Breccia and Novella Sandstone.

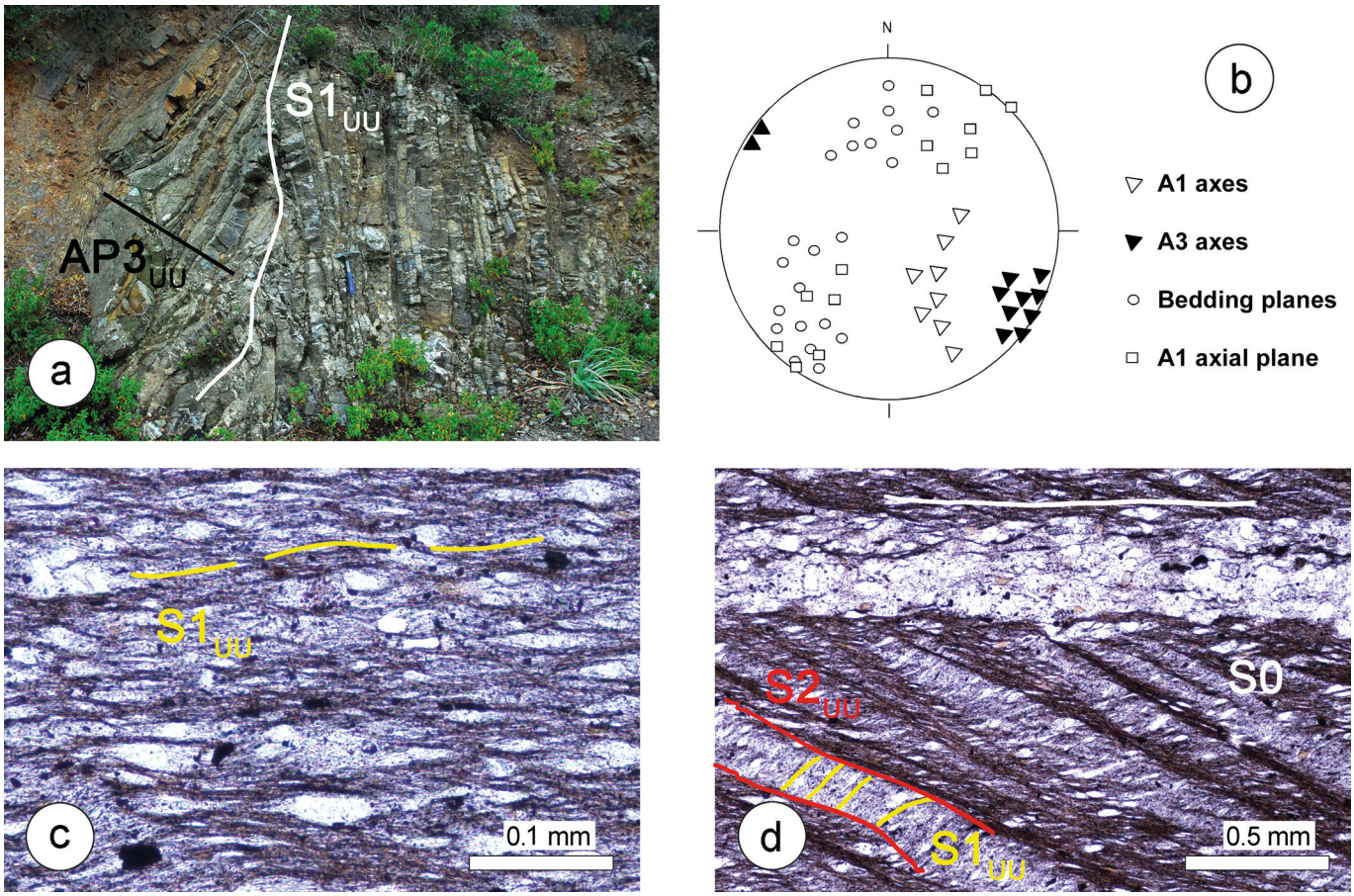

Fig. 2.7 - (a) $F1_{UU}$ phase isoclinal fold from the Lydienne Flysch. The axial-plane foliation ($S1_{UU}$) has been refolded by the $F3_{UU}$ folds, $AP3_{UU}$ indicates the Axial plane of the $F3_{UU}$ fold, hammer for scale. (b) Stereonet diagram for the outcrop shown in (a). Lower hemisphere, Schmidt projection. (c) $S1_{UU}$ foliation developed in a siltstone from Lydienne Flysch. (d) $S2_{UU}$ crenulation cleavage from San Martino Fm. In this thin section the bedding (S0) and the slaty cleavage related to the first folding phase ($S1_{UU}$) are also indicated.

volcanic), low-grade metamorphic, and carbonate sedimentary rocks. Intrusive rocks are represented by fine-grained syenogranites and monzogranites, while volcanic rocks comprise dacites and pyroclastic rhyolites containing varying amounts of Qtz. Clasts of aphyric to porphyritic basalts were also observed. Marroni et al. (2001) classified these rocks as transitional to tholeiitic within-plate basalts. Low-grade metamorphic pebbles, mainly Ms-bearing micaschists and Ms- and/or Bt-bearing gneisses, are common. Limestone pebbles are represented by carbonate platform-derived rocks, mainly grainstones and mudstones of Triassic and Jurassic age. The third tectonic slice cropping out in the San Colombano hill

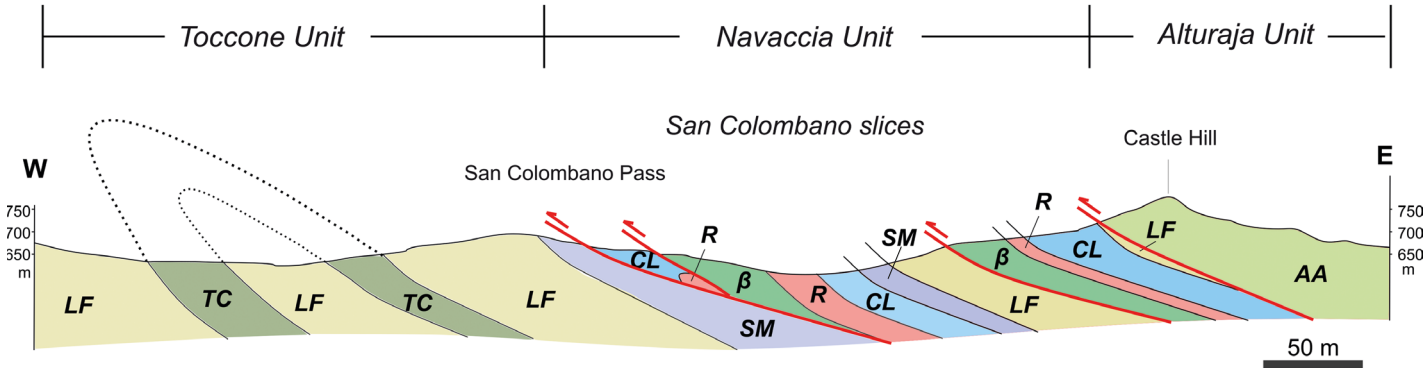

Fig. 2.8 - Geological cross-section of the San Colombano area. LF: Lydienne Flysch (late Hauterivian/Early Barremian/Early Turonian); TC: Toccone Breccia (late Barremian-Middle Aptian); SM: San Martino Fm. (Early Berriasian-Late Hauterivian/Early Barremian); CL: Calpionella Limestone (Tithonian-Early Berriasian); b: pillow basalts (Middle Jurassic); R: Radiolarites (Callovian-Kimmeridgian); AA: Alturaja Fm. (Late Barremian-Middle Aptian).

shows a complete succession from basalts to Lydienne Flysch and Toccone Breccia. The pillow lava basalts, characterized by pipe vesicles filled with carbonates, are topped by Chert, Calpionella Limestone and San Martino Fm., that transitions upward to the Lydienne Flysch. The next slice consists of Chert, which can be observed in an attractive outcrop characterized by sub-isoclinal folds. At the top is a slice of Lydienne Flysch. Finally, the uppermost part of the entire section is represented by the base of the Alturaja Unit, made, in this outcrop by a polymictic breccia of early to middle Aptian age, that is affected by brittle deformation close to a tectonic boundary.

STOP 2.9 - La Fuata pass: PANORAMA TOWARDS THE PUNTA DI CORBAIOLA STRUCTURE

We return to the RN197 road and follow it for approximately 5 km until we reach the junction with the road to Piana. We stop at La Fuata pass. Here, the impressive Punta di Corbajola structure can be fully observed (Fig. 2.9). The structure deforms the rocks belonging to the Punta Corbajola Subunit of the Navaccia Unit and is a map-scale isoclinal syncline with Calpionella Limestone at its core that can be correlated with the $D1_{UU}$ phase. At the base of Punta di Corbajola, the interference of this structure with $F3_{UU}$, low angle axial plane folds can be seen. To the NW, this syncline is followed by an anticline with basalts at its core. The landscape morphology clearly shows the location of the thrust juxtaposing Punta Corbajola Subunit over the Toccone Unit.

STOP 2.10 - La Fuata Pass: THE METAMORPHIC VOLPARONE BRECCIA (42°32'51.85"N 9° 4'32.21"E)

We return to La Fuata pass and stop at an abandoned quarry to observe the metabreccias belonging to the LU (Malasoma and Marroni, 2007). These are deformed and metamorphosed continental units located at the boundary between Hercynian and Alpine Corsica. These metabreccias are referred to as Volparone Breccia by Marroni et al. (2001) and have a thickness ranging from 10 to 70 m. The deformed clasts are mainly metagranites, metarhyolites, micaschists, marbles and mafic rocks (Fig. 2.10a,b).

Clasts are set in a foliated matrix, which shows evidence of being deformed by three folding phases. The clasts were significantly deformed during the initial deformation phase, characterized by a substantial amount of finite strain. Based on their petrographic and geochemical features, the mafic rocks are transitional to tholeiitic within-plate basalts (Marroni et al., 2001). Data on the metamorphism indicate that the first deformation phase occurred under *HP-LT* conditions of 1.15 and 1.05 GPa and 280–300 °C (Di Rosa et al., 2025). The lithological, deformational, and metamorphic features allow to correlate these metabreccias with those cropping out in the Corte area.

STOP 2.11 - La Fuata Hill: RELATIONSHIPS BETWEEN BASALTS AND CONTINENTAL-DERIVED CONGLOMERATES (45°55'52.9"N 9°08'35.6"E)

From the abandoned quarry, we walk east of La Fuata pass towards Cima Corbajola. We cross the tectonic boundary between the LU, represented by the Volparone Breccia, and the Toccone Unit, here represented by alternating layers of Toccone Breccia and Lydienne Flysch, with a basal section marked by thin limestone slices. The Toccone Unit, in turn, is thrust by the Corbajola Subunit of the Navaccia Unit, which is represented by basalts and their sedimentary cover. Along the path, the boundary between the Toccone Unit and the Corbajola Subunit is marked by a vertical shear zone cutting through the Toccone Breccia and the basalts. This geometry is the result of $D3_{UU}$ deformation, which affects all tectonic boundaries in the form of E-verging folds with gently dipping axial planes. At Cima Corbajola, the basalts are topped by a fine-grained conglomerate consisting of fragments derived from the continental crust, such as granitoids, limestones, rhyolites, and metamorphic rocks, set in an arenite matrix. These conglomerates are in turn topped by Jurassic limestones, which are deformed in a syncline with an N-S axis and a sub-horizontal axial plane. At the top of the hill, the overturned flank of this structure crops out, with the limestones topped by the conglomerates. This structure is bounded by an internal thrust within the Punta Corbajola Subunit, which is part of the anticline of basalts that was previously observed in the panoramic view. Along the overturned flank of this structure, pillow lava basalts overlie a coarse-grained, clast-supported conglomerates (F3 facies according to Mutti, 1992). The stratigraphic relationships between the basalts and the conglomerates can easily be observed along the cliff. The conglomerate clasts comprise granitoids, volcanic rocks (mainly dacites and rhyolites), low-grade metamorphic pebbles (micaschists and Ms-/Bt- bearing gneisses) and limestone pebbles (rocks derived from carbonate platforms, mainly grainstones and mudstones of Triassic and Jurassic age). Moreover, intrabasinal pebbles of pillow lava basalts, as well as soft clasts of red cherts and siliceous shales, can be identified. The presence of these clasts highlights the severe erosion and post-radiolarites emplacement

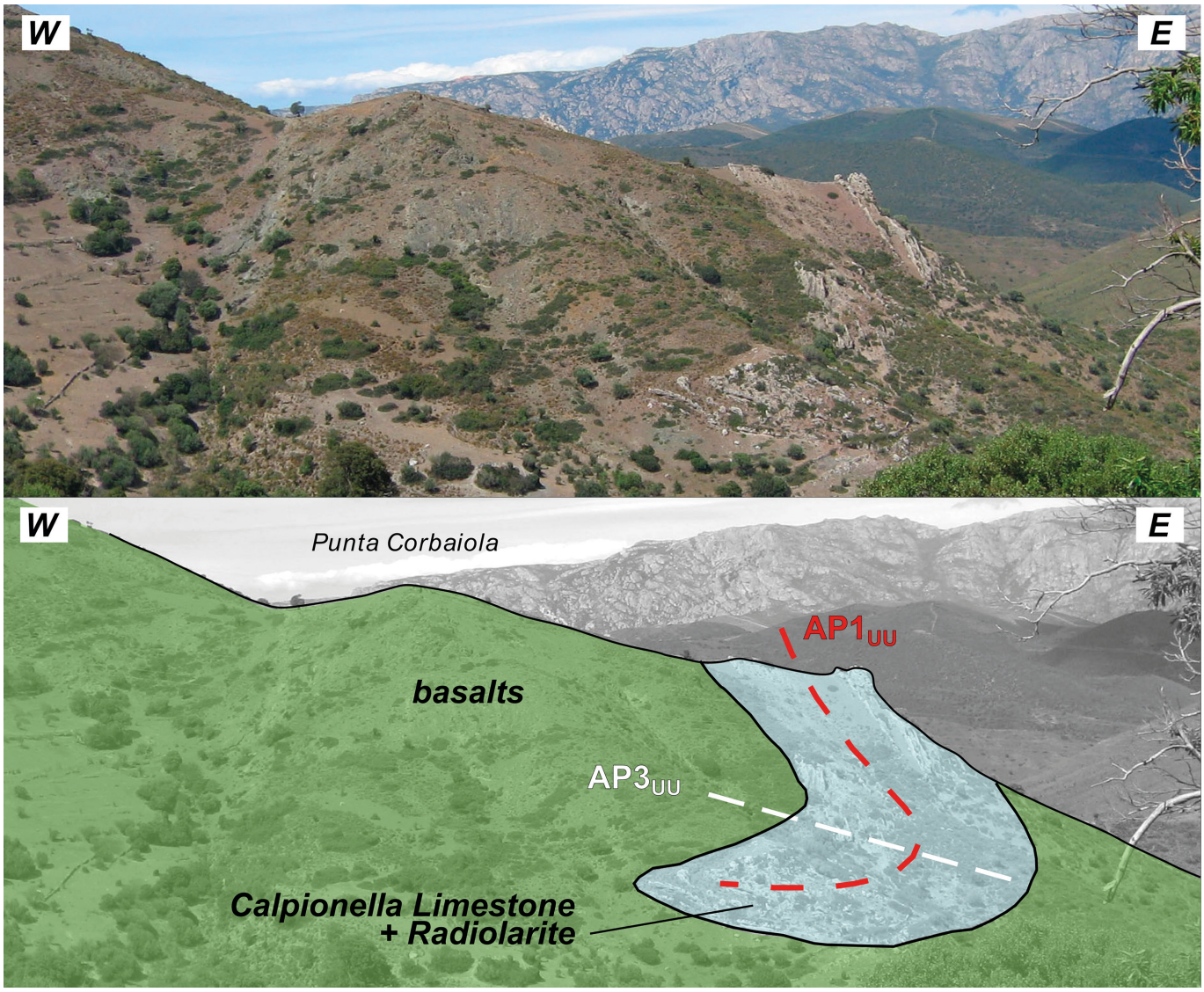

Fig. 2.9 - Panorama from La Fuata toward the Punta Corbaiola structure. $AP1_{UU}$: Axial plane of $F1_{UU}$ fold, $AP3_{UU}$: axial plane of $F3_{UU}$ folds.

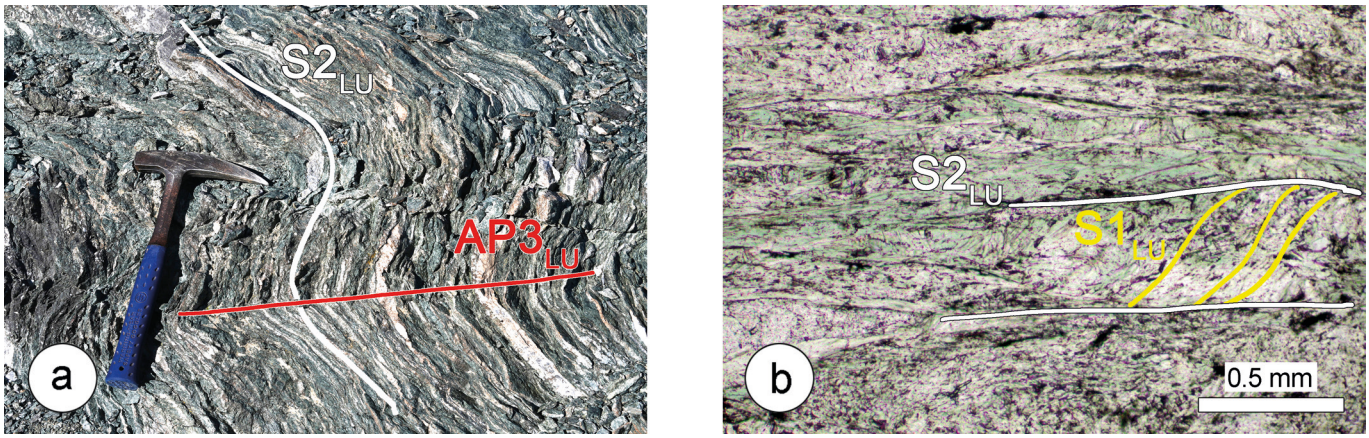

Fig. 2.10 - Metamorphic Volparone Breccia near La Fuata Pass. (a) Field occurrence of the Volparone Breccia. The main foliation ($S2_{LU}$) is refolded by the late $D3_{LU}$ phase (the axial plane $AP3_{LU}$ is indicated). (b) In thin section relics of the first folding phase foliation ($S1_{LU}$) can be recognized inside the S2 foliation ($S2_{LU}$).

of these deposits, which clearly indicate that this portion of oceanic crust was close to the continental margin.

STOP 2.12 - old Road Ponte Leccia - Île Rousse: THE SEDIMENTARY COVER OF THE HERCYNIAN BASEMENT (45°57'98.3"N 9°04'59.6"E)

From La Fuata pass, we head back towards the RN197 road, which we follow until we reach the coast. A well-exposed section of the sedimentary cover of the Variscan basement of Hercynian Corsica can be observed along the roadcut before reaching the junction for Palasca. The base of this cover comprises Middle Eocene polymictic conglomerates containing pebbles of all the lithologies that characterize the Hercynian basement. These conglomerates are topped by a thick layer of nummulite-bearing limestones of Middle Eocene age. Huge nummulites can be seen in the stones in the wall alongside the road. The conglomerates transition to Middle to Late Eocene (?) Shaly Flysch, which is characterized by a highly deformed alternation of shales and fine-grained arenites. At this point, the sedimentary succession of the Hercynian basement is interrupted by a W-verging thrust, as evidenced by the presence of conglomerates overlying the nummulite-bearing limestones. This thrust can be observed at the outcrop on the second bend of the road. The Shaly Flysch is characterized by a complex deformation pattern consisting of three superposed phases of deformation. It is overthrust by the Palasca Unit, which belongs to the Parautochthonous Units (Nardi et al., 1978). This unit is represented by a thick succession of well-bedded siliciclastic turbidites of Middle Eocene age known as the Annunciata Fm. (Durand-Delga, 1984). The boundary between the Palasca Unit and the Hercynian basement sedimentary cover is marked by slices of metagranitoids, metadolostones and metalimestones. Along the road cut, an example of Triassic dolomitic metalimestones can be observed. These slices can probably be regarded as belonging to the Fuata-Pedani Unit.

STOP 2.13 - Guardiola Area: STRATIGRAPHIC AND STRUCTURAL FEATURES OF THE NARBINCO FLYSCH (42°39'23.9"N 9°03'19.5"E)

From Belgodere village, we reach the coast at Lozari. Along the roadcut, immediately after the large beach of Lozari and before the Ostriconi beach, a continuous outcrop of the Narbinco Flysch (see Flysch Calcareo by Nardi et al., 1978) is exposed. The Narbinco Flysch belongs to the Bas-Ostriconi Unit of the UU. This unit comprises Late Cretaceous carbonate turbidites (Narbinco Flysch), which are associated with coarse-grained polymictic conglomerates (Cima Lo Caigo Conglomerate). The Narbinco Flysch consists of alternating layers of medium- to coarse-grained arenites and fine-grained rudites, as well as thick layers of marls and calcareous marls (Fig. 2.11a,b).

Lenticular coarse-grained beds (consisting of coarse sands and small pebbles) and megaripples can also be observed. The arenites from the Narbinco Flysch, characterized by a mixed siliciclastic-carbonatic composition, indicate a source area representing an upper continental crust domain. No ophiolitic or lower continental crust fragments were identified.

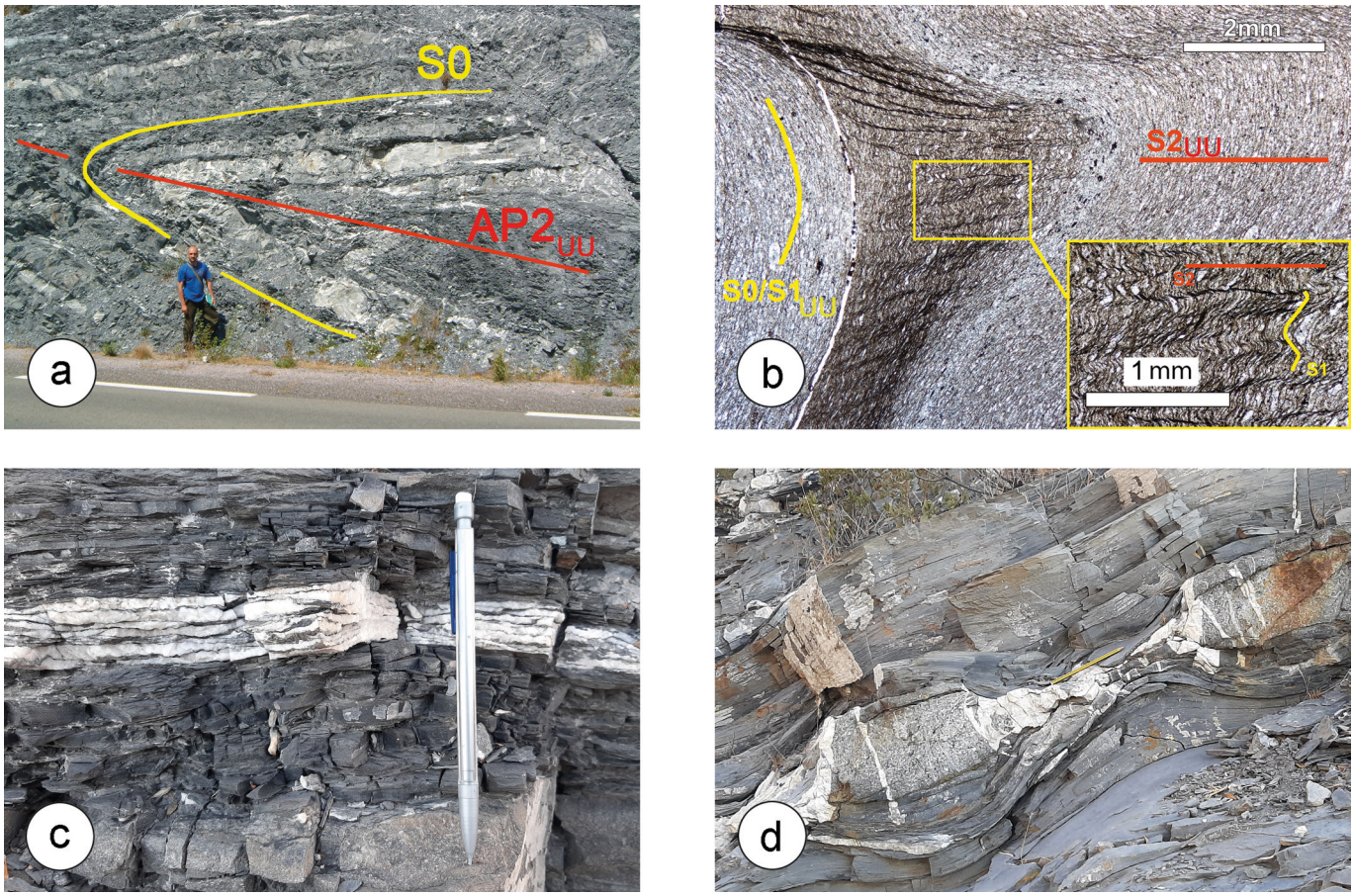

Fig. 2.11 - (a) Mesoscale isoclinal $F2_{UU}$ folds in the Narbinco Flysch. The bedding (S0) and the $AP2_{UU}$ axial plane are indicated. (b) microphotograph of the relationships between the $S1_{UU}$ and $S2_{UU}$ foliation in the hinge zone of the $F2_{UU}$ fold of Fig 2.11a. c) and (d) calcite-bearing veins showing different geometrical relationships with the bedding and the various geological structures.

This outcrop also allows the structural features resulting from a polyphase deformation history to be fully observed. In the roadcut, the most widespread structures are represented by tight $F2_{UU}$ folds with NW-SE trending axes and $S2_{UU}$ crenulation cleavage. The axial planes of the $F2_{UU}$ folds are folded by the gentle $F3_{UU}$ folds, which have sub-horizontal axial planes. Additionally, relics of an $S1_{UU}$ slaty cleavage characterized by aligned fine-grained phyllosilicates (Wm + Chl + Stp) and elongated Cal-Qtz-Ab aggregates can be found in the hinge zone of the $F2_{UU}$ folds.

The sedimentary section visible along the roadcut is pervaded by quartz- and calcite-bearing veins showing different geometrical relationships with the bedding and the various geological structures (Fig. 2.11c,d). Two types of veins can be found at very-low angle with bedding/S1 planes. They are cm-thick veins, with a long-strike continuity at the meter scale: i) mode I extension veins, localized at the shale/sandstone boundary with fibrous texture normal to vein wall and evidences of repeated crack-and-seal events; and ii) shear veins with fibrous texture, well visible slickenfibers and steps consistent with top-to-W shear, with a crack-and-seal texture defined by phyllosilicate inclusion bands subparallel to vein margins (Fig. 2.11c). Both these groups of veins are folded by F2 folds, as visible in Fig. 2.11a.

At high angle to bedding, localized in the coarser-grained beds two other systems of mineralization are visible (Fig. 2.11d). One system of quartz/calcite veins fills the neck space between boudins of coarse-grained layers, with cm-scale thickness in the range of competent layers with pinching shape, and mosaic to locally fibrous texture. A second system is characterized by thin veins (<1 mm to <5 cm) with sharp boundaries and organized in conjugate systems. They show fibrous textures with fibers oblique to normal to vein walls. Both these groups of veins sharply crosscut S1-parallel pressure solution seams are folded by F2 folds, together with bedding.

DAY 3: WALKING ACROSS THE HP METAMORPHIC OCEANIC CRUST OF THE INZECCA-LENTO AND MORTEDA-FARINOLE UNITS (SCHISTES LUSTRÉS COMPLEX)

Today, we complete our overview of the SL metaophiolites in the Golo Valley, along the western edge of Alpine Corsica. First, we will observe the Inzecca-Lento Unit, interpreted as a fragment of the Ligurian-Piedmont oceanic crust deformed under blueschist conditions during accretion at the Alpine prism at deep structural levels, and that formally belongs to the Upper Slices Complex of the SL, as defined in the introduction section (Fig. 3.1). Then, we will move to observe a well-exposed section of the Lower Slices Complex, which was not seen along the RD81 Bastia-Saint-Florent Road on the first day. As already mentioned, the Lower Slices Complex (see Morteda-Volpajola-Campitello Unit of Lahondère and Lahondère, 1988 and Brunet et al., 2000) also features a metaophiolitic section deformed by eclogite facies metamorphism, followed by retrograde blueschist metamorphism (Lahondère and Lahondère, 1988; Lahondère, 1991).

In the past 10 years, the Inzecca-Lento Unit has been the subject of extensive studies by the authors of this contribution. with the goal of better defining the stratigraphic and the structural arrangement of the units and place it in the frame of Alpine geodynamic evolution. It is therefore important for a better understanding of the stop of this day, to focus on the updated knowledge on the stratigraphic and structural features of this unit.

Despite polyphase deformation and associated HP metamorphism, it is possible to reconstruct the stratigraphic succession of the Inzecca-Lento Unit by integrating field data and comparing it with the less metamorphic succession of the Upper Units (UU) and Internal Ligurian Units of the Northern Apennines (Caron and Delcey, 1979; Durand-Delga, 1984; Padoa, 1999; Levi et al., 2007; De Cesari et al., 2024). The reconstructed succession (Fig. 3.2) comprises a metaophiolite

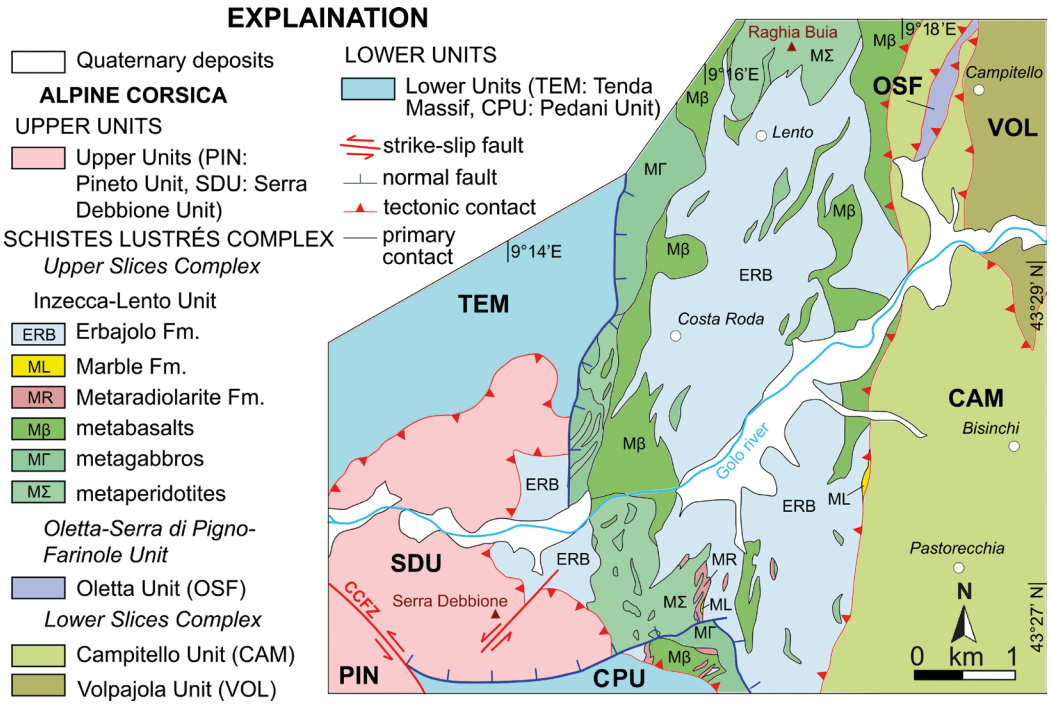

Fig. 3.1 - Geological map of the Inzecca-Lento Unit along the Golo valley (slightly modified after Levi et al., 2007).

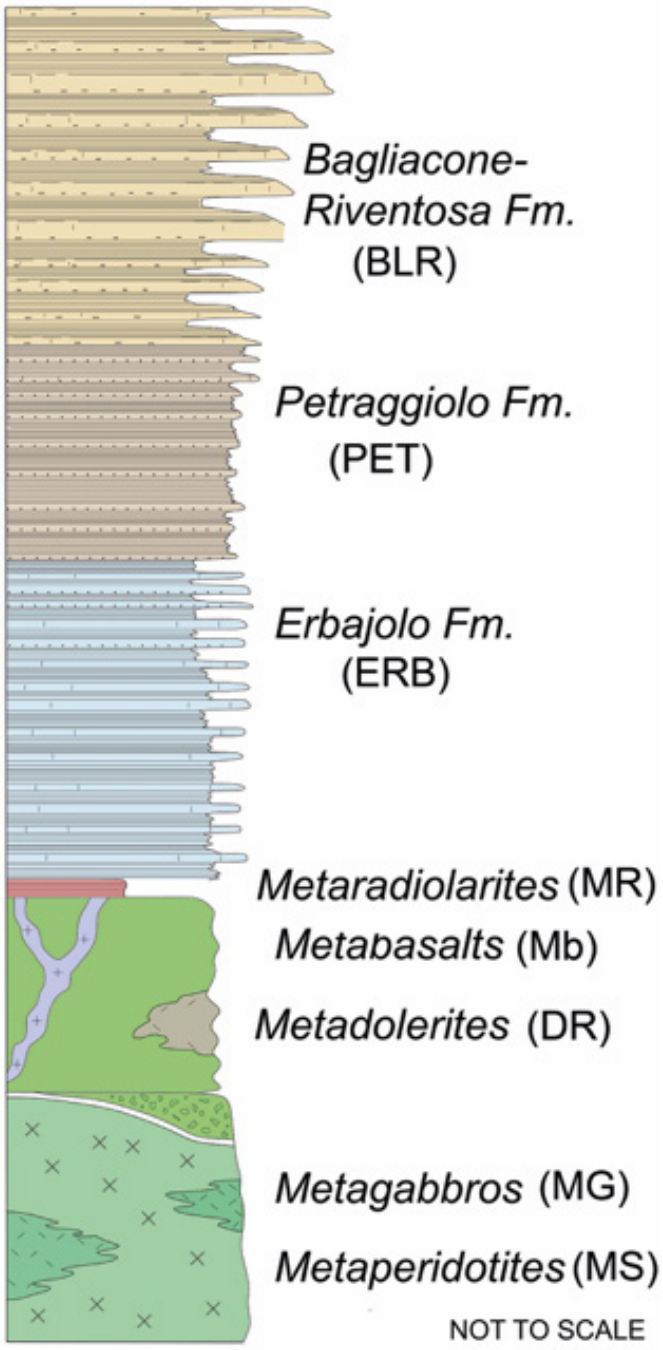

Fig. 3.2 - Stratigraphic log of the Inzecca-Lento Unit. MS: serpentinized peridotites; MG: metagabbros; Mb: metabasalts; DR: metadolerites; MR: metaradiolarites.; ERB: Erbajolo Fm.; PET: Petraggiolo Fm.; BLR: Bagliacone-Riventosa Fm. (slightly modified after De Cesari et al., 2024).

sequence dating from the Middle to Late Jurassic (Li et al., 2015) and a thick metasedimentary cover (Guelfi et al., 2025; 2026).

Specifically, the succession comprises the following, from bottom to top:

– a basement of metaperidotites, which are intruded by several bodies of metagabbros. The metaperidotites are generally highly sheared and serpentinized and are intersected by rare basaltic or rodingitized gabbroic dikes. In some outcrops, the serpentinites are topped by thin levels of metaophicalcites. The metagabbros range in composition from Mg- to Fe-gabbros, with subordinate metaplagiogranites (Ohnenstetter et al., 1976; Guelfi et al., 2025).
– a volcano-sedimentary complex ranging from few hundreds to few m in thickness, including massive or pillowed metabasalts with a MORB geochemical affinity (Saccani et al., 2008), which are generally associated with oceanic metabreccias. Locally, the volcanic sedimentary complex is absent, with the metasedimentary cover lying directly on top of the basement.

The metasedimentary cover includes, from bottom to top:

i) a thin succession of metaradiolarites (Metaradiolarite Fm., Late Jurassic).
ii) very thin and discontinuous sequences of marbles (Marble Fm., Early Cretaceous), whose protolith is likely represented by the Calpionella Limestone (Levi et al., 2007).
iii) the Cretaceous Erbajolo Fm. (Amaudric du Chaffaut et al., 1972), represented by a thick succession of dm-thick layers of micaschists and cm-thick layers of marbles alternated with massive, m-thick intervals of calcschists. This formation can be correlated with the weakly metamorphosed Palombini Shale Fm. of the Northern Apennines.
iv) near the village of Venaco, the Erbajolo Fm. is topped by the Petraggiolo and Bagliacone-Riventosa Fms., consisting of siliciclastic and carbonate metaturbidites (De Cesari et al., 2024).

The ophiolite sequence of the Inzecca-Lento Unit exhibits features like those of many other ophiolitic units in the Western Tethys, such as reduced basement thickness, absence of sheeted dikes, and the presence of ophicalcites and ophiolitic breccias (Marroni and Pandolfi, 2007). Similarly, the sedimentary cover succession can be compared with the Middle Jurassic to Early Paleocene sedimentary cover of the ophiolitic Internal Ligurian Units of the Northern Apennines (Abbate et al., 1980; Principi et al., 2004; Marroni et al., 2017) whereas the siliciclastic and carbonate metaturbidites that occur discontinuously on top of the Erbajolo Fm. may instead be correlated with the Val Lavagna Group of the Northern Apennines (Marroni and Pandolfi, 2001; Meneghini et al., 2020).

The Inzecca-Lento Unit shows a complex structural setting resulting from a polyphase deformation history, schematized in 4 deformation phases $D1_{SL}$ to $D4_{SL}$, and associated with development of a peak metamorphism under blueschist facies P-T conditions (Gibbons et al., 1986; Waters, 1990; Fournier et al., 1991; Caron, 1994; Daniel et al., 1996; Brunet et al., 2000; Martin et al., 2011; Vitale Brovarone et al., 2011; Vitale Brovarone and Herwartz, 2013; Rossetti et al., 2015). Despite the significant transposition associated with subsequent deformations (primarily the $D2_{SL}$ phase), evidence of the earliest deformation history can be found at both mesoscale and microscale in the low-strain domains of metabasalts, metagabbros, and marble bodies, where the impact of $D2_{SL}$-related deformations is generally weaker. Mesoscale $D1_{SL}$ structures are present in marble layers in the form of rare, generally rootless intrafolial isoclinal folds with acute hinge zones and strongly thinned limbs (Fig. 3.3a). The attitude of the $A1_{SL}$ axes cannot be clearly determined, because of the non-cylindrical nature of the $F1_{SL}$ folds.

An $S1_{SL}$ foliation, which is still well preserved in metagabbros and metabasalts, is the most penetrative structural element of this phase. It is associated with a $L1_{SL}$ mineral lineation trending NE to SW, marked by the preferred orientation of *HP* mineral grains, such as Ntr, Lws and Cr-Grt.

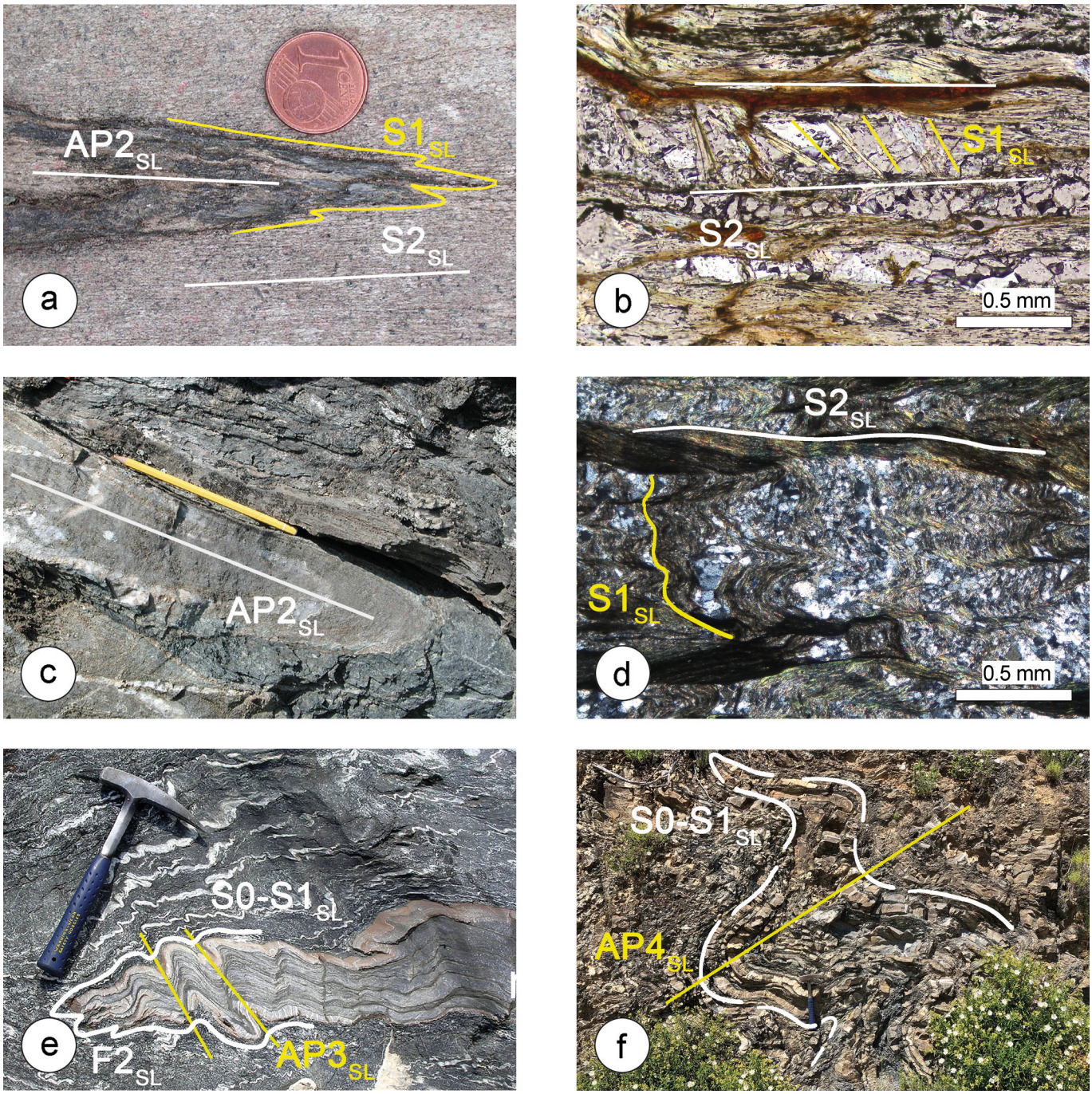

Fig. 3.3 - (a) Intrafolial $F1_{SL}$ fold in marble layer. (b) Microphotograph of the $S1_{SL}$ foliation within $S2_{SL}$ foliation in calcschists, PPL. (c) $F2_{SL}$ fold in the Erbajolo Fm., the white line indicates the axial planes ($AP2_{SL}$) of the $F2_{SL}$. (d) Microphotograph of the $S2_{SL}$ foliation with relics of the $S1_{SL}$ foliation within the microlithons, CPL. (e) $F3_{SL}$ folds deforming an isoclinal $F2_{SL}$ fold ($S0\text{-}S1_{SL}$ composite bedding-foliation surface is indicated). $PA2_{SL}$ and $PA3_{SL}$ indicate the axial planes of $F2_{SL}$ and $F3_{SL}$ folds. (f) $F4_{SL}$ folds with sub-horizontal axial planes indicate as $AP4_{SL}$ refold a composite $S0\text{-}S1_{SL}$ surface.

In metabasites, the $S1_{SL}$ foliation is preserved in $D2_{SL}$ microlithons as continuous schistosity (Passchier and Trouw, 2005). This schistosity is marked by the presence of oriented, elongated grains of Ntr, Grt, Qtz, and Ab in metabasalts and by Ntr, Lws, Ca-Grt and minor Qtz in metagabbros. An $S1_{SL}$ cleavage is rarely visible in the micaschists of the Erbajolo Fm. and is defined by a metamorphic mineral assemblage of Wm, Chl, Qtz and Cal. In the calcschists, the relic $S1_{SL}$ foliation can be identified in the hinge zone of the $F2_{SL}$ folds in the microlithons along the $S2_{SL}$ foliation (Fig. 3.3b).

The $S2_{SL}$ foliation in the Inzecca-Lento Unit is the primary planar anisotropy observed on a large scale in micaschists and calcschists. The $S2_{SL}$ foliation is a continuous foliation that often exhibits shear sense indicators in the form of σ-type tails around boudinaged Qtz veins. Once restored from subsequent deformations, the orientation of the $S2_{SL}$ foliation ranges from NE-SW in the northern areas to N-S and NW-SW in the southernmost area, while the sense of asymmetry of the kinematic indicators points to a top-to-NW sense of shear. In metabasalts, metagabbros and marbles the $S2_{SL}$ foliation is a crenulation cleavage.

In all the SL, the $S2_{SL}$ foliation is parallel to the axial plane

of $F2_{SL}$ isoclinal to sub-isoclinal and cylindrical folds. $F2_{SL}$ fold have similar geometry, subacute to rounded thickened hinge zones, and stretched limbs with boudinage, necking, and pinch-and-swell structures (Fig. 3.3c). The $A2_{SL}$ axes trend from NW-SE to NE-SW in different areas, whereas the plunge is always at a low angle. In thin sections, the $S2_{SL}$ foliation generally occurs as composite layering, with the metamorphic minerals that recrystallized during the $D2_{SL}$ phase superimposed on the pre-existing *HP* minerals. In the $F2_{SL}$ hinge zones only, the $S2_{SL}$ foliation occurs as crenulation cleavage. This is characterized by smooth cleavage domains showing a gradational to discrete transition to microlithons, where the $S1_{SL}$ foliation is visible (Fig. 3.3d). In the metabasalts, the $D2_{SL}$ deformation is associated with recrystallisation of Chl, Qtz, Ab, Ca-Na-Amp, Ep, and a small amount of Spl. Ca-Na-Amp typically occurs as pseudomorphs on previous Na-Amp. In the metagabbros, the $S2_{SL}$ foliation is characterized by Qtz ribbons and the growth of Chl and Wm around the pre-existing *HP* minerals.

In the metaradiolarites, the $S2_{SL}$ foliation can be classified as a disjunctive cleavage, with Wm-rich layers alternating with microlithons of Qtz grains. The Qtz grains, characterized by a planar shape fabric, show evidence of complete dynamic recrystallisation through grain boundary migration and subgrain rotation processes. In micaschists, the $S2_{SL}$ foliation is characterized by the development of Phl, Chl, Qtz, Ab and Cal. In these lithotypes, kinematic indicators, primarily in the form of porphyroclasts of Qtz and Amp, suggest a top-to-W sense of shear.

The third phase, $D3_{SL}$, includes $F3_{SL}$ folds and associated spaced $S3_{SL}$ axial-plane foliation, which overprints all $D2_{SL}$ structural elements. In metasedimentary rocks, the $F3_{SL}$ folds are nearly open and have rounded hinge zones. The $F3_{SL}$ folds always display marked asymmetric geometry, showing westward vergence (Fig. 3.3e). The $A3_{SL}$ axes trend approximately N-S with variable plunge angles, whereas the $AP3_{SL}$ axial planes are steeply inclined with predominantly N-S strikes. Generally, mesoscale $F3_{SL}$ folds are associated with $S3_{SL}$ foliation that can be classified as crenulation cleavage in micaschists and disjunctive cleavage in more competent lithotypes. At the microscale, the $S3_{SL}$ foliation is only recognized in the micaschists of the Erbajolo Fm., where it can be classified as a crenulation cleavage, characterized by smooth cleavage domains and a gradational transition to microlithons. In the micaschists, the fabric is characterized by displacement-controlled strain fringes developed around opaque minerals.

The last deformation phase $D4_{SL}$ produced gentle to open, long wavelength (up to several m), parallel $F4_{SL}$ folds, with sub-horizontal $PA4_{SL}$ axial planes (Fig. 3.3f). Locally, some minor-scale kink-folds occur. The $S4_{SL}$ foliation is a very spaced disjunctive cleavage, well-developed exclusively in the hinge zone of the $F4_{SL}$ folds. No metamorphic mineral assemblage related to the $D4_{SL}$ phase has been observed. This phase is characterized by widespread low-angle shear zones and S-C structures. After restoration from subsequent deformations, these structures display normal fault motion with a top-to-E sense of shear.

The available data (Fig. 3.4) for the Lento Unit along the Golo Valley (Levi et al., 2007) indicate that the peak metamorphic conditions were acquired during the $D1_{SL}$ deformation phase, with estimated parameters of $P = 0.80 \pm 0.20$ GPa and $T < 450$ °C (blueschist facies). De Cesari et al. (2024) estimated 245-275 °C and 1.2-1.0 GPa for the Inzecca-Lento Unit in the Venaco area, 230-250 °C and 1.0-0.8 GPa for the Petraggiolo Fm., and 280-300 °C and 1.2-1.0 GPa for the Bagliacone-Riventosa Fm. The $D2_{SL}$ phase, however, is associated with retrograde metamorphic assemblages developed at P-T conditions consistent with the blueschist-greenschist facies transition. The $D3_{SL}$ phase is finally characterized by the growth of very low-grade mineral assemblages such as Qtz + Cal + Chl +Wm.

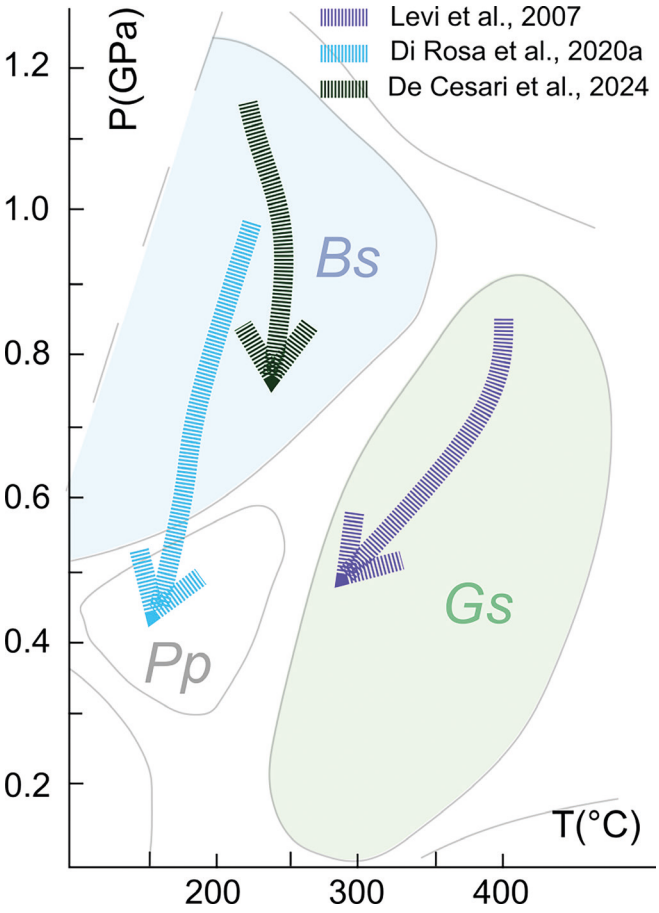

Fig. 3.4 - Estimated P-T path for the Inzecca-Lento Unit (after Levi et al., 2007; Di Rosa et al., 2020a; De Cesari et al., 2024). P-T grid for epidote-blueschist facies (continuous lines, Evans et al., 1990; abbreviations: BS epidote-blueschist facies; GS greenschist facies; Pp prehnite-pumpellyite facies.

DAY 3 STOPS DESCRIPTION

ITINERARY: Île Rousse, Ponte Leccia, Ponte Novu, Lento, Bigorno, Campitello, Accendi Pipa, Bastia.

STOP 3.1. - Road from Ponte Novu to Lento: BLUESCHIST FACIES METAGABBROS (42°29'42.3"N 9°17'04.6"E)

From Ile Rousse we drive on the RT30 until Ponte Leccia, where we take the RT20 toward Bastia. At the village of Ponte Novu (located 7 km east of Ponte Leccia), we take the road RD5 toward Lento. We stop along the road ca. 1 km after the intersection where a section of metagabbros crop out. The metagabbros occur as whitish, strongly foliated rocks showing strong deformation partitioning. Low-strain domains are characterized by relics of the magmatic assemblage, represented by porphyroclasts of Cpx. In contrast, high-strain domains lack these magmatic relics and have more pervasive

foliation. At map-scale, these metagabbros lie at the core of the map-scale $F2_{SL}$ folds. The main foliation identified in this outcrop is a composite anisotropy, resulting from the overprinting of $S2_{SL}$ on $S1_{SL}$ (Fig. 3.5a). The $S1_{SL}$ foliation is mainly identifiable in thin sections, where it is preserved throughout the microliths between the $S2_{SL}$ foliation (Fig. 3.5b). In the metagabbros, the $S1_{SL}$ foliation is defined by Na-Amp + Lws + Wm +Qtz. Qtz grains show evidence of dynamic recrystallisation. The $S2_{SL}$ foliation is characterized by Qtz ribbons and the growth of Chl and Wm around pre-existing *HP* minerals.

STOP 3.2. - Road from Ponte Novu to Lento: METASEDIMENTS OF THE OPHIOLITE SEQUENCE (42°30'15.5"N 9°17'38.6"E)

We continue along the RT20 to Lento crossing the metasediments of the Erbajolo Fm., represented here by carbonate turbidites and $CaCO_3$-free hemipelagites. The outcrop shows the metamorphic equivalent of these carbonate turbidites in the form of alternating marbles, calcschists and schists (i.e., limestones, marlstones, and shales, respectively) (Fig. 3.5c). These rocks show evidence of the polyphase deformation (Fig. 3.5d) affecting the Inzecca-Lento Unit, with

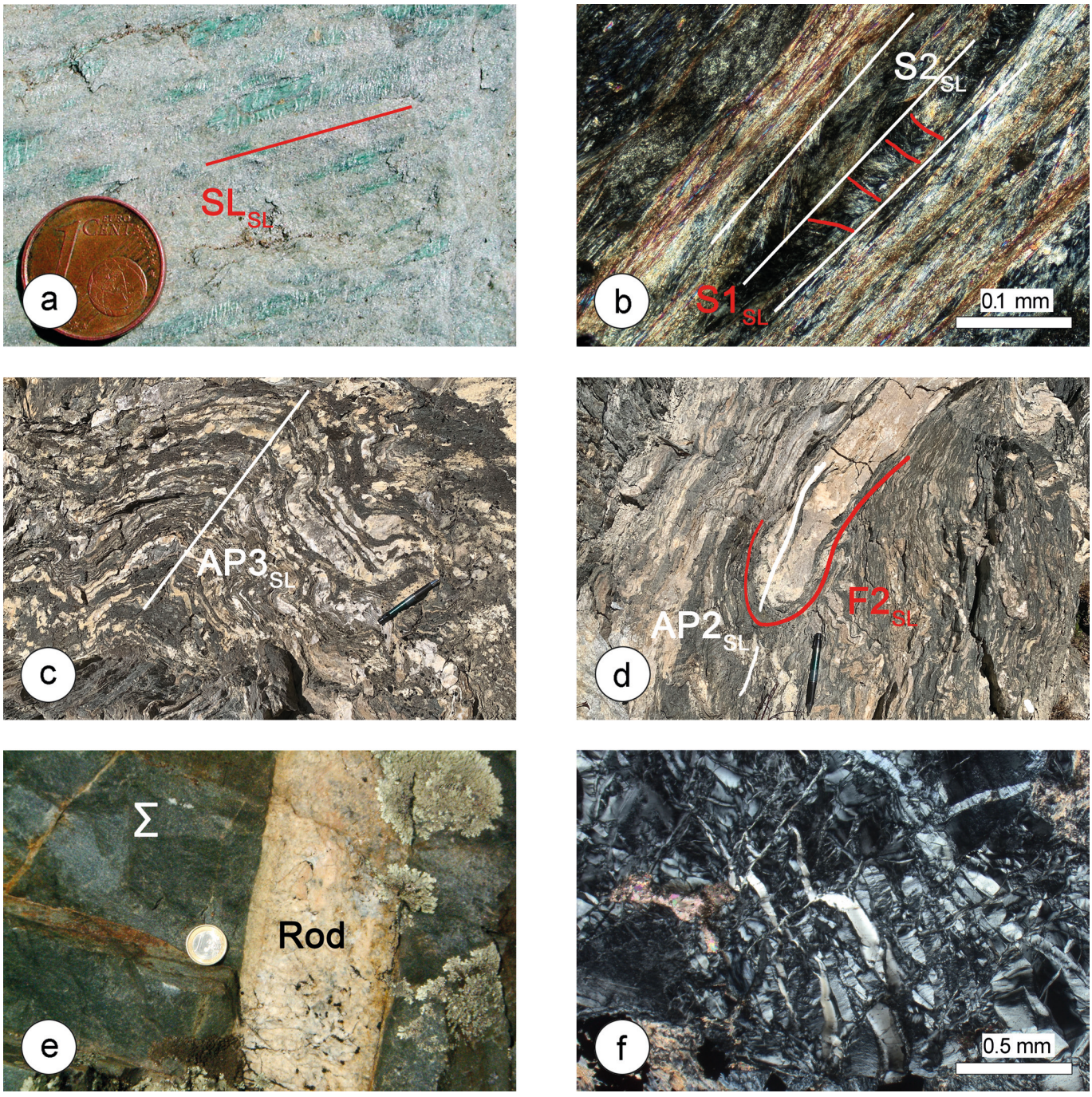

Fig. 3.5 - Lento Unit (a) $S2_{SL}$ main foliation in metagabbros. Pale green mineral is fuchsite and its elongation indicate the stretching lineation (SL_{SL}). (b) Photomicrograph of metagabbro showing relics of $S1_{SL}$ foliation preserved throughout the microliths between the $S2_{SL}$ foliation, CPL. (c and d) Field occurrence of the Erbajolo Fm. The hinges zones of an $F3_{SL}$ fold (c) and $F2_{S}L$ fold (d) can be recognized. (Label, $AP3_{SL}$: A3 fold axial plane; $AP2_{SL}$: A2 fold axial plane). (e) field occurrence of metaperidotites (S) cut by a dyke of metarodingites (Rod). (f) Photomicrograph of serpentinized peridotites: mesh texture defined by relics of clinopyroxene, orthopyroxene, and chromium-spinel, wrapped in a fine-grained matrix of serpentine and magnetite, CPL.

the main visible elements at outcrop-scale being isoclinal to sub-isoclinal $F2_{SL}$ folds, deformed by $F3_{SL}$ and $F4_{SL}$ folding. Within the micaschists, the $S1_{SL}$ foliation is rarely recognizable, and only as a relic within the microlithons alongside the $S2_{SL}$ foliation, primarily in the hinge zone of the $F2_{SL}$ folds. In this lithotype, the relic $S1_{SL}$ foliation can be classified as continuous cleavage, defined by a metamorphic mineral assemblage consisting of Wm, Chl, Qtz, and Cal. The $S2_{SL}$ foliation in thin sections is characterized by syn-kinematic metamorphic minerals that have recrystallized on pre-existing *HP* minerals. Along the limbs of the $F2_{SL}$, the main foliation is represented by composite $S2_{SL}$ + $S1_{SL}$ foliation. In contrast, in the $F2_{SL}$ hinge zone where the $S1_{SL}$ foliation is preserved, the $S2_{SL}$ foliation is classified as a crenulation cleavage. This is occurring as smooth cleavage domains showing a gradational to discrete transition to the microlithons. In micaschists, the $S2_{SL}$ foliation is characterized by the development of Wm, Chl, Qtz, Ab, and Cal.

STOP 3.3 - road from Lento to Bigorno: SERPENTINIZED PERIDOTITES (42°31'43.6"N 9°17'36.1"E)

We continue to drive on the RD5 to Lento. After approximately 2 km, before reaching the village of Bigorno, we stop at a well-exposed outcrop of a highly fractured yet homogeneous body of serpentinized peridotites. These rocks originated from pristine lherzolite and are characterized by a medium to high degree of serpentinization (approximately 60-90% serpentine minerals). Occasionally, a tectonic texture marked by oriented mm sized Opx and Cpx crystals, as well as dikes of rodingitized gabbros (Fig. 3.5e), can be observed. The main feature of this peridotite body is a complex network of veins filled with both massive and fibrous infillings of minerals, such as Srp and Cal.

In thin sections, a mesh texture defined by relics of Cpx, Opx, and Cr-Spl, wrapped in a fine-grained matrix of Srp and Mag, is well visible. In peridotites that have undergone limited serpentinization, microstructural evidence indicates that their primary texture was probably tectonic, consisting of large, oriented Opx porphyroclasts within a fine-grained, recrystallized, protogranular aggregate of Opx, Cpx, and Ol. In the studied thin sections, Ol has almost entirely been replaced by Srp, although it is still occasionally present in the mesh-textured domains (Fig. 3.5f). Opx and Cpx have partially transformed into 'bastite' (i.e., fine-grained aggregates of Srp fibers that have replaced and mimicked the Px). Spl remains unaltered, even in the more serpentinized samples.

STOP 3.4 - road from Bigorno to Campitello: SLICE OF CONTINENTAL METAGRANITOIDS (42°31'30.0"N 9°18'37.4"E)

In this outcrop, we observe a slice of metagranitoids like that observed in the stop 1.3. The occurrence of this slice indicates that we have crossed the boundary between the Upper and Lower Slices Complexes of the SL. These metagranitoids are associated with remnants of the sedimentary cover represented by metaconglomerates and metasandstones (not observed in this outcrop).

STOP 3.5. - Accendipipa area: AN OPHIOLITE SEQUENCE AND ITS SEDIMENTARY COVER DEFORMED UNDER ECLOGITE FACIES METAMORPHIC CONDITIONS (42°30'27.3"N 9°19'38.4"E)

We take road D7 up to Volpajola, then we take the road D15 towards south. Reached the T20, we turn right and after 4 km we park on the right. An exceptional section of an ophiolite sequence that reached a metamorphic peak achieved under eclogite facies conditions (Lahondère and Guerrot, 1997) (Fig. 3.6) and have subsequently underwent retrograde blueschist and greenschist metamorphism (Lahondère and Lahondère, 1988; Lahondère, 1991) is exposed in this area. This sequence was studied in detail by Lahondére and Guerrot (1997) and consists of serpentinized peridotites, metabasalts and quartzites (representative of the oceanic radiolarites).

From the parking lot, we walk toward west up to the ridge. After passing a fence, we continue along the ridge toward NE until the cliff (42°30'34.5"N 9°19'32.7"E). The outcrop manly consists of white quartzites and cm thick violet manganesiferous layers rich in piemontite and spessartine deformed by impressive sheath folds (Fig. 3.7a) regarded as having formed under eclogite facies metamorphic conditions. The interaction between these old sheath folds and the subsequent deformation phase, represented by close-to-isoclinal

Fig. 3.6 - This figure shows the walking route to follow starting from T20 road to reach the outcrop of Stop 3.5.

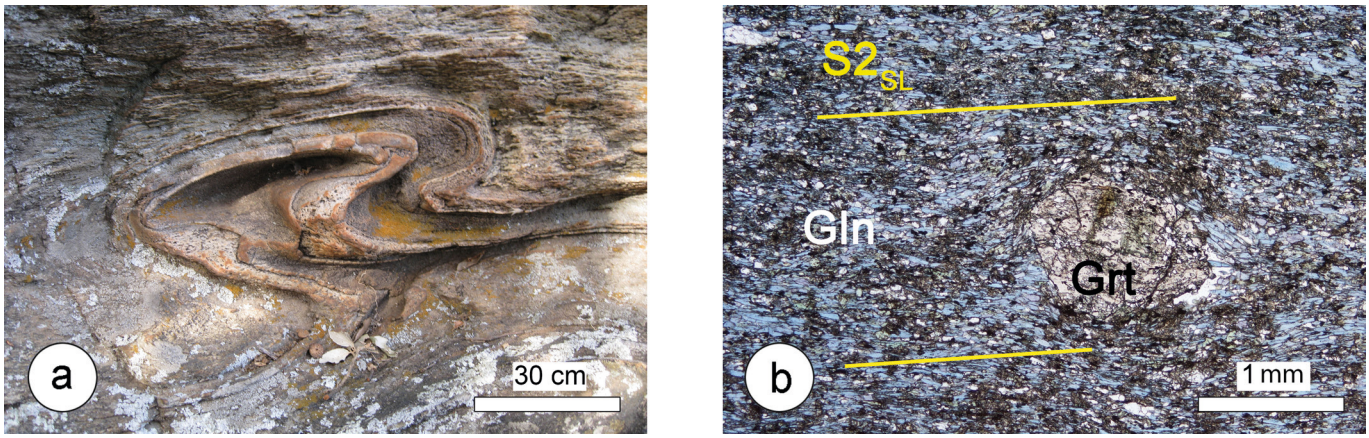

Fig. 3.7 - Accendipipa Stop 3.5. (a) Outcrop of the quarzites showing an isoclinal $F2_{SL}$ fold deformed by a $F3_{SL}$ fold. (b) Microphotograph of the eclogite facies paragneisses (Gln, glaucophane; Grt, garnet), CPL. The main foliation $S2_{SL}$, is also indicated.

folds, produced complex interference patterns that can be clearly seen in the outcrop (Fig. 3.7a). At the microscopic scale, quartzites preserve relics of Gln and Grt (Alm) locally replaced by Chl and Ep (Fig. 3.7b).

STOP 3.6 - Accendi Pipa area: OPHIOLITE SEDIMENTARY COVER UNDER ECLOGITE FACIES METAMORPHISM (45°50'97.4"N 9°32'60.9"E)

Walking westward at the same altitude, we transition from metabasalts and quartzites to micaschists and calcschists containing rounded boudins of marbles and paragneiss. This succession is generally considered to be the remains of an ophiolite sedimentary cover. In this outcrop, a layer of paragneisses containing rounded boudins of metabasalts is exposed (Lahondère and Guerrot, 1997). The main foliation consists of minerals that developed during eclogite facies metamorphism, such as Grt and Jd. These minerals are found as relics in a matrix of Qtz, Wm, Gln, Ab, Ep, Chl, and Cal.

However, boudins of paragneisses that have not been affected by retrograde metamorphic processes can be found. These boudins consist of Qtz, Jd, Na-Amp, Wm, Chl, Alm, Chr, Ap, and Fe-, Ti-, and Zr-oxides. The paragneisses underwent eclogite facies metamorphism (2.0 GPa and approximately 500 °C; Lahondère and Guerrot, 1997), followed by retrograde blueschist facies metamorphism (0.8-1.0 GPa and 350 ± 25 °C; Lahondère and Lahondère, 1988; Lahondère, 1991) (Fig. 3.7b). The crystallization age of this paragenesis was determined using the Sm-Nd systematics on whole rock and on separated Grt, Amp, and Cpx mineral phases. The obtained isochron indicates an age of 83.8 ±4.9 Ma (Lahondère and Guerrot, 1997).

DAY 4: A JOURNEY WITHIN THE HP CONTINENTAL CRUST OF THE LOWER UNITS

The fourth day of the trip focuses on the LU representative of the thinned continental margin of the Europe plate. These units are involved in the continental collision that predated the collision in the Middle to Late Eocene period. The reconstructed log of these units includes a polymetamorphic basement that records Panafrican and Variscan orogenic events, and that was then intruded by Permo-Carboniferous magmatic rocks (Ménot and Orsini, 1990; Rossi et al., 2009; 2015). Both the polymetamorphic basement and the magmatic rocks were covered by sedimentary successions of Permian volcaniclastic rocks, Mesozoic carbonates, and Middle to Late Eocene siliciclastic turbidites (Durand-Delga, 1984). The LU underwent significant deformation and metamorphic overprint during their involvement in continental subduction, as evidenced by pervasive *HP* metamorphism. These units differ from each other about the P-T conditions of the

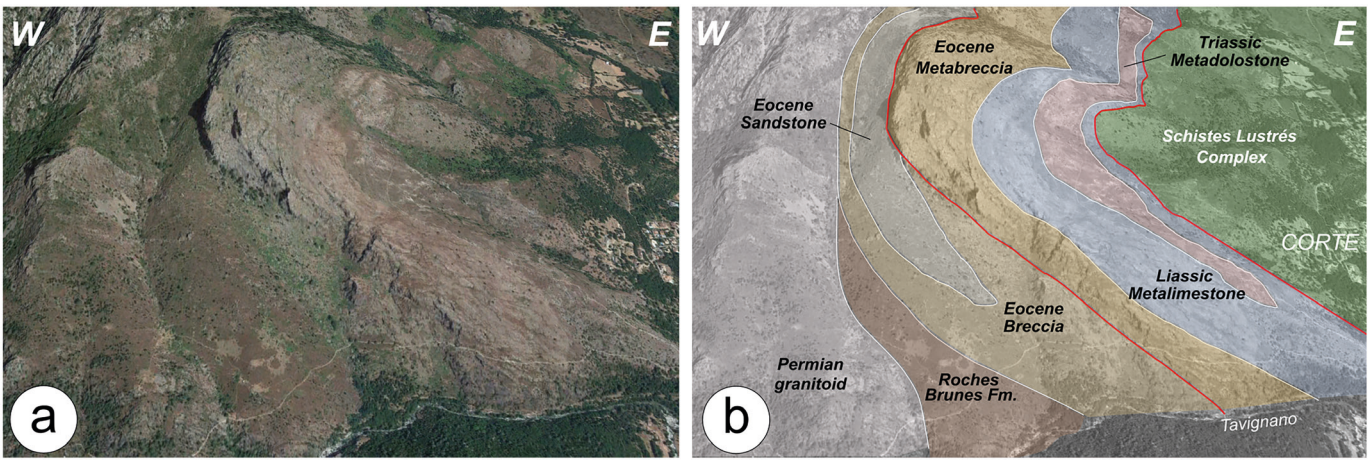

Fig. 4.1 - (a) Panoramic view and (b) schematic representation of the main geological features in the Tavignano area west of Corte. The view faces S to N.

metamorphic peak, as well as to the path followed during exhumation (Di Rosa et al., 2020a; Frassi et al., 2023). The field trip focuses on the Catiglione-Popolasca Unit, which is one of the most representative LU.

DAY4 STOP DESCRIPTION

ITINERARY: Île Rousse, Ponte Leccia, Corte, Castirla bridge, Castiglione, Popolasca, Ponte Leccia, Île Rousse.

STOP 4.1 - Tavignano valley: WALKING ACROSS THE LOWER UNITS UP TO HERCYNIAN CORSICA (parking: 42°18'29.1"N 9°08'50.6"E)

From Ile Rousse we move to Corte through the roads RT30 and RT20. In the town of Corte, we stop at the parking lot (42°18'29.1"N 9°08'50.6"E) where the trail along the Tavignano valley starts. The promenade along the trail provides an excellent opportunity to observe the lithologies of the LU in a section close to Hercynian Corsica (Fig. 4.1).

The first outcrops on the trail expose the Hettangian-

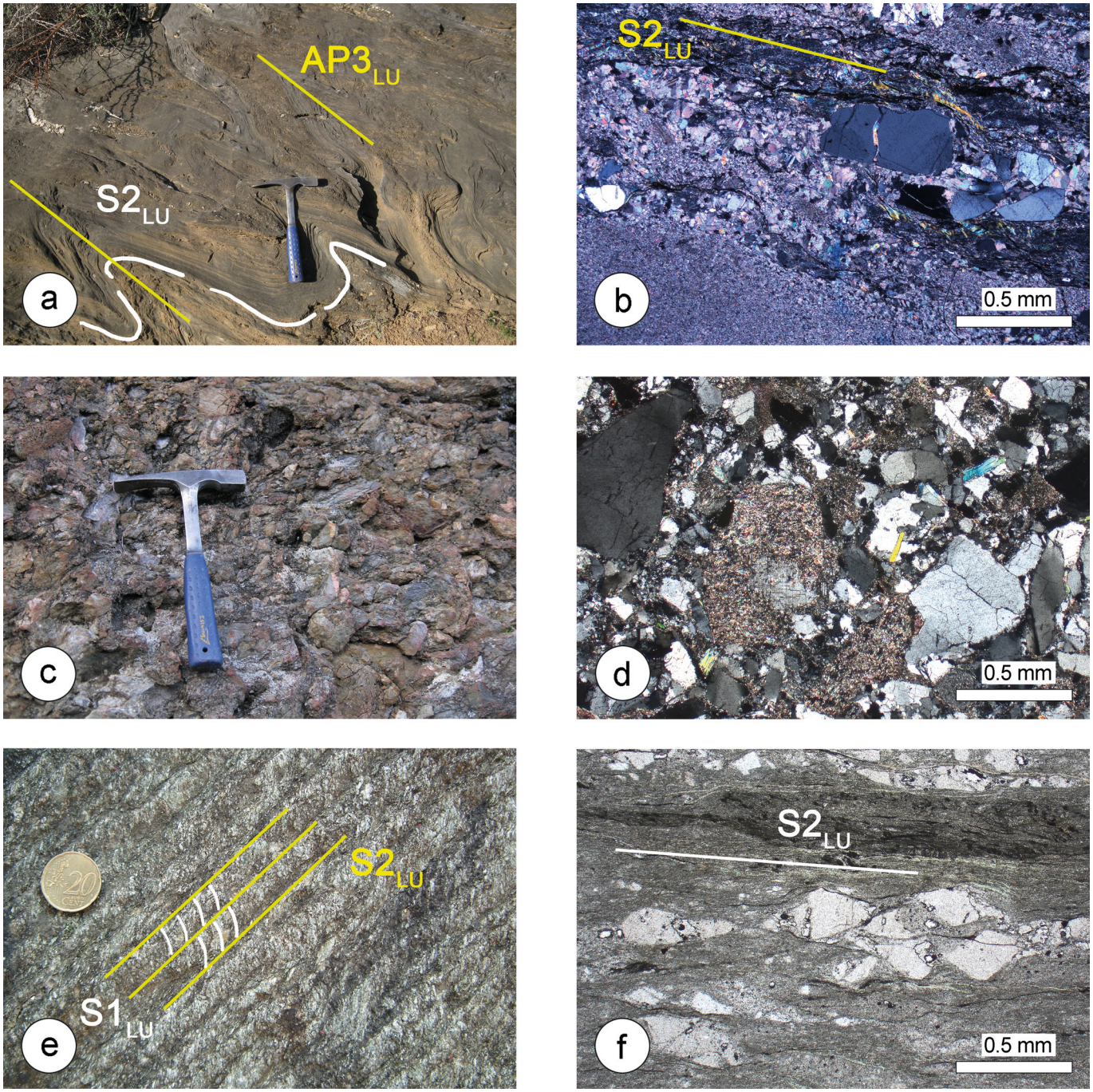

Fig. 4.2 - (a-d) Meso- and microscale features of selected rock types along the path of the Tavignano Valley: (a) $D2_{LU}$ folds in the Metalimestone and Metadolostone Fm. of the Castiglione-Popolasca Unit. The attitude of the $S2_{LU}$ foliation as well as that of the $AP3_{LU}$ axial plane foliation is shown; (b) bedding in the Detritic Metalimestone Fm. of the Castiglione-Popolasca Unit. The attitude of the $S2_{LU}$ foliation is shown, CPL; mesoscale (c) and microscale, CPL (d) example of undeformed Eocene conglomerates belonging to the sedimentary cover of the Hercynian Corsica. (e-f) Features of the Permian Metavolcanic and Metavolcaniclastic Fm. of the Castiglione-Popolasca Unit along the Golo valley: (e) relationship between the $S1_{LU}$-$S2_{LU}$ foliations at the mesoscale and (f) microscale occurrence of the $S2_{LU}$ foliation, PPL.

Sinemurian Metalimestone and Metadolostone Fm. consisting of folded, medium-to-thick beds of metalimestones and metadolostones (Fig. 4.2a). The $S1_{LU}$ foliation and the boudinaged layers of metadolostones are folded by sub-isoclinal, west-verging $F2_{LU}$ folds and by open and almost recumbent $F3_{LU}$ folds. The Metalimestone and Metadolostone Fm. is topped through an angular unconformity by the Eocene Metabreccia Fm. (cf. Volparone Breccia of Malasoma and Marroni, 2007), consisting of elongated clasts of orthogneisses, paragneisses, micaschists and metagranitoids enclosed in a fine-grained matrix of metapelites to metarenites.

This metamorphic sequence belongs to the Castiglione-Popolasca Unit, that, records P-T conditions during the $D1_{LU}$ phase ranging from P = 1.2-1.1 GPa and T = 250-330 °C, to P = 0.8-0.6 GPa and T = 320-350 °C (Di Rosa et al., 2017a; 2019c) (Fig. 4.2b). This evolution indicates that exhumation started at the end of the $D1_{LU}$ phase, as documented in the other LU (Di Rosa et al., 2020b and reference therein). Continuing along the path, we cross the boundary between the Metabreccia Fm. of the Castiglione-Popolasca Unit and the Eocene conglomerates that form the cover of Hercynian Corsica.

This boundary is marked by a significant difference in deformation in the metabreccia and conglomerate clasts (flattened versus rounded clasts). The Eocene conglomerates (Fig. 4.2c,d) are folded by an upright synform containing Eocene sandstones at its core. Outcrops of Eocene sandstones can be seen along the footpath. After a small valley, the polydeformed and polymetamorphic assemblage of micaschists, paragneiss, quartzites, and amphibolites of Roches Brunes Fm., can be observed (Rossi et al., 1994). The last outcrop that we visit along the trail (42°18'22.8"N 9°07'44.0"E) offers a well-exposed section of the Permo-Carboniferous Bt-bearing monzogranites intruded in the Roches Brunes Fm. (Rossi et al., 2015).

STOP 4.2. - Castirla bridge: DEFORMATION HISTORY IN THE META-ARKOSES (42°23'00.5"N 9°08'19.1"E)

We then return to Corte and follow the Golo valley along the RT20 until we reach the village of Francardo where we take the RD84 toward Castirla and we stop at the Castirla bridge over the Golo river. In this outcrop, the structural relationships between the $D1_{LU}$, $D2_{LU}$ and $D3_{LU}$ can clearly be detected in the Permian Metavolcanic and Metavolcaniclastic Fm. belonging the Castiglione-Popolasca Unit. The formation is represented here by meta-arkoses showing pervasive $S1_{LU}$ foliation, deformed by well-spaced, steeply dipping $S2_{LU}$ foliation (Fig. 4.2e). These relationships can be observed in the Barbanello road 20 m away from the bridge. In turn, the $S2_{LU}$ foliation is deformed by open $F3_{LU}$ folds with a sub-horizontal axial plane. Under a microscope, the meta-arkoses have a 'porphyric' appearance, characterized by coarse-grained porphyroclasts wrapped in a fine-grained matrix made up of neoblasts formed by a dynamic recrystallisation mechanism (Fig. 4.2f). The $S1_{LU}$ foliation can be classified as a continuous schistosity, characterized by granoblastic layers consisting of Qtz and Fsp porphyroclasts, alternating with aligned Wm, Chl, Qtz, and Ab layers. The $S2_{LU}$ axial-plane foliation is a well-developed, discrete crenulation cleavage characterized by aligned Wm + Chl + Qtz + Fe-oxides layers. Thin Qtz and Cal veins cut through all the $D1_{LU}$ structures. Qtz porphyroclasts show intracrystalline deformation (e.g., undulose extinction, deformation lamellae) and dynamic subgrain rotation recrystallisation producing core-and-mantle structures with σ-type old grains along the $S2_{LU}$. Kinematic criteria after the restoration of the $D3_{LU}$ folds indicate a top-to-W sense of shear.

STOP 4.3. - Castiglione Village: EOCENE METABRECCIAS (42°25'04.3"N 9°07'44.1"E)

From the Castirla bridge, we proceed north on the RD18, and we stop at the village of Castiglione. From the parking lot, we move down towards the town, we turn left (towards east) and after 20 meters on the right we can see a good exposure of the Eocene Metabreccia Fm. belonging to the Castiglione-Popolasca Unit (Fig. 4.4a).

This Metabreccia Fm. consists of clasts of granitoids, metavolcanites, metabasites and limestones set in an arenite matrix (Fig. 4.4a,b). The clasts, aligned along the main $S1_{LU}$ + $S2_{LU}$ composite foliation, have a flattened shape comparable to a type II ellipsoid in the Flinn (1962) classification diagram. The clasts lithotype clearly indicate the Variscan basement and its Late Paleozoic-Mesozoic sedimentary cover as the source area. Their pristine angular to subangular shape suggests deposition in an area very close to the source. In thin section, the breccia matrix is characterized by a fine-grained foliated fraction mainly composed of Chl + Wm + Ab + Qtz + Cal + Kfs wrapping around lithic, Qtz, Kfs, Bt, and rare Pl porphyroclasts. The matrix is affected by polyphase deformation characterized by two different foliations. The $S2_{LU}$ foliation is a dominant anisotropy that can be classified as zonal and anastomosing crenulation cleavage. It is characterized by a clear change in the cleavage domains and microlithons,

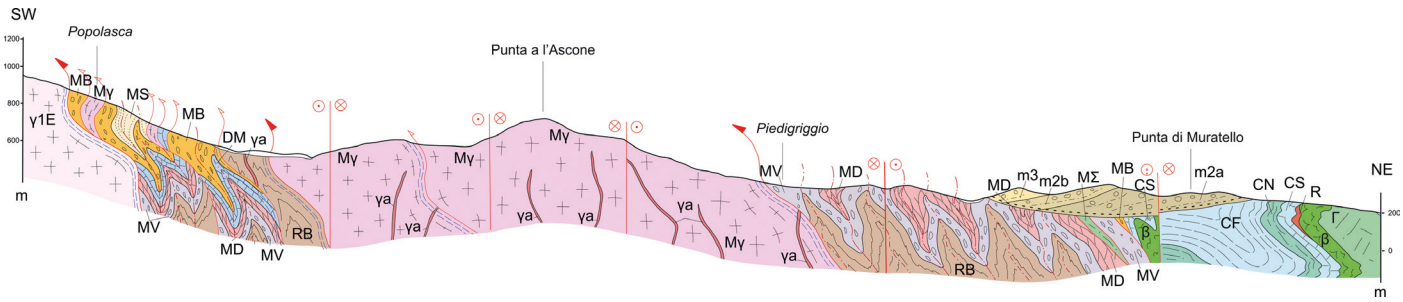

Fig. 4.3 - Geological cross-section showing the Alpine stack of units above the Hercynian Corsica along the Popolasca-Punta di Muratello transect. Hercynian Corsica: g1E (Permo-Carboniferous monzogranites). Castiglione-Popolasca Unit (Lower Units): Mγ (metagranitoids), RB (Roches Brunes Fm.), MV (Metavolcanic and Metavolcaniclastic Fm.), MD (Metadolostone Fm.), DM (Detritic Metalimestone Fm.), MB (Metabreccia Fm.) and MS (Metasandstone Fm.). Croce d'Arbitro Unit (Lower Units): Mγ (metagranitoids) and γa (mafic dykes). Piedigriggio-Prato Unit (Lower Units): RB (Roches Brunes Fm.), MV (Metavolcanic and Metavolcaniclastic Fm.), MD (Metadolostone Fm.) and MB (Metabreccia Fm.). The Inzecca-Lento Unit (Schistes Lustés Complex): MΣ (serpentinized peridotites). The Pineto-Serra Debbione Unit (Upper Units): Γ (gabbros), β (basalts), R (radiolarites), CS (Calpionella Limestone Fm.), CN (San Martino Fm.) and CF (Lydienne Flysch). Francardo Basin (Miocene deposits): m2b (Taverna Fm.), m2a (Ortone Fm.) and m3 (Francardo Fm.). Slightly modified after Malasoma et al. (2020).

where relics of the $S1_{LU}$ foliation, marked by layers of Chl + Wm + Ab + Qtz, are preserved.

STOP 4.4. - road from Castiglione to Popolasca: EOCENE METASANDSTONES (42°25'10.5"N 9°07'52.6"E)

From Castiglione village, we move back along the road D118 towards Popolasca village, and we stop after 300-350 m to observe the metaturbidites of the Metasandstone Fm. of the Castiglione-Popolasca Unit. The formation is characterized by metarenites, metasiltstones and metapelites layers (Fig. 4.4c) preserving the primary features, such as graded bedding and sedimentary laminations. The $S1_{LU}$ foliation is a pervasive and continuous foliation in the metaturbidites that is preserved within the microlithons of the $S2_{LU}$ main foliation.

The $S2_{LU}$ foliation is associated to tight to isoclinal, non-cylindrical folds $F2_{LU}$ whose axial planes are deformed by asymmetric, open and E-verging $F3_{LU}$ folds which have sub-horizontal axial planes. In thin sections, these metasandstones are characterized by deformed porphyroclasts of Qtz, K-Fsp, Chl and Ab in a fine-grained composite layering. This layering is defined by the overprinting of the $S2_{LU}$ foliation, which is mainly composed by Chl + Wm + Qtz + Ab, on the $S1_{LU}$. In the $F2_{LU}$ hinge-zone, the $S2_{LU}$ foliation can be classified as zonal crenulation cleavage characterized by smooth cleavage

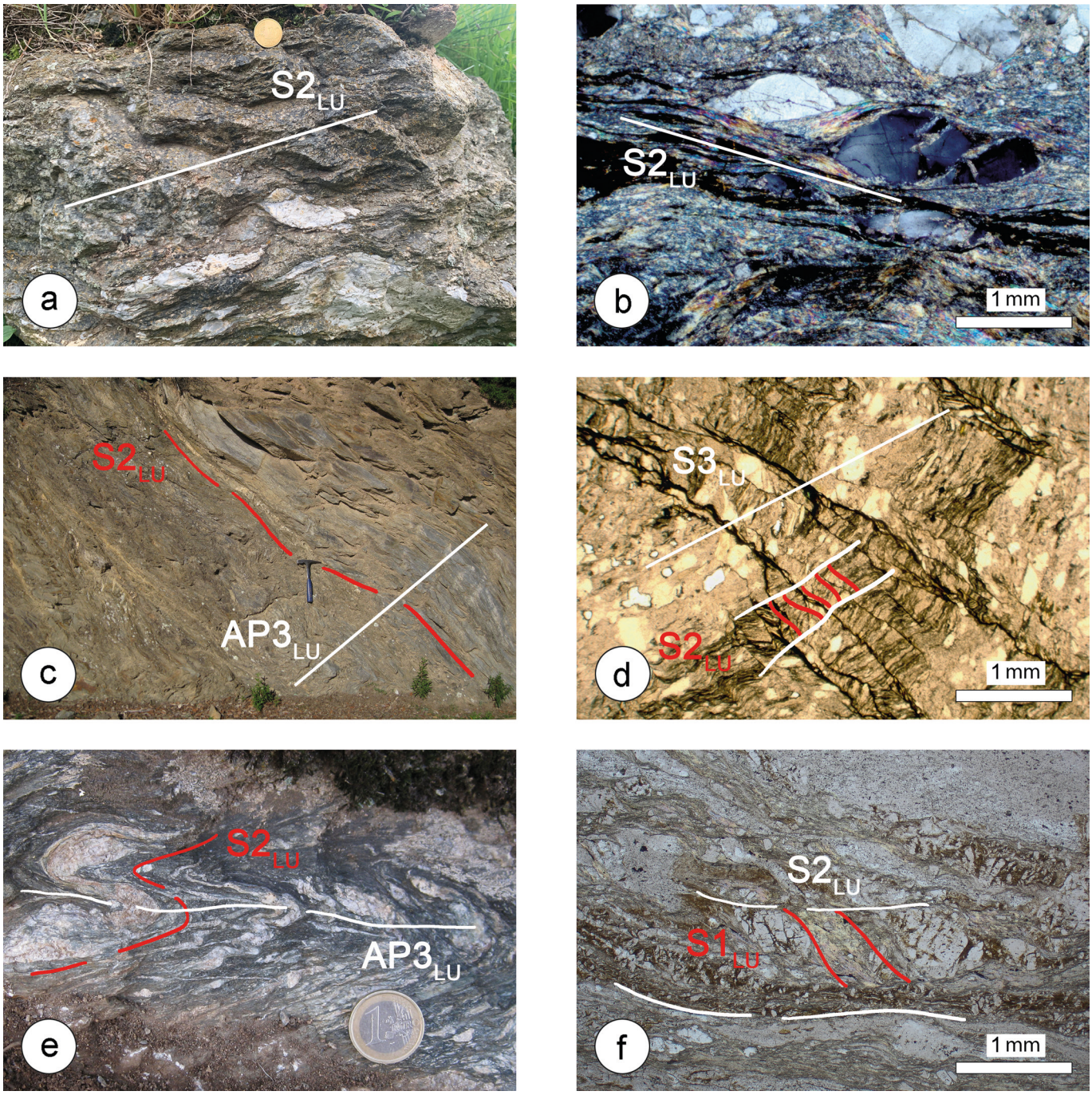

Fig. 4.4 - Meso- and microphotographs showing selected rock types of the Castiglione-Popolasca Unit north of the Golo Valley. (a) the Metabreccia Fm. near Castiglione Village. The attitude of the $S2_{LU}$ foliation is shown. (b) $S2_{LU}$ foliation in the Metasandstone Fm. marked by the recrystallization of chlorite and white mica, CPL. (c) $D2_{LU}$-$D3_{LU}$ phase in the Metasandstone Fm. (d) relationships between the $S2_{LU}$ and $S3_{LU}$ foliations in the hinge zone of an $F3_{LU}$ fold, PPL. (e) attitude of the S2LU foliation in the metagranitoids at Popolasca village, and (f) relics of S1LU foliation within the $S2_{LU}$ foliation in the metagranitoids, PPL.

domains showing a gradational to discrete transition to the microlithons. In these microlithons the $S1_{LU}$ can be classified as continuous foliation marked by syn-kinematic grown of Chl + Wm + Ab + Qtz. In contrast, the $S2_{LU}$ foliation is characterized by the growth of new Chl + Wm + Qtz + Cal of a smaller grain size compared to those that recrystallized during the $D1_{LU}$ phase (Fig. 4.4d). The $S3_{LU}$ foliation is classifiable as spaced crenulation cleavage. There is no evidence of recrystallisation associated with the $S3_{LU}$ foliation.

STOP 4.5. - Popolasca Village: HIGHLY DEFORMED METAGRANITOIDS (42°26'00.2"N 9°07'53.0"E)

We continue along the road until the Popolasca Village where a slice of strongly deformed sheared metagranitoids belonging to the Castiglione-Popolasca Unit can be observed. This slice, which is associated with slices of metabreccias and metalimestones, occurs at the boundary with the Hercynian Corsica. In the field, the sheared granitoids exhibit low-*T* cataclastic-mylonitic deformation characterized by the development of continuous foliation trending N-S and sub-vertical, i.e. parallel to the boundaries of the Castiglione-Popolasca Unit. The main foliation is a composite, $S1_{LU}$ + $S2_{LU}$ anisotropy defined by the preferred shape orientation of Qtz + feldspar ± Bt grains, as well as thin lepidoblastic layers (Wm ± Chl ± Stp). The main foliation is associated with a stretching/mineral composite lineation (Lp), which is highlighted by Qtz ribbons and K-Fsp porphyroclasts (LS fabric). The approximately E-W trending Lp_{LU} lineation is located along the dip-slip direction of the foliation plane. The attitudes of the foliation and lineation are strongly influenced by subsequent deformation phases and asymmetric folds with sub-horizontal axial planes and N-S-trending axes (Fig. 4.4e). These folds have been attributed to the $F3_{LU}$ folds identified in the sedimentary cover rocks based on the deformation style, geometry, and orientation of structural elements.

In the thin section, the metagranitoids exhibit protomylonitic to ultramylonitic foliation, characterized by discontinuous layers of recrystallized Wm and Bt, as well as granoblastic layers of fine-grained, recrystallized Qtz and Pl, which wrap around weakly elongated Fsp grains and Qtz crystals (Fig. 4.4f). The S-C' fabric, the σ-type porphyroclasts of feldspar and the bookshelf structures (with synthetic and antithetic fractures) indicate a top-to-W sense of shear. The dominant mylonitic foliation is characterized by the planar distribution of mica and chlorite, as well as the preferred orientation of Qtz and Fsp. Deformation is heterogeneous; relics of the protolith and of older paragenesis are preserved in lenses alternating with phyllosilicate layers, in which S-C and S-C' domains can be distinguished. Relics of Qtz and feldspars are characterized by cataclastic flow, and the fractures are filled with by Wm, Chl and fine-grained Qtz. Mylonitic domains of Qtz and feldspars are characterized by bulging recrystallisation and subgrain rotation. In the thin sections of metapelites, the $S2_{LU}$ foliation is a crenulation cleavage characterized by a new generation of Chl + Wm + Qtz + Ab + Cal.

STOP 4.6. - road from Popolasca to Ponte Leccia: MIOCENE DEPOSITS OF FRANCARDO BASIN (42°26'54.7"N 9°11'02.4"E)

From the village of Popolasca, we continue along the road

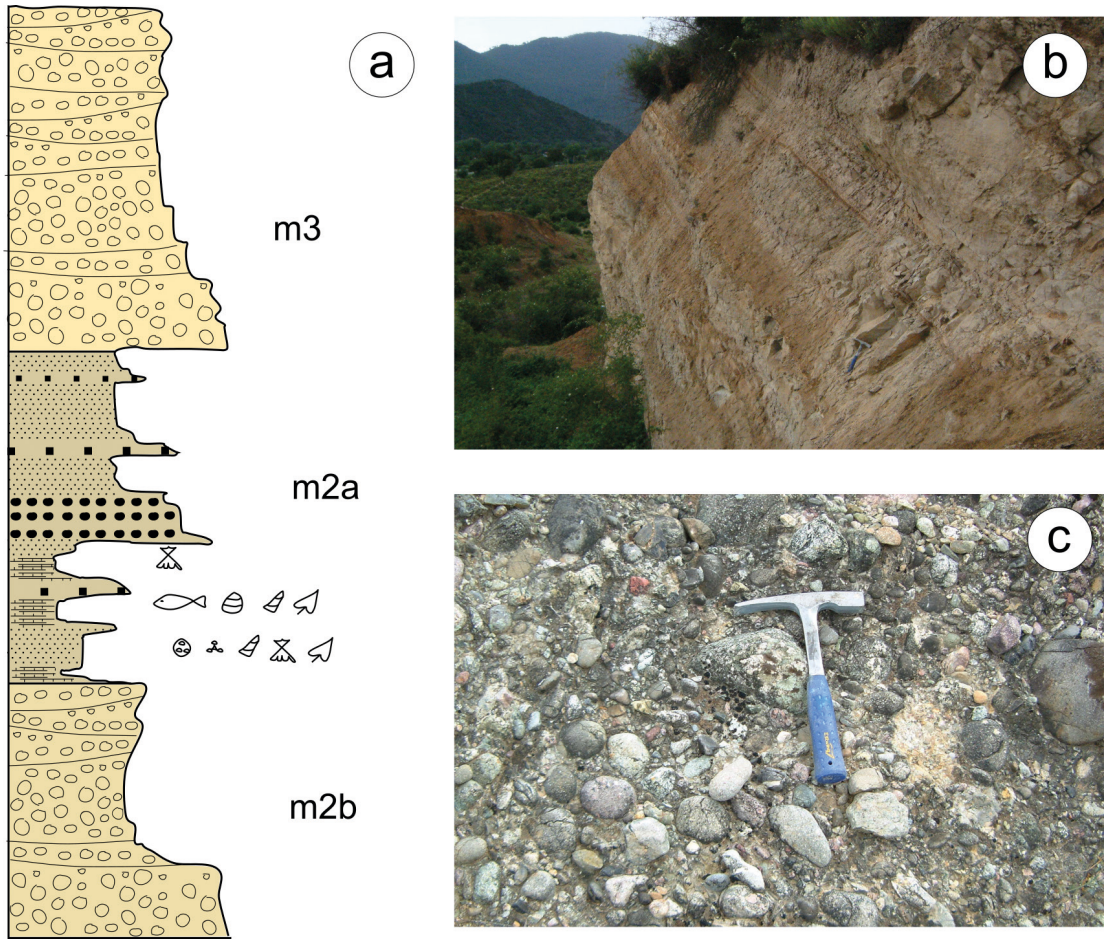

Fig. 4.5 - (a) Stratigraphic log of the Miocene deposits from the Francardo Basin (from Cubells et al. (1994). m2b: Taverna Fm. (late Burdigalian); m2a: Ortone Fm. (late Burdigalian); m3: Francardo Fm. (Langhian). Mesophotographs showing (b) an alternance of conglomerates and sandstones in the Francardo Fm., and (c) the fluvial conglomerates of the Ortone Fm.

RD18. The Miocene Francardo Basin stretches approximately 7 km along the left bank of the Golo river. The basin, which is between Burdigalian and Tortonian in age, has a maximum thickness of approximately 500 m. The stratigraphic succession (Fig. 4.5a) has been divided into three formations: the Ortone, the Taverna and the Francardo Fms. (Ferrandini and Loye-Pilot, 1992; Cubells et al., 1994). Cubells et al. (1994) stated that sedimentation in the Francardo-Ponte Leccia Basin is controlled by extensional and transcurrent tectonics. The stop shows the early Burdigalian Ortone Fm. (Fig. 4.5b) (about 150 m thick) consisting of fining-upward conglomerates interpreted as an alluvial fan deposited in a continental environment (Cubells et al., 1994). The conglomerates are poorly sorted, clast-supported and characterized by angular to sub-rounded clasts of granitoids, siliciclastic conglomerates, volcanic rocks, micaschists, limestones and nummulites-bearing calcarenites, as well as a small amount of ophiolitic rocks.

Return to Île Rousse.

CONCLUSIONS

Alpine Corsica provides a comprehensive overview of the axial zone of a collisional belt of Alpine age. The stratigraphic, structural, and metamorphic features visible on the outcrops proposed in this field journey through Alpine Corsica units allows to explore the evolution of a portion of the Ligurian-Piedmont Basin and its adjacent continental margins from the ocean formation to its involvement into subduction and collision. The history started with the Middle Triassic-Middle Jurassic rifting and subsequent opening of the Ligurian-Piedmont Oceanic Basin between the Europe and Adriatic continental margins (Lavier and Manatschal, 2006; Marroni and Pandolfi, 2007; Péron-Pinvidic and Manatschal, 2009; Masini et al., 2013; Ribes et al., 2019). Spreading in this basin was only active from the Middle to Late Jurassic (Abbate et al., 1980; Lagabrielle and Lemoine, 1997; Principi et al., 2004; Marroni and Pandolfi, 2007; Sanfilippo and Tribuzio, 2013; Tribuzio et al., 2016), after which a long period of deep-sea pelagic sedimentation ensued, with no tectonic or volcanic events (Marroni et al., 2017). This quiet period was interrupted in the Late Cretaceous, probably during the Campanian stage, by the onset of east-dipping subduction at the ocean-continental transition on the Adria continental margin (Elter and Pertusati, 1973; Lagabrielle and Polino, 1988; Schmid et al., 1996; Michard et al., 2002; Molli, 2008; Handy et al., 2010; Marroni et al., 2017). Spanning from the Late Cretaceous to the Paleocene, this subduction resulted in the development of an accretionary wedge, in which slices of ophiolites and their sedimentary cover were deformed and metamorphosed (Principi and Treves, 1984; Malavieille et al., 1998; Marroni et al., 2004). Since the Paleocene/Eocene boundary, the thinned Europe continental margin has been involved in subduction, producing slices of continental rock affected by HP metamorphism (Bezert and Caby, 1988; Egal, 1992; Brunet et al., 2000; Tribuzio and Giacomini, 2002; Malasoma et al., 2006; Molli et al., 2006; Malasoma and Marroni, 2007; Molli and Malavieille, 2011; Di Rosa et al., 2017b). These oceanic and continental units were then assembled during the continental collision that formed the present-day tectonic architecture of Alpine Corsica. Unlike the Alps, this collisional belt never reached maturity due to the opening of the Ligurian-Balearic back-arc basin in the Oligocene, which isolated Alpine Corsica and abruptly interrupted the contractional stage (Guéguen et al., 1998; Faccenna et al., 2004; Fellin et al., 2005). The Alpine Corsica region is thus a segment of the Alps that has remained frozen since the Oligocene. As a result, the tectonic structures formed during the initial continental collision of the Alpine belt can be clearly seen here.

Venturing out through the different groups of units of the tectonic stack allows us to gain details on the processes shaping the oceanic and continental domains involved in this evolution. Despite high-grade metamorphism and pervasive deformation, the ophiolite sequences and the oceanic units of the SL provide important information on the architecture of the oceanic lithosphere. These sequences formed at an ultra-slow-spreading ridge from the Middle to Late Jurassic (Marroni and Pandolfi, 2007; Sanfilippo and Tribuzio, 2013; Tribuzio et al., 2016). This is evident from the widespread occurrence of ophiolitic sedimentary breccias and basaltic lava flows lying directly on top of mantle peridotites and gabbros. However, the SL are best known for oceanic slices that were accreted at different depths within the alpine accretionary wedge (Caron and Péquinot, 1986; Lahondère, 1991; Jolivet et al., 1998; levi et al., 2007; Vitale Brovarone et al., 2011). This is indicated by P-T metamorphic peaks ranging in the different slices from eclogite to blueschist facies. This occurrence provides a good opportunity to study both the accretion- and exhumation-related deformations in oceanic slices involved in the subduction at different depths. By contrast, the LU reveal the deformation and metamorphic history of continental fragments originating from a thinned continental margin and involved in subduction tectonics (Bezert and Caby, 1988; Malasoma et al., 2006; Malasoma and Marroni, 2007; Garfagnoli et al., 2009; Di Rosa et al., 2020b). The metamorphism of the LU does not exceed blueschist facies and still allows a complete reconstruction of the stratigraphic setting of these units. This stratigraphy provides details on how the rifting and post-rifting events impacted the Europe continental margins, as well as the characteristics of the deposits associated with the continental collision stage. The UU observed in the Balagne Nappe represent slices of an oceanic area close to the Europe continental margin (Durand-Delga, 1984; Durand-Delga et al., 1997, 2005; Marroni and Pandolfi, 2003; Pandolfi et al., 2016), as suggested by the coarse-grained continental deposits found in the basalts, as well as in the sedimentary cover of the ophiolites, such as the Calpionella Limestone, Lydienne Flysch and Toccone Breccia. From a stratigraphic perspective, the ophiolite sequence of the Balagne Nappe is a distinctive and singular fragment of oceanic crust that is not present in any other unit of the Alpine-Apennine collisional belt. In addition, the Balagne Nappe underwent deformation in the accretionary wedge at a shallow level, as indicated by its prehnite-pumpellyite facies metamorphism (Marroni and Pandolfi 2003; Di Rosa et al., 2025). This indicates that Balagne nappe is likely to be the fragment to be lastly accreted to the accretionary wedge, as indicated by its sedimentary cover, which extends to the Campanian.

The trip through Alpine Corsica also offers the opportunity to observe the mutual relationships between UU, SL, and LU. The characteristics of the units bounding shear zones indicate their origin in either contractional or extensional tectonics, thus allowing a better understanding of how the coupling of ocean-derived and continental-derived slices occurred during all the geodynamic evolution. Alpine Corsica is a true natural laboratory for teaching and research activities, which must receive greater recognition in the future. This paper, and the proposed field journey across the collisional belt of Alpine Corsica, contributes to this goal.

ACKNOWLEDGEMENTS

The project was supported by Fondi d'Ateneo by Michele Marroni and Luca Pandolfi. Michele Marroni and Luca Pandolfi are indebted to Michel Durand-Delga, Piero Elter and Alberto Puccinelli for introducing them to Corsican geology. Emilio Saccani and Gianfranco Principi are acknowledged for their stimulating suggestions.

REFERENCES

Abbate E., Bortolotti V. and Principi G., 1980. Appennine ophiolites: a peculiar oceanic crust. Ofioliti, 1: 59-96.

Agard P., Omrani J., Jolivet L., Whitechurch H., Vrielynk B. Spakman W., Monié P., Meyer B. and Wortel R., 2011. Zagros orogeny: a subduction dominated processes. Geol.Mag., 148(5-6): 692-725.

Alessandri J.A., Magné J., Pilot M.D. and Samuel E., 1977. Le Miocène de la région de Corte-Francardo. Bull. Soc. Sci. Hist. Nat. Corse, 622: 51-54.

Amaudric du Chaffaut S., 1975. L'unité de Corte: un témoin de "Piémontais externe" en Corse? Bull. Soc. Géol. France, 7: 739-745.

Amaudric du Chaffaut S. and Saliot P., 1979. La region de Corte: secteur-clé pour la comprehension du métamorphisme alpin en Corse. Bull. Soc. Géol. France, 21: 149-154.

Amaudric du Chaffaut S., Caron J.M., Delcey R. and Lemoine M., 1972. Données nouvelles sur la stratigraphie des schistes lustrés de Corse: La série de l'Inzecca. Comparaison avec les Alpes Occidentales et l'Apennin ligure. Acad. Sci. Paris, 275: 2611-2614.

Amaudric du Chaffaut S., Kienast J.R. and Saliot P., 1976. Répartition de quelques minéraux de métamorphisme alpin en Corse. Bull.Soc.Géol.France, 18(5): 1179-1182.

Argand E., 1924. Des Alpes et de l'Afrique. Bull. Soc. Vaudoise Sci.Nat., 55: 233-236.

Baud J.P., Boyon M.J. and Rollet M., 1974. Observations sur le roches vertes en Haute Balagne. Reunion annuelle des sciences de la Terre. Bull. Soc. Géol. France 2: 35.

Beltrando M., Zibra I., Montanini A. and Tribuzio R., 2013. Crustal thinning and exhumation along a fossil magma-poor distal margin preserved in Corsica: A hot rift to drift transition? Lithos, 169-189: 99-112.

Berno D., Sanfilippo A., Zanetti A. and Tribuzio R., 2019. Reactive melt migration controls the trace element budget of the lower oceanic crust: insights from the troctolite-olivine gabbro association of the Pineto Ophiolite (Corsica, France). Ofioliti, 44(2): 71-82.

Bezert P. and Caby R., 1988. Sur l'âge post-bartonien des événements tectonométamorphiques alpins en bordure orientale de la Corse cristalline (Nord de Corte). Boll. Soc. Géol. France, 4(6): 965-971.

Bill M., Bussy F., Cosca M.A., Masson H. and Hunziker J.C., 1997. High-precision UPb and 40Ar/39Ar dating of an Alpine ophiolite (Gets nappe, French Alps): Ecl. Geol. Helv., 90: 43-54.

Boccaletti M., Elter P. and Guazzone G., 1971. Plate tectonic models for the development of the Western Alps and Northern Apennines. Nature, 234: 108-111.

Bosma W., 1956. Contribution à la géologie de la Balagne (Corse). Thèse Sc. Geol. Instituut Amsterndam, 128 pp.

Bracciali L., Marroni M., Pandolfi L. and Rocchi S., 2007. Petrography and geochemistry of western Tethys Mesozoic sedimentary covers (Alpine Corsica and Northern Apennines): a valuable tool in constraining sediment provenance and margin configuration. In: J. Arribas, S. Critelli, M.J. Johnsson (Eds.), Sedimentary provenance and petrogenesis: perspectives from petrography and geochemistry. Geol. Soc. Am. Spec. Pap., 420: 73-93.

Brunet C., Monié P., Jolivet L. and Cadet J.P., 2000. Migration of compression and extension in the Tyrrhenian Sea, insights from 40Ar/39Ar ages on micas along a transect from Corsica to Tuscany. Tectonophysics, 321: 127-155.

Burkhard M., 1992. Calcite twins, their geometry, appearance and significance as stress-strain markers and indicators of tectonic regime: a review. J. Struct. Geol., 20: 1-18.

Cabanis B., Cochemé J.J., Vellutini P.J., Joron J.L. and Treuil M., 1990. Post-collisional Permian volcanism in northwestern Corsica: an assessment based on mineralogy and trace-element geochemistry. J. Volc. Geotherm. Res., 44: 51-67.

Caron J.M., 1994. Metamorphism and deformation in Alpine Corsica. Schweiz. Miner. Petr. Mitt., 74(1): 105-114.

Caron J.M. and Delcey R., 1979. Lithostratigraphie des Schistes Lustrés corses: diversité des séries post-ophiolitiques. C. R. Acad. Sci. Paris, 288: 1525-1528.

Caron J.M. and Péquignot G., 1986. The transition between blueschist and lawsonite bearing eclogites. Example of Corsican metabasalt. Lithos, 19: 205-218.

Caron J.M., Kienast J.R. and Triboulet C., 1981. High-pressure/low-temperature metamorphism and polyphase Alpine deformation at Sant'Andrea di Cotone (Eastern Corsica, France). Tectonophysics, 78: 419-451.

Cavazza W., DeCelles P.G., Fellin M.G. and Paganelli L., 2007. The Miocene Saint Florent Basin in northern Corsica: stratigraphy, sedimentology, and tectonic implications. Basin Res., 19(4): 507-527.

Cavazza W., Zattin M., Ventura B. and Zuffa G.G., 2001. Apatite fission track analysis of Neogene exhumation in northern Corsica (France). Terra Nova, 13: 51-57.

Ceriani S., Fügenschuh B. and Schmid S.M., 2001. Multi-stage thrusting at the "Penninic Front" in the Western Alps between Mont Blanc and Pelvoux massifs. Int. J. Earth Sci. (Geol. Rundsch), 90: 685-702.

Chamot-Rooke N., Gaulier J.M. and Jestin F., 1999. Constraints on Moho depth and crustal thickness in the Liguro-Provençal basin from a 3D gravity inversion: geodynamic implications. In: B. Durand, L. Jolivet, F. Horvath and M. Sérranne (Eds.), The Mediterranean basin: Tertiary extenson within the Alpine Orogen. Geol. Soc. London Spec. Publ., 156: 37-61.

Chemenda A.I., Mattauer M., Malavieille J. and Bokun A.N., 1995. A mechanism for syn-collisional deep rock exhumation and associated normal faulting: Results from physical modeling. Earth Planet. Sci. Lett., 132: 225-232.

Chopin C., Beyssac O., Bernard S. and Malavieille J., 2008. Aragonite-grossular intergrowths in eclogite-facies marble, Alpine Corsica. Eur. J. Miner., 20: 857-865.

Conti M., Marcucci M. and Passerini, P., 1985. Radiolarian cherts and ophiolites in the Northern Apennines and Corsica. Age, correlations and tectonic frame of siliceous deposition. Ofioliti 10: 203-224.

Cubells J.F., Ferrandini, J., Ferrandini, M., Gaudant, J. and Loye-Pilot M.D. 1994. Presence du genre Aphanius NARDO, famille des Cyprinodontidae, dans le Miocene du Bassin de Francardo Ponte Leccia (Corse). Geol. Mediterr. 21:19-24

Dal Piaz G.V. et al., 1977. I complessi ofiolitici e le unità cristalline della Corsica alpina. Ofioliti, 2 (2-3): 265-324.

Dallan L. and Nardi R., 1984. Ipotesi dell'evoluzione dei domini "liguri" della Corsica nel quadro della paleogeografia e della paleotettonica delle unità alpine. Boll. Soc. Geol. It., 103: 515-527.

Dallan L. and Puccinelli A., 1995. Geologia della regione tra Bastia e St-Florent (Corsica Settentrionale). Boll. Soc. Geol. It., 114: 23-66.

Daniel J.M., Jolivet L., Goffé B. and Poinssot C., 1996. Crustal-scale strain partitioning: footwall deformation below the Alpine Oligo-Miocene detachment of Corsica. J. Struct. Geol., 18(1): 41-59.

De Cesari F., Di Rosa M., Sanità E., Pandolfi L. and Marroni M., 2024. Long-lived sedimentation in the Western Tethys oceanic basin: revisiting the metasediments of Bagliacone-Riventosa Formation (Corsica, France), Int. Geol. Rev., 67(7): 906-932. (10.1080/00206814.2024.2411537)

De Wever P., Danielan T., Durand-Delga M., Cordey F. and Kito F., 1987. Datations des radiolarites post-ophiolitique de Corse alpine à l'aide des radiolaires. C. R. Acad. Sci. Paris, 305: 893-900.

Deseta N., Andersen T.B. and Ashwal L.D., 2014. A weakening mechanism for intermediate-depth seismicity? Detailed petrographic and microtextural observations from blueschist facies pseudotachylites, Cape Corse, Corsica. Tectonophysics, 610: 138-149.

Di Rosa M., De Giorgi A., Marroni M. and Vidal O., 2017a. Syn-convergence exhumation of continental crust: evidence from structural and metamorphic analysis of the Monte Cecu area, Alpine Corsica (Northern Corsica, France). Geol. J., 52: 919-937.

Di Rosa M., De Giorgi A., Marroni M. and Pandolfi L., 2017b. Geology of the area between Golo and Tavignano Valleys (Central Corsica): a snapshot of the continental metamorphic units of Alpine Corsica. J. Maps, 13: 644-653.

Di Rosa M., Frassi C., Marroni M., Meneghini F. and Pandolfi L. 2019a. Did the "Autochthonous" Europe foreland of Corsica Island (France) experience Alpine subduction? Terra Nova, 32: 34-43.

Di Rosa M., Meneghini F., Marroni M., Hobbs N. and Vidal O., 2019b. The exhumation of continental crust in collisional belts: insights from the deep structure of Alpine Corsica in the Cima Pedani area. J. Geol., 127(3): 263-288.

Di Rosa M., Frassi C., Meneghini F., Marroni M., Pandolfi L. and De Giorgi A., 2019c. Tectono-metamorphic evolution in the Europe continental margin involved in the Alpine subduction: new insights from the Alpine Corsica, France. C. R. Acad. Sci. Paris, 351(5): 384-394.

Di Rosa M., Meneghini F., Marroni M., Frassi C. and Pandolfi L., 2020a. The coupling of high-pressure oceanic and continental units in Alpine Corsica: evidence for syn-exhumation tectonic erosion at the roof of the plate interface. Lithos, 354-355: 105328, https://doi.org/10.1016/j.lithos.2019.105328.

Di Rosa M., Frassi C., Malasoma M., Marroni M., Meneghini F. and Pandolfi L., 2020b. Syn-exhumation coupling of the oceanic and continental units along the western edge of the Alpine Corsica : a review. Ofioliti, 45(2): 71-102 DOI: 10.4454/ofioliti.v45i2.4534

Di Rosa M., Sanità E., Frassi C., Lardeaux J.-M., Corsini M., Marroni M. and Pandolfi L., 2023. A journey of the continental crust to and from mantle depth: The P-T-t-d path of Venaco unit, Alpine Corsica (France). Geol. J., 59(2), 422-440. https://doi.org/10.1002/gj.4872

Di Rosa M., Sanità E., Malasoma, A., Pandolfi, L. and Marroni, M., 2025. Switching from contractional to extensional tectonics along the Alpine Front: structural and metamorphic evidence from the Balagne area (northern Corsica, France). J. Struct. Geol., 199, 105471. https://doi.org/10.1016/j.jsg.2025.105471

Dickinson W.R., 1985. Interpreting provenance relations from detrital modes of sandstones. In: Provenance of arenites (pp. 333-361). Dordrecht: Springer Netherlands.

Doglioni C., 1991. A proposal of kinematic modelling for W-dipping subductions - Possible applications to the Tyrrhenian-Apennines system. Terra Nova, 3: 423-434.

Donatio D., Marroni M. and Rocchi S., 2013. Serpentinization history in mantle section from a fossil slow-spreading ridge sequence: Evidences from Pomaia quarry (Southern Tuscany, Italy). Ofioliti, 38(1): 15-28.

Durand-Delga M., 1974. La Corse. Géol. France, 2: 465-478.

Durand-Delga M., 1984. Principaux traits de la Corse Alpine et correlations avec les Alpes Ligures. Mem. Soc. Geol. It., 28: 285-329.

Durand-Delga M., Fondecave-Wallez M.J. and Rossi P., 2005. L'unité ophiolitique de Pineto (Corse): signification du détritisme continental dans sa couverture de flysch albo-cénomanien. C. R. Geosci., 337(12): 1084-1095.

Durand-Delga M., Peybernès B. and Rossi P., 1997. Arguments en faveur de la position, au Jurassique, des ophiolites de Balagne (Haute-Corse, France) au voisinage de la marge continentale européenne. C. R. Acad. Sci. Paris, 325: 973-981.

Durand-Delga M. et al., 1978. Corse. Guides Géol. Régionaux, Masson èd. 208 pp.

Egal E., 1992. Structures and tectonic evolution of the external zone of Alpine Corsica. J. Struct. Geol., 14: 1215-1228.

Egal E. and Caron J.M., 1988. Tectonique polyphasée dans l'Eocène autochtone à la bordure ouest de la Nappe de Balagne (Corse). Bull. Soc. Géol. France, 8: 315-321.

Elter P. and Pertusati. P.C., 1973. Considerazioni sul limite Alpi-Appennino e sulle relazioni con l'arco della Alpi Occidentali. Mem. Soc. Geol. It., 12: 359-375.

Evans B.W., 1990. Phase relations in epidote-blueschists. Lithos, 25; 3-23.

Faccenna C., Piromallo C., Crespo-Blanc L., Jolivet L. and Rossetti F., 2004. Lateral slab deformation and the origin of Western Mediterranean arcs. Tectonics, 23: TC1012.

Faccenna C., et al., 2014. Mantle dynamics in the Mediterranean. Rev.Geophys. 52:283-322.

Faure M. and Malavieille J., 1981. Étude structurale d'un cisaillement ductile: le charriage ophiolitique corse dans la région de Bastia. Bull. Soc. Géol. France, 23(4): 335-343.

Favre P. and Stampfli G.M., 1992. From rifting to passive margin: the example of the Red Sea, Central Atlantic and Alpine Tethys. Tectonophysics, 215: 69-97.

Fellin M.G., Picotti V. and Zattin M., 2005. Neogene to Quaternary rifting and inversion in Corsica: Retreat and collision in the western Mediterranean. Tectonics, 24 (1): doi:10.1029/2003TC001613.

Ferrandini J. and Loye-Pilot M.D., 1992. Tectonique en distension et décrochement au Burdigalien-Tortonien en Corse: l'exemple du bassin de Francardo-Ponte Leccia (Corse centrale). Géol. Alp., 1: 30-31.

Ferrandini M., Ferrandini J., Loye-Pilot M.D., Butterlin J., Cravatte J. and Janin M.C., 1998. Le Miocène du bassin de Saint Florent (Corse): modalités de la transgression du Burdigalien supérieur et mise en évidence du Serravallien. Geobios, 31(1): 125-137.

Ferrandini J., Ferrandini M., Rossi P. and Savary-Sismondini B., 2010. Définition et datation de la formation de Venaco (Corse): dépot d'origine gravitaire d'âge Priabonien. C. R. Geosci., 342: 921-929.

Flinn D., 1962. On Folding during Three-Dimensional Progressive Deformation. Quarterly J. Geol. Soc. London, 118: 385-428. https://doi.org/10.1144/gsjgs.118.1.0385

Fournier M., Jolivet L., Goffé B. and Dubois R., 1991. The Alpine Corsica metamorphic core complex. Tectonics, 10: 1173-1186.

Frassi C., Di Rosa M., Farina F., Marroni M. and Pandolfi L., 2022. Anatomy of a deformed upper crust fragment from Western Alpine Corsica (France): insights into continental subduction processes. Int. Geol. Rev., 65(1): 40-60. (https://doi.org/10.1080/00206814.2022.2031315)

Froitzheim N. and Manatschal G., 1996. Kinematics of Jurassic rifting, mantle exhumation, passive margin formation in the Austroalpine and Penninic nappes (Eastern Switzerland). Geol. Soc. Am. Bull., 108: 1120-1333.

Garfagnoli F., Menna F., Pandeli E. and Principi G., 2009. Alpine metamorphic and tectonic evolution of the Inzecca-Ghisoni area (southern Alpine Corsica, France). Geol. J., 44: 191-210.

Gattacceca J., Deino A., Rizzo R., Jones D.S., Henry B., Beaudoin B. and Vedeboin F., 2007. Miocene rotation of Sardinia: new paleomagnetic and geochronological constraints and geodynamic implications. Earth Planet. Sci. Lett., 258: 359-377.

Gibbons W. and Horak J., 1984. Alpine metamorphism of Hercynian horneblende granodiorite beneath the blueschist facies Schistes Lustrés nappe of NE Corsica. J. Metam. Geol., 2: 95-113.

Gibbons W., Waters C. and Warburton J., 1986. The blueschist facies Schistes Lustrés of Alpine Corsica: a review. Geol. Soc. Am. Mem., 164: 301-331.

Gueguen E., Doglioni C. and Fernandez M., 1998. On the post-25 Ma geodynamic evolution of the western Mediterranean. Tectonophysics, 298: 259-269.

Guelfi R., Maremmani A., Di Rosa M., Meneghini F., Pandolfi L. and Marroni M., 2025. Adding pieces to the puzzle of the Western Tethys Oceanic Basin structure: the architecture of the Inzecca Unit in the Noceta-Vezzani area (Alpine Corsica, France). Episodes, 48(2): 163-179. https://doi.org/10.18814/epiiugs/2025/025006

Guelfi R., De Cesari F., Maremmani A., Di Rosa M., Nannini D., Marroni M., Pandolfi L. and Sanità E., 2026. Lithostratigraphy and structural setting of the Inzecca Unit (Schistes Lustrés Complex, Alpine Corsica, France): Clues from the Venaco-Altiani area. J. of Maps, 22(1): 2599906.

Gueydan F., Brun J-P, Phillippon M. and Noury M., 2017. Sequential extension as a record of Corsica rotation during Apennines slab roll-back. Tectonophysics, 710: 149-161.

Gueydan F., Leroy Y.M., Jolivet L. and Agard P., 2003. Analyses of continental midcrustal strain localization induced by microfaulting and reactionsoftening. J. Geophys. Res., 108: 2064-2081.

Guieu G., Loye-Pilot M.D., Lahondère D. and Ferrandini J., 1994. Carte Géol. France (1/50000), feuille Bastia (1111). BRGM, Orléans, pp. 50

Handy M.R., Schmid S.M., Bousquet R., Kissling E. and Bernoulli D., 2010. Reconciling plate-tectonic reconstructions of Alpine Tethys with the geological-geophysical record of spreading and subduction in the Alps. Earth Sci. Rev., 102: 121-158.

Harris L., 1985. Progressive and polyphase deformation of the Schistes Lustrés in Cap Corse, Alpine Corsica. J. Struct. Geol., 7(6): 637-650.

Ingersoll R.V. and Suczek C.A., 1979. Petrology and provenance of Neogene sand from Nicobar and Bengal fans, DSDP sites 211 and 218. J. Sed. Petr., 49(4): 1217-1228.

Jakni B., Poupeau G., Sosson M., Rossi P., Ferrandini J. and Guennoc P., 2000. Dénudations cénozoiques en Corse: une analyse thermochronologique par traces de fission sur apatites. C. R. Acad. Sci. Paris, 331: 775-782.

Jolivet J., 1993. Extension of thickened continental crust, from brittle to ductile deformation: examples from Alpine Corsica and Aegean Sea. Ann., 36(2): 139-153.

Jolivet L., Daniel J.M. and Fournier M., 1991. Geometry and kinematics of ductile extension in Alpine Corsica. Earth Planet. Sci. Lett., 104: 278-291.

Jolivet L., Dubois R., Fournier M., Goffé B., Michard A. and Jordan C., 1990. Ductile extension in Alpine Corsica. Geology, 18: 1007-1010.

Jolivet L., Faccenna C., Goffé B., Mattei M., Rossetti F., Brunet C., Storti F., Funiciello R., Cadet J.-P., D'Agostino N. and Parra T., 1998. Midcrustal shear zones in post-orogenic extension: Example from the Tyrrhenian Sea. J. Geoph. Res., 103: 12-123.

Lacazedieu A. (1974) - Contribution à l'étude géologique de la partie nord-est de la Balagne sédimentaire (Corse). Thèse 3 e cycle, univ. Paul-Sabatier (Toulouse), 124 pp.

Lacombe O. and Jolivet L., 2005. Structural and kinematic relationships between Corsica and the Pyreneeses-Provence domain at the time of the Pyrenean orogeny. Tectonics, 24: TC1003, doi: 10.1029/2004TC001673

Lagabrielle Y. and Lemoine M., 1997. Alpine, Corsican and Appennine ophiolites: the slowspreading ridge model. C. R. Acad. Sci. Paris, 325: 909-920.

Lagabrielle Y. and Polino R., 1988. Un schéma structural du domaine des Schistes Lustrés ophiolitifères au nord-ouest du massif du Mont Viso (Alpes sudoccidentales) et ses implications. C. R. Acad. Sci. Paris, 323: 957-964.

Lahondère D., and Guerrot C., 1997. Datation Sm-Nd du métamorphisme éclogitique en Corse alpine: un argument pour l'existence au Crétacé supérieur d'une zone de subduction active localisée sous le bloc corso-sarde. Géol. France, 3: 3-11.

Lahondère D., Rossi P. and Lahondère J.C., 1999. Structuration alpine d'une marge continentale externe: le massif du Tenda (Haute-Core). Implication géodynamiques au niveau de la transversale Corse-Appennins. Géol. France, 4: 27-44.

Lahondère J.C., Conchon O., Lahondère D., Dominici R. and Vautrelle C., 1983. Carte Géol. France (1/50000), feuille Bastia (1104). BRGM, Orléans.

Lahondére D., 1988. Le métamorphisme éclogitique dans les orthogneiss et les métabasites ophiolitiques de la région de Farinole (Corse). Bull. Soc. Géol. France, 8: 579-585.

Lahondére, J.C., Lahondére, D. 1988. Organisation structurale des schistes Lustrés du Cap Corse (Haute Corse). C. R. Acad. Sci. Paris, 307: 1081-1086.

Lahondere D., 1991. Les schistes bleus et les éclogites à lawsonite des unités continentales et océaniques de la Corse alpine: Nouvelles données pétrologiques et structurales. Ph.D. thesis. Université Montpellier.

Laporte D., Fernandez A. and Orsini J.B., 1991. Le complexe d'Ile Rousse, Balagne, Corse du Nord-Ouest: pétrologie et cadre de mise en place des granitoïdes magnésiopotassiques. Géol. France, 4: 15-30.

Lavier L. and Manatschal G., 2006. A mechanism to thin the continental lithosphere at magma-poor margins. Nature, 440(7082): 324-328.

Law R.D., 2014. Deformation thermometry based on quartz c-axis fabrics and recrystallization microstructures: a review. J. Struct. Geol., 66: 129-161.

Levi N., Malasoma A., Marroni M., Pandolfi L. and Paperini M., 2007. Tectono- metamorphic history of the ophiolitic Lento Unit (northern Corsica): evidences for the complexity of accretion-exhumation processes in a fossil subduction system. Geod. Acta, 20(1): 99-118.

Li X.H., Faure M., Rossi P., Lin W. and Lahondère D., 2015. Age of Alpine Corsica ophiolites revisited: Insights from in situ zircon U-Pb age and O-Hf isotopes. Lithos, 220: 179-190.

Maggi M., Rossetti F., Corfu F., Theye T., Andersen T.B. and Faccenna C., 2012. Clinopyroxene-rutile phyllonites from East Tenda Shear Zone (Alpine Corsica, France): pressure-temperature-time constraints to the Alpine reworking of Variscan Corsica. J. Geol. Soc. London, 169: 723-732.

Malasoma A. and Marroni M., 2007. HP/LT metamorphism in the Volparone Breccia (Northern Corsica, France): evidence for involvement of the Europe/Corsica continental margin in the Alpine subduction zone. J. Metam. Geol., 25: 529-545.

Malasoma A., Marroni M., Musumeci G. and Pandolfi L., 2006. High pressure mineral assemblage in granitic rocks from continental units, Alpine Corsica, France. Geol. J., 41: 49-59.

Malasoma A., Morelli G., Di Rosa M., Marroni M., Pandeli E., Principi G. and Pandolfi L., 2020. The stratigraphic and structural setting of metamorphic continental units from Alpine Corsica: clues from the area between Asco and Golo valleys (Central Corsica, France). J. Maps, 16(2): 313-323.

Malavieille J., 1983. Etude tectonique de la nappe de socle Centuri (zone de Schistes Lustrés de la Corse); Consequence pour la géométrie de la chaine alpine. Bull. Soc. Géol. France, 25: 195-204.

Malavieille J., Chemenda A. and Larroque C., 1998. Evolutionary model for the Alpine Corsica: mechanism for ophiolite emplacement and exhumation of high-pressure rocks. Terra Nova, 10: 317-322.

Malusà M.G., Faccenna C., Baldwin S.L., Fitzgerald P.G., Rossetti F., Balestrieri M.L., Danisik M., Ellero A., Ottria G. and Piromallo C., 2015. Contrasting styles of (U)HP rock exhumation along the Cenozoic Adria-Europe plate boundary (Western Alps, Calabria, Corsica). Geochem. Geophys. Geosyst., 16: 1786-1824.

Malusà M., Polino R. and Zattin M., 2009. Strain partitioning in the axial NW Alps since the Oligocene. Tectonics, 28(3), https://doi.org/10.1029/2008TC002370

Maluski H., Mattauer M. and Matte P.H., 1973. Sur la presence de decrochement alpins en Corse. C. R. Acad. Sci. Paris, 276: 709-712.

Manatschal G., 1995. Jurassic rifting and formation of a passive continental margin (Platta and Err nappes, Eastern Switzerland): geometry, kinematics and geochemistry of fault rocks and comparison with Galicia margin. Diss. ETH, Nr. 11188, Zurich.

Marino M., Monechi S. and Principi G., 1995. New calcareous nannofossil data on the Cretaceous-Eocene age of Corsican turbidites. Riv. Ital. Pal. Strat., 101: 49-62.

Marroni M. and Pandolfi L., 2001. Debris flow and slide deposits at the top of the Internal Liguride ophiolitic sequence, Northern Apennines, Italy: a record of frontal tectonic erosion in a fossil accretionary wedge. Isl. Arc, 10: 9-21.

Marroni M. and Pandolfi L., 2003. Deformation history of the ophiolite sequence from the Balagne Nappe, northern Corsica: insights in the tectonic evolution of the Alpine Corsica. Geol. J., 38: 67-83.

Marroni M. and Pandolfi L., 2007. The architecture of an incipient oceanic basin: a tentative reconstruction of the Jurassic Liguria-Piemonte basin along the Northern Apennine-Alpine Corsica transect. Int. J. Earth Sci., 96: 1059-1078.

Marroni M., Molli G., Ottria G. and Pandolfi L., 2001. Tectono-sedimentary evolution of the External Liguride units (Northern Appennines, Italy). Insights in the pre-collisional history of a fossil ocean-continent transition zone. Geodin. Acta, 14: 307-320.

Marroni M., Meneghini F. and Pandolfi L., 2017. A revised subduction inception model to explain the Late Cretaceous, double-vergent orogen in the pre-collisional Western Tethys: evidence from the Northern Apennines. Tectonics, 36: 2227-2249.

Marroni M., Pandolfi L. and Meneghini F., 2004. From accretion to exhumation in a fossil accretionary wedge: a case history from Gottero Unit (Northern Apennines, Italy). Geod. Acta, 17: 41-53.

Marroni M., Pandolfi L. and Perilli N., 2000. Calcareous nannofossil dating of the San Martino Formation from the Balagne ophiolite sequence (Alpine Corsica): comparison with the Palombini Shale of the Northern Apennine. Ofioliti, 25: 147-156.

Marroni M., Pandolfi L., Saccani E., Sanità E. and Tagliacollo L., 2026. A snapshot of the volcanic activity during the early evolution of the Ligurian-Piedmont Ocean: Insights from the pillow lava sequence of the Balagne Nappe (Alpine Corsica). Ofioliti, submitted.

Martin A.J., Rubatto D., Vitale Brovarone A. and Hermann J., 2011. Late Eocene lawsonite-eclogite facies metasomatism of a granulite sliver associated to ophiolites in Alpine Corsica. Lithos, 125: 620-640.

Masini E., Manatschal G. and Mohn G., 2013. The Alpine Tethys rifted margins: Reconciling old and new ideas to understand the stratigraphic architecture of magma-poor rifted margins. Sedimentology, 60(1): 174-196.

Mattauer, M. and Proust F., 1975. Données nouvelles sur l'evolution structurale de la Corse alpine. C. R. Acad. Sci. Paris, 281: 1681-1684.

Mattauer M. and Proust F., 1976. La Corse alpine: un modèle de genèse du métamorphisme haute pression par subduction de croute continentale sous du matérial océanique. R. Acad. Sci. Paris, 282: 1249-1252.

Mattauer M., Faure M. and Malavieille J., 1981. Transverse lineation and large-scale structures related to Alpine obduction in Corsica. J. Struct. Geol., 3: 401-409.

Mattauer M., Proust F. and Etchecopar A., 1977. Linéation "a" et mécanisme de cisellement simple liés au chevauchement de la nappe de Schistes Lustrés en Corse. Bull. Soc. Géol. France, 14: 841-945.

Meneghini F., Pandolfi L. and Marroni M., 2020. Recycling of heterogeneous material in the subduction factory: evidence from the sedimentary mélange of the Internal Ligurian Units, Italy. J. Geol. Soc., 177: 587-599.

Ménot R.P. and Orsini J.B., 1990. Evolution du socle anté-stéphanien de Corse: événements magmatiques et métamorphiques. Schweiz. Miner. Petr., 70: 35-53.

Meresse F., Lagabrielle Y., Malavieille J. and Ildefonse B., 2012. A fossil ocean-continent transition of the Mesozoic Tethys preserved in the Schistes Lustrés nappe of northern Corsica. Tectonophysics, 579: 4-16.

Michard A., Chalouan A., Feinberg H., Goffé B. and Montigny R., 2002. How does the Alpine belt end between Spain and Morocco? Bull. Soc. Géol. France, 173(1): 3-15.

Michard A. and Martinotti G., 2002. The Eocene unconformity of the Brianconnais domain in the French-Italian Alps, revisited (Marguareis massif, Cuneo); a hint for a Late Cretaceous-middle Eocene frontal bulge setting. Geodin. Acta, 15: 289-301.

Mohn G., Manatschal G., Beltrando M., Masini E. and Kusznir N., 2012. Necking of continental crust in magma-poor rifted margins: Evidence from the fossil Alpine Tethys margins. Tectonics, 31 (1): doi:10.1029/2011TC002961.

Mohn G., Manatschal G., Muntener O., Beltrando M. and Masini E., 2009. Unravelling the interaction between tectonic and sedimentary process during lithospheric thinning in the Alpine Tethys margins. Int. J. Earth Sci., 99: S75-S101.

Molli G., 2008. Northern Apennine-Corsica orogenic system: an updated overview. In: S. Siegesmund, B. Fugenschuh and N. Froitzheim (Eds.), Tectonic aspects of the Alpine-Dinaride-Carpathian System. Geol. Soc. London Spec. Publ., 298: 413-442.

Molli G. and Malavieille J., 2011. Orogenic processes and the Corsica/Apennines geodynamic evolution: insights from Taiwan. Int. J. Earth Sci., 100: 1207-1224.

Molli G. and Tribuzio R., 2004. Shear zones and metamorphic signature of subducted continental crust as tracers of the evolution of the Corsica/Northern Apennine orogenic system. In: G.I. Alsop, R.E. Holdsworth, K.J.W. McCaffrey and M. Handy, (Eds.), Flow processes in faults and shear zones. Geol. Soc. London Spec. Publ., 224: 321-335.

Molli G., Tribuzio R. and Marquer D., 2006. Deformation and metamorphism at the eastern border of Tenda Massif (NE Corsica): a record of subduction and exhumation of continental crust. J. Struct. Geol., 28: 1748-1766.

Mutti E., 1992. Turbidite Sandstones. San Donato Milanese. Agip-Istituto di Geologia, Università di Parma, 275 pp.

Nardi R., 1968a. Contributo alla geologia della Balagne (Corsica nord-occidentale). Mem. Soc. Geol. It., 7: 471-489.

Nardi R., 1968b. Le unità alloctone della Corsica e la loro correlazione con le unità delle Alpi e dell'Appennino. Mem. Soc. Geol. It., 7: 323-344.

Nardi R., Puccinelli A. and Verani M., 1978. Carta geologica della Balagne "sedimentaria" (Corsica) alla scala 1:25.000 e Note Illustrative. Boll. Soc. Geol. It., 97: 3-22.

Ohnenstetter M., Ohnenstetter D. and Rocci G., 1976. Étude des métamorphismes successifs des cumulats ophiolitiques de Corse. Bull. Soc. Géol. France, 18(1): 115-134.

Padoa E., 1999. Les ophiolites du massif de l'Inzecca (Corse alpine): lithostratigraphie, structure géologique et évolution géodynamique. Géol. France, 3: 37-48.

Pandeli E., Giusti R., Elter F.M., Orlando A. and Orti L. 2018. Structural setting and metamorphic evolution of a contact aureole: the example of the Mt. Capanne pluton (Elba Island, Tuscany, Italy). Ofioliti, 43(1): 41-73.

Pandolfi L., 1997. Stratigrafia ed evoluzione strutturale delle successioni torbiditiche cretacee della Liguria orientale (Appennino Settentrionale). Tesi di dottorato, Università di Pisa.

Pandolfi L., Marroni M. and Malasoma A., 2016. Stratigraphic and structural features of the Bas-Ostriconi Unit (Corsica): paleogeographic implications. C. R. Geosci., 348: 630-640.

Paquette J.L., Ménot R.P., Pin C. and Orsini J.B., 2003. Episodic and short-lived granitic pulses in a post-collisional setting: evidence from precise U-Pb zircon dating through a crustal cross-section in Corsica. Chem.Geol., 198: 1-20.

Passchier C.W. and Trouw R.A.J., 2005. Microtectonics: Berlin, New York, Springer, 16, pp. 366.

Pequignot G.,1984. Métamorphisme et tectonique dans les Schistes Lustrés à l'Est de Corte (Corse). Ph.D. Thesis Univ. Claude-Bernard (Lyon), pp. 145

Péron-Pinvidic G. and Manatschal G., 2009. The final rifting evolution at deep magma-poor passive margins from Iberia-Newfoundland: A new point of view. Int. J. Earth Sci., 98: 1581-1597.

Peybernès B., Durand-Delga M., Rossi P. and Cugny, P., 2001. Nouvelles datations micropaléontologiques dans les séquences intra- et post-ophiolitiques de la nappe de Balagne (Corse) et essai de reconstitution d'un segment de la marge occidentale de l'océan liguro piémontais, Ecl. Geol. Helv., 94: 95-105.

Principi G. and Treves B., 1984. Il sistema corso-appenninico come prisma d'accrezione. Riflessi sul problema generale del limite Alpi-Appennini. Mem. Soc. Geol. It., 28: 49-576.

Principi G., Bortolotti V., Chiari M., Cortesogno L., Gaggero L., Marcucci M., Saccani E. and Treves B., 2004. The pre-orogenic volcano-sedimentary covers of the western Tethys oceanic basin: a review. Ofioliti, 29(2): 177-211.

Pupin J.-P., 1980. Zircon and granite petrology. Contrib. Min. Petrol. 73:207-220.

Ravna E.J.K., Andersen T.B., Jolivet L. and De Capitani C., 2010. Cold subduction and the formation of lawsonite-eclogite from prograde evolution of eclogitized pillow lava from Corsica. J. Metam. Geol., 28: 381-395.

Rehault J.P., Boillot G. and Mauffred A., 1984. The western Mediterranean Basin geological evolution. Mar. Geol., 55: 447-477.

Renna M.R., Tribuzio R., Sanfilippo A. and Tiepolo M. 2017. Zircon U-Pb geochronology of lower crust and quartzo-feldspathic clastic sediments from the Balagne ophiolite (Corsica). Swiss Journal of Geosciences 110: 479-501.

Renna M.R., Tribuzio R., Sanfilippo A. and Thirlwall M. 2018. Role of melting process and melt-rock reaction in the formation of Jurassic MORB-type basalts (Alpine ophiolites). Contributions to Mineralogy and Petrology 173 31.

Ribes C., Manatschal G., Ghienne J.-F., Karner G.D., Johnsonm C.A., Flgueredo P.H., Incerpi N. and Epin M.-E., 2019. The syn-rift stratigraphic recrord across a fossil hyper-extended rifted margin: the example of the northwestern Adriatic margin exposed in the Central Alps. Int. J. Earth Sci., 108(6): 2071-2095.

Rosenbaum G., Lister G.S. and Duboz C., 2002. Relative motion of Africa, Iberia and Europe during Alpine orogeny. Tectonophysics, 359: 117-129.

Rossetti F., Glodny J., Theye T. and Maggi M., 2015. Pressure temperature deformation- time of the ductile Alpine shearing in Corsica from orogenic construction to collapse. Lithos, 218-219: 99-116.

Rossi P., Cocherie A. and Fanning M., 2015. Evidence in Variscan Corsica of a brief and voluminous Late Carboniferous to Early Permian volcanic-plutonic event contemporaneous with a high-temperature/low-pressure metamorphic peak in the lower crust. Bull. Soc. Géol. France, 186(2-3): 171-192.

Rossi P., Durand-Delga M., Caron J.M., Guieu G., Conchon O., Libourel G. and Loye-Pilot M., 1994. Carte Géologique de la France (1/50,000), feuille Corte (1110). BRGM, Orléans.

Rossi P., Durand-Delga M., Lahondère J.C., Baud J.P., Egal E., Lahondère D., Laporte D., Lluch D., Loyle M.D., Ohnenstetter M. and Palagi P., 2001. Carte Géologique de la France (1/50,000), feuille Santo Pietro di Tenda (1106). BRGM, Orléans.

Rossi P., Oggiano G. and Cocherie A., 2009. A restored section of the "southern Variscan realm" the Corsica-Sardinia microcontinent. C.R. Geosci., 341: 224-238.

Rossi P., Cocherie A., Lahondère D. and Fanning, C.M., 2002. La marge européenne de la Téthys jurassique en Corse: datation de trondhjémites de Balagne et indices de croûte continentale sous le domaine Balano-Ligure. C. R. Geosci., 334: 313-322.

Routhier P., 1956. Étude géologique de la Balagne sédimentaire (Corse septentrionale). Bull. Serv. Cart. Géol. France, LIV 249 (èd.1957), 266-2933.

Saccani, E., 2003. New geochemical and petrological data on Corsica ophiolites: Possible geodynamic implications for the Alpine Corsica-Apennine system. Atti del Convegno: La geologia del Mare Tirreno e degli Appennini. Geol. Acta, 2: 162-164.

Saccani E., Padoa E. and Tassinari R., 2000. Preliminary data on the Pineto gabbroic massif and Nebbio basalts: progress toward the geochemical characterization of Alpine Corsica ophiolites. Ofioliti, 25: 75-86.

Saccani E., Principi G., Garfagnoli F. and Menna F., 2008. Corsica ophiolites: geochemistry and petrogenesis of basaltic and metabasaltic rocks. Ofioliti, 33(2): 187-207.

Sagri M., Aiello E. and Certini L., 1982. Le unità torbiditiche cretacee della Corsica. Rend. Soc. Geol. It., 5: 87-91.

Sallarès V. and Ranero C.R., 2005. Structure and tectonics of the erosional convergent margin of Antofagasta, north Chile (23°30'S). J. Geophys. Res., 110: B06101.

Sanfilippo A. and Tribuzio R., 2013. Origin of olivine-rich troctolites from the oceanic lithosphere: a comparison between the Alpine Jurassic ophiolites and modern slow spreading ridge. Ofioliti, 38(1): 89-99.

Sanfilippo A., Tribuzio R., Tiepolo M. and Berno D., 2015. Reactive flows as dominant evolution process in the lowernmost oceanic crust: evidence from olivine of the Pineto ophiolite (Corsica). Contrib. Miner. Petrol., 170(4): 38

Schmid S. and Kissling E., 2000. The arc of the Western Alps in the light of geophysical data on deep crustal structure. Tectonics, 19: 62-85.

Schmid S.M., Pfiffner O.A., Froitzheim N., Schönborn G. and Kissling E., 1996. Geophysical-geological transect and tectonic evolution of the swiss-italian Alps. Tectonics, 15(5): 1036-1064.

Staub R., 1924. Der Bau der Alpen. Beitr. z. geol. Karte. Schweiz. Neue Folge, 52: 107.

Treves B. and Harper G.D., 1994. Exposure of serpentinites on the ocean floor: sequence of faulting and hydrofracturing in the Northern Apennine ophicalcites. Ofioliti, 19: 435-466.

Tribuzio R. and Giacomini F., 2002. Blueschist facies metamorphism of peralkaline rhyolites from Tenda crystalline massif (northern Corsica): evidence for involvement in the Alpine subduction event? J. Metam. Geol., 20: 513-526.

Tribuzio R., Renna M.R., Braga R. and Dallai L. 2009). Petrogenesis of Early Permian olivine-bearing cumulates and associated basalt dykes from Bocca di Tenda (Northern Corsica): Implications for post-collisional Variscan evolution. Chemical Geology 259: 190-203.

Tribuzio R., Garzetti F., Corfu F., Tiepolo M. and Renna M.R. 2016. U-Pb zircon geochronology of the Ligurian ophiolites (Northern Apennine, Italy): Implications for continental breakup to slow seafloor spreading. Tectonophysics 666: 220-243.

Vitale Brovarone A., Beltrando M., Malavieille J., Giuntoli F., Tondella E., Groppo C., Beyssac O. and Compagnoni R., 2011. Inherited Ocean-Continent Transition zones in deeply subducted terranes: Insights from Alpine Corsica. Lithos, 124: 273-290.

Vitale Brovarone A. and Herwartz D., 2013. Timing of HP metamorphism in the Schistes Lustrés of Alpine Corsica: new Lu-Hf garnet and lawsonite ages. Lithos, 172-173: 175-191.

Vitale Brovarone A., Beyssac O., Malavieille J., Molli G., Beltrando M. and Compagnoni R., 2012. Stacking and metamorphism of continuous segments of subducted lithosphere in a high-pressure wedge: The example of Alpine Corsica (France). Earth Sci. Rev., 116: 35-56.

Vitale Brovarone A., Picatto M., Beyssac O., Lagabrielle Y. and Castelli D., 2014. The blueschist-eclogite transition in the Alpine chain: P-T paths and the role of slow-spreading extensional structures in the evolution of HP-LT mountain belts. Tectonophysics, 615: 96-121.

Warburton J., 1986. The ophiolite-bearing Schistes Lustrés nappe in Alpine Corsica: a model for the emplacement of ophiolites that have suffered HP/LT metamorphism. Geol. Soc. Am. Mem., 164: 313-331.

Warr L.N, 2021. IMA-CNMNC approved mineral symbols. Mineral. Mag., 85: 291-320.

Waters C.N., 1990. The Cenozoic tectonic evolution of Alpine Corsica. J. Geol. Soc. London, 147: 811-824.

Zarki-Jakni B., Van Der Beek P., Poupeau G., Sosson M., Labrin E., Rossi P. and Ferrandini J., 2004. Cenozoic denudation of Corsica in response to Ligurian and Tyrrhenian extension: results from apatite fission track thermochronology. Tectonics, 23: TC1003, doi: 10.1029/ 2003TC001535.

Zuffa G.G., 1980. Hybrid arenites; their composition and classification. J. Sedim. Res., 50(1), 21-29.

Received, November 27, 2025
Accepted, December 24, 2025